



Application of Finite Element Method for Estimation of Acoustic Parameters

Ph.D. Thesis

Nikolaos M. Papadakis

20/11/2017

Application of Finite Element Method for Estimation of Acoustic Parameters

Χρήση της Μεθόδου των Πεπερασμένων
Στοιχείων για τον Υπολογισμό
Ακουστικών Μεγεθών

Διδακτορική Διατριβή

Νικόλαος Μ. Παπαδάκης

20/11/2017

Πολυτεχνείο Κρήτης
Τμήμα Μηχανικών Παραγωγής και Διοίκησης

Technical University of Crete

School of Production Engineering & Management

University Campus

73100, Chania, Greece

Phone: +30 28210 37255, 37305

<http://www.pem.tuc.gr>

info@pem.tuc.gr

To my mother

Aggeliki

Everything is simpler than you think

and at the same time more complex than you imagine

Johann Wolfgang von Goethe

Advisory Committee

Georgios E. Stavroulakis (Supervisor)

Professor, School of Production Engineering & Management,
Technical University of Crete, Greece

Daphne Manoussaki (Co-supervisor)

Asst. Professor, School of Electrical and Computer Engineering,
Technical University of Crete, Greece

Christopher Provatidis (Co-supervisor)

Professor, School of Mechanical Engineering
National Technical University of Athens, Greece

Examination Committee

Aristomenis Antoniadis

Professor, School of Production Engineering & Management,
Technical University of Crete, Greece

Dimitrios Sotiropoulos

Professor, School of Production Engineering & Management,
Technical University of Crete, Greece

Konstantinos-Alketas Oungrinis

Assoc. Professor, School of Architecture,
Technical University of Crete, Greece

Konstantinos Providakis

Professor, School of Architecture,
Technical University of Crete, Greece



This dissertation is distributed according to the terms and conditions of the Creative Commons License, Attribution – Non Commercial – No Derivatives 4.0 International (CC BY-NC-ND 4.0)¹ or later.

ABSTRACT

In the field of computational acoustics, the calculation of the impulse response of a space is of vital importance. Acoustic parameters, frequency response and the cumulative spectral decay can directly be extracted from the impulse response. This thesis contributes on the development and utilization of a Finite Element Method in the Time Domain for estimating the impulse response and acoustic parameters of a room.

A methodology is developed for resolving the most crucial elements involving the Finite Element Method in the Time Domain. In order to develop an accurate method, we considered different modeling parameters (source selection, modeling of walls and acoustic material) and different parameters for the numerical scheme (finite element meshes, time stepping method, time stepping scales).

For this purpose the impulse responses and the acoustic parameters of a reverberant space were computed and then compared with the measured ones. The results showed that the Time Domain Finite Element Method is an applicable method that provides good results for the calculation of the impulse response and acoustic parameters in a reverberant room.

As a utilization of the Time Domain Finite Element Method the method was applied in a Virtual Reverberation Chamber for the calculation of the absorption coefficients of an acoustic panel. The results showed that the method can be used for the prediction of the absorption characteristics of acoustic panels of various shapes prior to their manufacture.

ΠΕΡΙΛΗΨΗ

Στον τομέα της υπολογιστικής ακουστικής, ο υπολογισμός της κρουστικής απόκρισης ενός χώρου είναι μεγάλης σημασίας. Η πλειονότητα των ακουστικών παραμέτρων, όπως και η συχνοτική απόκριση του χώρου μπορούν να εξαχθούν από την κρουστική απόκριση. Η διατριβή συμβάλλει στην ανάπτυξη και αξιοποίηση της Μεθόδου Πεπερασμένων Στοιχείων στο Πεδίο του Χρόνου για τον υπολογισμό της κρουστικής απόκρισης και των ακουστικών παραμέτρων ενός χώρου.

Στην διπλωματική αναπτύχθηκε μεθοδολογία για την επίλυση των πιο κρίσιμων θεμάτων που αφορούν τη Μέθοδο των Πεπερασμένων Στοιχείων στο Πεδίο του Χρόνου. Τα βήματα που ελήφθησαν υπόψη για την ανάπτυξη μιας αξιόπιστης μεθόδου ήταν η κατάλληλη επιλογή πηγής, η κατάλληλη μοντελοποίηση των τοίχων, οι χρονικές κλίμακες, τα πλέγματα των πεπερασμένων στοιχείων, η μοντελοποίηση του υλικού ακουστικής απορρόφησης και η μέθοδος χρονισμού.

Για το σκοπό αυτό υπολογίστηκαν οι κρουστικές αποκρίσεις και οι ακουστικές παράμετροι ενός χώρου αντήχησης και στη συνέχεια συγκρίθηκαν με τις αντίστοιχες που βρέθηκαν μετά από μέτρηση. Τα αποτελέσματα έδειξαν ότι η Μέθοδος των Πεπερασμένων Στοιχείων στο Πεδίο του Χρόνου μπορεί να παρέχει καλά αποτελέσματα για τον υπολογισμό της κρουστικής απόκρισης και των ακουστικών παραμέτρων σε ένα χώρο αντήχησης.

Ως αξιοποίηση της Μεθόδου των Πεπερασμένων Στοιχείων στο Πεδίο του Χρόνου, έγινε εφαρμογή σε ένα εικονικό θάλαμο αντήχησης για τον υπολογισμό των συντελεστών απορρόφησης ενός ακουστικού στοιχείου. Τα αποτελέσματα έδειξαν ότι η μέθοδος μπορεί να χρησιμοποιηθεί για την πρόβλεψη των χαρακτηριστικών απορρόφησης ακουστικών στοιχείων διαφόρων σχημάτων πριν από την κατασκευή τους.

CONTRIBUTION TO THE STATE OF THE ART

Finite Element Method (FEM) is among the most widely used numerical methods in acoustics. However few researchers have addressed the issue of using the method in the Time Domain (TDFEM) for room acoustics applications. For this reason the aim of this thesis was to broaden the current knowledge of TDFEM especially for measurements of impulse responses and acoustic parameters. We initiated this research by assembling all the right elements for an applicable and effective TDFEM [1, 2]. The same elements were used to simulate diffraction effects from sound barriers [3]. This thesis also provided additional contribution regarding the measurement methods that were essential for the experimental evaluation of TDFEM [4, 5].

The first contribution is the utilization of the TDFEM for measuring the absorption coefficient of acoustics panels [6]. In reality measuring the absorption coefficient of an acoustic panel requires the usage of a reverberation chamber. This process is time-consuming and costly. For this thesis the process of measuring the absorption coefficient of an acoustic panel was simulated with the use of the TDFEM. A 'virtual reverberation' method was created and the implementation of the process provided good results. With the use of this process the absorption coefficient of acoustic panels with variant shapes can be measured. The same method can also be utilized for the measurement of other acoustic characteristics of materials such as the diffusion coefficient.

The second contribution involves mesh restriction requirements for room acoustic application of TDFEM. Experimental data showed that the cross correlation coefficient between calculated and impulse response has a decreasing step over time [7]. The same results were obtained after some theoretical calculations that are presented in this thesis. The importance of these findings is significant. Mesh restrictions imposed so far in the field of acoustics provides good results but mainly for calculations in the frequency domain. For calculations in the time domain it appears that mesh restriction requirements depends on the time duration of the impulse response. Hence it depends on the

reverberation time and volume of the room since the duration of the impulse response is affected by these characteristics. Longer impulse responses require smaller mesh size than the current restrictions for more accurate calculations.

This study also contributes to a new understanding of the choice of measurement method according to levels of background noise. For the evaluation of the TDFEM precise measurements were required. The most common methods for impulse response and reverberation time measurements in acoustic spaces are the Exponential Sine Sweep (ESS) and Maximum Length Sequence (MLS). The ESS and MLS methods were applied for impulse response measurements with a varying level of background noise [4]. Results show that for reverberation time measurements the mean absolute error and standard deviation for the MLS method starts to rise at lower background noise levels compared to the ESS method. For low background noise levels the two methods provide similar results. Implications of the findings suggest the proposed method for measurement according to the levels of the background noise.

Last but not least a novel alternative sound source for acoustic measurements was tested. A dodecahedral loudspeaker is commonly required for precise impulse response and reverberation time measurements. A common directional loudspeaker was utilized to mimic the sound field created by a dodecahedral loudspeaker [5]. For this purpose the directional loudspeaker was placed in twelve positions similar to the positions of the cones of the dodecahedral loudspeaker. For each position impulse response were measured and finally added up creating a single impulse response for the directional loudspeaker. The impulse response was also obtained with the use of a dodecahedral loudspeaker. The findings suggest that reverberation time measurements with the proposed method can provide usable results for acoustic spaces. According to the results the proposed method is one of the best alternative methods for measuring reverberation time when a dodecahedral speaker is not available.

PUBLICATIONS

1. Papadakis, N. and G.E. Stavroulakis, Validation of Time Domain Finite Element method via calculations of acoustic parameters in a reverberant space, in 10th HSTAM International Congress on Mechanics. 2013: Chania, Crete, Greece.
2. Papadakis, N. and G.E. Stavroulakis. Time domain finite element method for the calculation of impulse response of enclosed spaces. Room acoustics application, in Mechanics of Hearing: Protein to Perception: Proceedings of the 12th International Workshop on the Mechanics of Hearing. 2015. AIP Publishing.
3. Papadakis, N.M. and G.E. Stavroulakis, Estimation Of Insertion Loss of Sound Barriers via Finite Element Method, in 9th GRACM International Congress on Computational Mechanics. 2018: Chania, Crete, Greece.
4. Antoniadou, S., N.M. Papadakis, and G.E. Stavroulakis, Measuring Acoustic Parameters with ESS and MLS: Effect of Artificially Varying Background Noises, in Euronoise 2018. 2018: Heraclion, Crete, Greece.
5. Papadakis, N.M., A. Serras, and G.E. Stavroulakis, Mimicking the Sound Field of a Dodecahedral Loudspeaker by a Common Directional Loudspeaker for Reverberation Time Measurements, in Euronoise 2018. 2018: Heraclion, Crete, Greece.
6. Papadakis, N. and G.E. Stavroulakis, Virtual Reverberation Chamber Method with the use of Time Domain Finite Element Method (Submitted to) Building Acoustics, 2017.
7. Papadakis, N.M. and G.E. Stavroulakis, Effect of Mesh Size for Modeling Impulse Responses of Acoustic Spaces via Finite Element Method in the Time Domain, in Euronoise 2018. 2018: Heraclion, Crete, Greece.

ACKNOWLEDGEMENTS

I wish to express my sincere gratitude to my supervisor, Professor Georgios Stavroulakis, for his continued support and invaluable guidance throughout my graduate career. His priceless insights and constructive criticisms helped me shape myself into the competitive academic environment. I am forever indebted to him as he was able not only to impart knowledge, but also his work ethic which I intend to follow for the rest of my academic career and life.

I also wish to express my appreciation to the committee member, Assistant Professor Dafni Manousaki, for her assistance, guidance and encouragement. I have been greatly benefited from her numerous comments and helpful discussions spanning mathematics to career development.

I would also like to acknowledge and extend my sincere thanks to the committee member, Professor Christoforos Provatidis, for his contribution to the completion of this thesis.

Finally I would like to thank all my family and friends for their support and understanding during this time.

TABLE OF CONTENTS

1. ABSTRACT	IX
2. ΠΕΡΙΛΗΨΗ	X
3. CONTRIBUTION TO THE STATE OF THE ART	XI
4. PUBLICATIONS	XIII
5. ACKNOWLEDGEMENTS	XIV
6. TABLE OF CONTENTS	XV
7. LIST OF FIGURES	XXI
8. LIST OF TABLES	XXV
9. ABBREVIATIONS	XXVI
1. INTRODUCTION	1
1.1 PROJECT SCOPE AND RESEARCH METHODS.....	3
1.2 THESIS STRUCTURE.....	5
2. ELEMENTS OF ACOUSTICS	7
2.1 BASIC SOUND FIELD QUANTITIES.....	8
2.1.1 Sound Pressure.....	9
2.1.2 Density, Particle Velocity, Particle Displacement	10
2.1.3 Speed of sound.....	11
2.1.4 Impedance	12
2.2 WAVE ACOUSTICS AND EQUATIONS	13

2.2.1	Derivation of the wave equation.....	13
2.2.1.1	Euler’s equation.....	14
2.2.1.2	Equation of continuity.....	16
2.2.1.3	Thermodynamic Law and Wave Equation	18
2.2.2	Other Forms of the Wave Equation	19
2.2.2.1	Linearized inhomogeneous wave equation.....	20
2.2.2.2	Lossy wave equation for propagation of sound in fluids	21
2.2.3	Boundary conditions	22
2.2.3.1	Dirichlet boundary condition.....	23
2.2.3.2	Neumann boundary condition.....	23
2.2.3.3	Robin or impedance boundary condition.....	23
2.2.4	Helmholtz Equation	24
2.2.5	Eigenfrequencies, Eigenmodes, Eigenvalues	24
2.2.6	Other modeling approaches	26
2.2.6.1	Geometrical acoustics	26
2.2.6.2	Statistical acoustics	28
2.2.7	Schroeder Frequency	28
2.3	IMPULSE AND FREQUENCY RESPONSE.....	29
2.3.1	Impulse Response.....	30
2.3.2	Frequency Response	31
2.3.3	Cumulative Spectral Decay	34

2.3.4	Auralization.....	36
2.4	ACOUSTIC PARAMETERS AND ABSORPTION COEFFICIENT	37
2.4.1	Reverberation time - RT.....	37
2.4.2	Early decay time - EDT	40
2.4.3	Clarity – C80, C50.....	40
2.4.4	Definition – D_{50}	41
2.4.5	Centre time - T_s	41
2.4.6	Strength - G.....	42
2.4.7	Other acoustic parameters.....	44
2.4.8	Absorption coefficient.....	44
3.	FINITE ELEMENT METHOD, ACOUSTICS AND FORMULATIONS.....	47
3.1	INTRODUCTION	48
3.2	FINITE ELEMENT METHOD IN ACOUSTICS.....	49
3.2.1	Literature review-Applications of the Finite Element Method and the TDFEM in Acoustics.....	50
3.2.2	Alternative Time Domain Methods.....	51
3.2.2.1	Finite Difference Method in Acoustics	52
3.2.2.2	Boundary Element Method in Acoustics.....	53
3.3	BASIC STEPS OF THE FINITE ELEMENT METHOD	54
3.3.1	Definition of governing equations.....	54
3.3.2	Weak Integral Formulation.....	55
3.3.2.1	Derivation of the Weak Formulation.....	55

3.3.2.2	Test Functions - Galerkin's method	56
3.3.3	Discretization	57
3.3.4	Approximation of variables and calculation of elementary matrices 59	
3.3.4.1	Shape functions.....	60
3.3.5	Assembling – Imposition of constraints	63
3.3.6	Solution and convergence study.....	64
3.3.6.1	Solution.....	64
3.3.6.2	Postprocessing.....	64
3.3.6.3	Numerical Error.....	64
3.4	FINITE ELEMENT FORMULATION OF THE WAVE EQUATION	66
3.4.1	Derivation of Acoustic Matrices	67
3.4.2	Acoustic Boundary Conditions	70
4.	SETUP OF THE FINITE ELEMENT METHOD AND IMPLEMENTATIONS	72
4.1	SETUP OF THE FINITE ELEMENT METHOD.....	73
4.1.1	Source selection	73
4.1.1.1	Gaussian Pulse Point Source.....	73
4.1.2	Impedances of walls	77
4.1.3	Time step.....	84
4.1.4	Finite element meshes.....	90
4.1.5	Modeling of the acoustic material	96
4.1.6	Stepping method.....	97

4.1.7	Solver.....	99
4.1.8	Type of Elements	100
4.2	IMPLEMENTATIONS OF TIME DOMAIN FINITE ELEMENT METHOD .	102
4.2.1	Reverberant room Modeling.....	102
4.2.2	Reverberant room with Acoustic Material Modeling.....	105
4.2.2.1	‘Virtual reverberation chamber’ method.....	105
4.2.2.2	Setup of the calculation for the ‘virtual reverberation chamber’ method	107
4.2.3	Reverberant room Modeling (Frequency Domain).....	110
5.	ACOUSTIC MEASUREMENTS.....	112
5.1	SETUP OF ACOUSTIC MEASUREMENTS.....	113
5.1.1	Impulse Response Measurements	113
5.1.2	Impulse Response Measurement Techniques.....	114
5.1.3	Choice of Measurement technique.....	115
5.1.4	Maximum Length Sequence (MLS) Measurement Technique.....	116
5.1.5	Calibration of the loudspeaker	118
5.1.6	Calibration of the Microphone.....	120
5.2	IMPLEMENTATIONS	121
5.2.1	Reverberant room Measurements.....	121
5.2.2	Reverberant room with Absorptive Material Measurements	124
6.	COMPARISON OF FEM MODELING AND MEASUREMENTS.....	128

6.1	IMPULSE RESPONSES, FREQUENCY RESPONSES AND ACOUSTIC PARAMETERS	129
6.1.1	Impulse Response.....	129
6.1.1.1	Probable causes for differences between measured and calculated impulse responses.....	131
6.1.2	Frequency responses- Cumulative Spectral Decays.....	133
6.1.3	Acoustic parameters.....	136
6.1.4	Application of the TDFEM in real life rooms.....	138
6.2	ABSORPTION COEFFICIENT OF ACOUSTIC MATERIAL.....	139
6.2.1	Absorption Coefficient.....	139
6.2.2	Applications for a 'virtual' reverberation chamber.....	140
6.3	EIGENFREQUENCIES-EIGENMODES	141
7.	CONCLUSION AND FUTURE RESEARCH.....	146
7.1	CONCLUSIONS	147
7.2	FUTURE WORK.....	149
8.	APPENDIX.....	152
8.1	DERIVATION OF THE FEM FORMULATION VIA THE PRINCIPLE OF MINIMUM POTENTIAL ENERGY	152
9.	BIBLIOGRAPHY.....	156

LIST OF FIGURES

Figure 2-1 Sound pressure acting on a small volume.....	15
Figure 2-2 Medium flow through a small volume.....	16
Figure 2-3 Boundary conditions [28].....	22
Figure 2-4 Impulse Response of a room	31
Figure 2-5 Linear Time Invariant System	32
Figure 2-6 Relationship between Impulse Response and Frequency Response...	32
Figure 2-7 Cumulative Spectral Decay of a room	35
Figure 2-8 Energy decay curve for a sound that is switched off in time $t=0$	38
Figure 2-9 Energy Decay Curve of an actual Room	39
Figure 2-10 Interaction of sound waves with a surface [68].....	45
Figure 3-1 Examples of elements in two and three dimensions	58
Figure 3-2 Tetrahedral Finite Element in Cartesian coordinates	61
Figure 3-3 Tetrahedral Finite Element in a Transformed Coordinate system	62
Figure 4-1 Spectrum of Gaussian Pulse Point Source.....	74
Figure 4-2 Gaussian Pulse Point Source in small time increments (2d)	75
Figure 4-3 Gaussian Pulse Point Source in small time increments (3d)	76
Figure 4-4 Dependence of the Absorption Coefficient of Materials to the angle of incidence (Materials with different Impedances) [127].....	79
Figure 4-5 Gaussian Pulse Point Source in small time increments within a room with reflective walls (2d).....	80

Figure 4-6 Gaussian Pulse Point Source in small time increments within a room with all walls reflective but the right which is fully absorptive (2d).....	81
Figure 4-7 Gaussian Pulse Point Source in small time increments within a room with all walls reflective but the right which is lightly absorptive (2d).....	82
Figure 4-8 Comparison of the same moment in time of a room with all reflective walls, a room with all walls but right reflective (right wall absorptive) and a room with all walls reflective but right (right wall lightly absorptive)	83
Figure 4-9 Acoustic Pressure of a room with reflective walls.....	84
Figure 4-10 Acoustic Pressure in a room with absorptive walls (t=0 sec to t=0.6 sec).....	88
Figure 4-11 Impulse Response (Point 1).....	89
Figure 4-12 Impulse Response (Point 2).....	89
Figure 4-13 Impulse Response (Point 3).....	89
Figure 4-14 Comparison of the Impulse Responses.....	90
Figure 4-15 2d space dimensions and Points	90
Figure 4-16 Impulse Response calculations in a 3d space with different meshes (Mesh 1,2: $\lambda/h < 5$, mesh 3: $\lambda/h = 5$, mesh 4: $\lambda/h > 5$)	93
Figure 4-17 Impulse Response calculations in a 3d space with different meshes (Mesh 1: $\lambda/h < 3$, mesh 2: $\lambda/h = 3$)	95
Figure 4-18 Comparison of the Impulse Responses for different meshes (Gray: Mesh 1, $\lambda/h < 3$, Black: mesh 2, $\lambda/h = 3$)	95
Figure 4-19 Lagrange 2nd order tetrahedron element [103]	100
Figure 4-20 Reverberant room with computed points.....	104
Figure 4-21 Meshing of the Reverberant room.....	104

Figure 4-22 Reverberant room with acoustic material	108
Figure 4-23 Placement of Sources (spheres) and Calculation Points (points) ...	109
Figure 4-24 Meshing of the reverberant room with the acoustic material.....	109
Figure 5-1 MLS sequence generation with shift registers	116
Figure 5-2 Dialog box for the measurement of the impulse response using MLS	118
Figure 5-3 Frequency Response for Compensation (Loudspeaker Calibration)	120
Figure 5-4 Reverberant room with measured and computed points.....	123
Figure 5-5 Maximum Length Sequence Impulse Response Measurements.....	124
Figure 5-6 Reverberant room with acoustic material	126
Figure 5-7 Reverberant Room with Acoustic Material	127
Figure 6-1 Measured and Computed Impulse Responses for three points in the Reverberant Room	130
Figure 6-2 Averaged cross-correlation coefficients for Measured and Calculated impulse responses.....	131
Figure 6-3 Measured and Computed Frequency Responses for three points in the reverberant room	134
Figure 6-4 Measured (gray) and Computed (light blue) Cumulative Spectral Decays for three points in the reverberant room.....	135
Figure 6-5 Measured and calculated absorption coefficient of an acoustic panel	140
Figure 6-6 Absolute error and percent error for measured and calculated absorption coefficient of an acoustic panel	140

Figure 6-7 Eigen frequencies, Eigen modes and Sound Pressure Levels in the Reverberant Room	142
Figure 6-8 Calculated frequency responses for three measurement points in the reverberant room	143
Figure 6-9 Isosurface for Eigenfrequency 110.47 Hz	144
Figure 6-10 Isosurface for Eigenfrequency 123.49 Hz.....	145
Figure 6-11 Isosurfaces for Eigenfrequency 169.2 Hz	145

LIST OF TABLES

Table 2-1 Overview of General Room Acoustical Parameters (ISO 3382)	37
Table 4-1 Shape functions for Lagrange 2nd order three dimensional element [103].....	101
Table 4-2 Source Placement and Points of Calculation.....	110
Table 5-1 Average Measured Reverberation times, standard deviations and average absorption coefficients of room surfaces	123
Table 5-2 Reverberant Room Conditions	126
Table 5-3 Receiving and Source Points	126
Table 6-1 Measured and calculated Reverberation Time of the reverberant space	136
Table 6-2 Measured and calculated Early Decay Time of the reverberant space	136
Table 6-3 Measured and calculated Clarity of the reverberant space.....	137
Table 6-4 Measured and calculated Definition of the reverberant space.....	137
Table 6-5 Averages of measured and calculated acoustic parameters.....	137
Table 6-6 Analytical, FEM (Helmholtz) and TDFEM Eigen frequencies for the reverberant room	143

ABBREVIATIONS

Acronym	Meaning
AFT	Advancing Front Technique
BEM	Boundary Element Method
BiCGStab	BiConjugate Gradient Stabilized
CFL	Courant–Friedrichs–Lewy
CIP	Constrained Interpolation Profile
EDT	Early Decay Time
FDM	Finite Difference Method
FEA	Finite Element Analysis
FEM	Finite Element Method
FFT	Fast Fourier Transform
FGMRES	Flexible Generalized Minimum RESidual)
GMRES	Generalized Minimum RESidual
IIR	Infinite Impulse Response
IR	Impulse Response
IRS	Inverse Repeated Sequence
LEE	Linearized Euler Equation
LSS	Logarithmic Sine Swip
LTI	Linear Time Invariant
MLS	Maximum Length Sequence
MUMPS	MUltifrontal Massively Parallel sparse direct Solver
ODE	Ordinary Differential Equation
PARDISO	PARallel Sparse DIrect SOLver
PDE	Partial Differential Equation
PML	Perfectly Matched Layer
QRD	Quadratic Residue Diffuser
RASTI	Rapid Speech Transmission Index

RT	Reverberation Time
SPL	Sound Pressure Level
STI	Speech Transmission Index
TDBEM	Time Domain Boundary Element Method
TDFDM	Time Domain Finite Difference Method
TDFEM	Time Domain Finite Element Method
TDFVM	Time Domain Finite Volume Method

Chapter 1

1. INTRODUCTION



The acoustics of rooms, music halls, public spaces, schools, as well as the outside environment is an area of significant importance. Computational acoustic simulation can help to predict and adjust the acoustical characteristics of spaces prior to their manufacturing. With the consistent progress of computer technology, computational acoustic simulation has become a popular, indispensable, and powerful tool for sound design of architectural and urban spaces. There are many expectations for a variety of applications for prediction of room acoustics and noise propagation, development of acoustic materials and optimization of sound environments. At present and in the near future computational acoustics will be widely used in the fields of architectural acoustics, environmental acoustics and noise control.

Especially room Impulse Response (IR) modeling has been a subject of interest to acousticians for many years. The room impulse response is the output of the space when presented with a brief input signal, called an impulse. With the calculation of the room impulse response the majority of the acoustic parameters that define a space can be derived. Almost all the acoustic parameters that can be measured in an area can result from the impulse response. Indicatively we can mention the Reverberation Time, Early Decay Time, Clarity, Speech Transmission Index as well as the Frequency Response and the Cumulative Spectral Decay of a space. Hence the acoustic behavior of an existing space is known if the impulse response is known. Similarly we can predict the acoustic behavior of a space prior of its construction if we are able to model the acoustic space and calculate the impulse response. Therefore the importance of the theoretical calculation of the impulse response of a room is significant.

On a commercial scale, mainly for large spaces, acoustic parameters and the impulse response are calculated by applying principles of Statistical and especially Geometric Acoustics. Geometric acoustics is a branch of acoustics that studies propagation of sound on the basis of the concept of rays considered as lines propagating acoustic energy. Geometric acoustics is widely used in modeling room impulse responses because it is relatively easy to implement and provides good results in the mid and high frequency range. A short review of Geometric along with Statistical acoustics will be presented in the next chapter. Although these methods are helpful especially for practical application stages, they cannot adequately predict the impulse response of a space where the dimensions are such that they are affected by wave phenomena (e.g. standing waves). Wave based considerations are required for most rooms within the lower frequency range where the wave phenomena are eminent. Hence a wave acoustics approach is necessary for an accurate calculation of the impulse response and acoustic parameters of a space. The wave equation governs any sound field and a room's impulse response is given by solving the wave equation with appropriate boundary conditions. For a wide range of frequencies within the audible range the wave phenomena greatly affect the correct prediction of the impulse response.

Wave methods are based on the numerical solution of the wave equation. Methods such as the Finite Element Method, Boundary Element Method (BEM) and Finite Difference Method (FDM) have many applications on the field of acoustics. Wave-based acoustic simulation techniques are steadily increasing their practicality and applicability in real life problems. With the rapid progress of computer technology wave based methods will become even more applicable for conducting acoustical investigations and carrying out design processes. Various applications of wave-based simulations are expected to be executed effectively. These methods enable us to investigate the sound fields in far more detail than Geometrical Acoustics. Of specific interest is the area of room acoustic simulation. The Finite Element Method has shown that it has the potential to be the most prominent method in the field of room acoustics. For this reason it seemed prudent to undertake a study of the Finite Element Method in the field of room acoustics for measuring the impulse response and acoustics parameters of a space.

1.1 PROJECT SCOPE AND RESEARCH METHODS

While there are many applications of the finite element method in the field of acoustics, few researchers have addressed the problem of calculating the impulse response and the derived acoustic parameters by applying the method in the time domain for room acoustics applications [8, 9]. Hence the goal of this investigation became trying to find out the applicability of the Time Domain Finite Element Method in the field of room acoustics. The main purpose of this thesis is to research a TDFEM that can derive accurately the impulse response and acoustic parameters of a room. A method that is practical and has little error compared with the actual measured results. This dissertation aims to address the discrepancies found when comparing the modeled and the measured room impulse responses. A goal of this thesis is to better match the modeled and the measured room impulse responses and to better understand why the simulations and the measurements of the room impulse responses may differ

even for simple cases like small reverberant rooms. Moreover this thesis will attempt to predict and solve problems that may arise in its implementation in real life rooms.

For this purpose, a methodology for acoustic analysis with finite elements in the time domain is proposed. The first step of this work is the theoretical calculation of the impulse response of an existing reverberant space with the finite element method. We develop a methodology for resolving the most crucial elements of an accurate method: source selection, correct modeling of walls, time step-time scales, finite element meshes, modeling of acoustic material and time stepping method. The impulse responses of the reverberant space were measured with the Maximum Length Sequence (MLS) technique and compared with the computed ones. With the help of simulations the numerical accuracy of the finite elements in acoustic analysis was tested. Acoustic parameters such as Reverberation Time, Early Decay Time, Clarity and Definition were extracted from the impulse responses along with the Cumulative Spectral Decays and Frequency Responses and compared with measured ones.

On the second part of the thesis a utilization of the time domain finite element method is presented. The theoretical capability of calculating the impulse response and consecutively the room reverberation time provides the ability of theoretical calculation of the absorption coefficient of an acoustic panel. A virtual replication of the reverberation chamber method that is used for the measurement of the absorption coefficient of materials was performed. A reverberation chamber is an acoustic space that is used for the measurement of absorption characteristics of acoustic materials. The process was carried out for the theoretical calculation of the reverberation time of a reverberant room, with and without a test specimen. Then the absorption coefficient was calculated from the differences both for measured and calculated results. The application of this method is useful for calculation of the acoustic behavior of materials prior to their manufacture and prediction of the influence of the shape of the absorption material. This method will help in the development and optimization of acoustic panels.

1.2 THESIS STRUCTURE

The thesis is divided into six main chapters: Elements of Acoustics, Finite Element Method in Acoustics and Formulations, Setup of Finite Element Method and Implementations, Acoustic Measurements, Comparison of Finite Element Method Modeling and Measurements and finally Conclusion and Future Work.

The chapter of Elements of Acoustics contains the necessary background information required to contextualize the extent of this research problem. The relevant theoretical fundamentals of Acoustics are presented in four parts: basic quantities, wave acoustics and equations, impulse and frequency response and finally acoustic parameters and absorption coefficient.

The chapter of the Finite Element Method, Acoustics and Formulations provides an introduction of the finite element method, a literature review of the applications of the Finite Element Method and the TDFEM in Acoustics, the basic steps of the method and the finite element formulation for the solution of the wave equation that was used for this thesis.

The Setup of Finite Element Method and Implementations includes the steps that were taken into account for the development of an accurate method such as source selection, correct modeling of walls, time step-time scales, finite element meshes, modeling of acoustic material and the time stepping method. Detailed setup of implementations of the method is presented for different cases.

The Acoustic Measurements chapter contains details about the actual measurements in a reverberant space such as the selection of the measurement method, speaker calibration, microphone calibration and application of ISO 354. Detailed setup of implementation of the measurements is presented for different cases.

Comparison of Finite Element Method Modeling and Measurements present the findings of the previous sections, comparison of theoretical and experimental results as well with discussion of the results.

Finally the conclusions of the thesis are summarized in chapter 7. Also many avenues for future research are identified.

An additional finite element formulation of the wave equation is presented in the Appendix, followed by the Bibliography.

Chapter 2

2. ELEMENTS OF ACOUSTICS



The chapter of Elements of Acoustics contains the necessary background information in the field of acoustics required to contextualize the extent of this thesis. It is divided into four subsections which are: Basic Sound Field Quantities, Wave Acoustics and Equations, Impulse and Frequency Response and finally the Acoustics Parameters and Absorption Coefficient. The Basic Sound Field Quantities section presents the quantities that will be used and calculated throughout this thesis. The section of Wave Acoustics and Equations contains necessary information about the wave and the Helmholtz equation. Especially different forms of the wave equation will be presented and discussed. Impulse and Frequency response section presents the importance and utilization of the impulse response in the field of acoustics. Finally the Acoustic parameters and Absorption Coefficient section presents the parameters and the absorption coefficient that were calculated, measured and compared in this thesis.

2.1 BASIC SOUND FIELD QUANTITIES

Acoustics as a science may be defined as the generation, transmission, and reception of energy as vibrational waves in matter [10]. The phenomenon of sound in a medium essentially involves time-dependent changes of density, with which are associated time-dependent changes of pressure, temperature and positions of the fluid particles [11]. Hence, sound can be defined as mechanical disturbance due to particle movement in a medium. The most common medium for sound propagation is air. Sound can also propagate to other media mediums such as water, metal, wood etc.

The sensation of sound is the most familiar acoustic phenomenon. For the average young person, the mechanical disturbance due to particle movement in air is interpreted as sound if the frequency content is between 20 Hz to 20,000 Hz. However, in a broader sense acoustics also includes the ultrasonic frequencies above 20,000 Hz and the infrasonic frequencies below 20 Hz.

Elasticity is an important characteristic of a medium necessary for transmitting sound and is a common property of gases, liquids, and solid-state materials. When the molecules in an elastic medium are displaced from their normal configurations, an internal restoring force arises. A force proportional to the displacement acts on the molecules to restore them to their original position. The particles then are set in vibratory motion and an elastic wave will be propagated through the medium. The wave propagates at a speed that depends on the elastic properties of the medium. It is this elastic restoring force, coupled with the inertia of the system that enables matter to participate in oscillatory vibrations and thereby generate and transmit acoustic waves.

The waves transmitted in air are longitudinal, since fluids cannot exhibit shear motion. Longitudinal waves are characterized by the oscillation of the wave motion being in the direction of the wave propagation. Examples include the simple sinusoidal vibrations produced by a tuning fork which are then transported through air, complex vibrations generated by a bowed violin string

and oscillations of a speaker cone. For this thesis we shall consider longitudinal waves in air.

2.1.1 Sound Pressure

Sound pressure is particularly important for the field of acoustics. Sound pressure or acoustic pressure is the local pressure deviation from the ambient (average, or equilibrium) atmospheric pressure, caused by a sound wave. The deflection of the molecules results in varying the local medium density and pressure from its equilibrium level [12]. Sound pressure is measured in pascals [Pa], which has a dimension $[N/m^2]$. The total pressure p_T at certain location is:

$$p_T = p_0 + p \quad (2-1)$$

where:

- p_T Total pressure at a certain location
- p_0 Static pressure or Equilibrium pressure
- p Sound pressure

The static pressure at a point in the medium is the pressure that would exist at that point with no sound waves present. At normal barometric pressure, p_0 equals approximately 10^5 Pa. Standard atmospheric pressure is usually taken to be 0.760 m Hg at 0°C. This is a pressure of 101 325 Pa. In this thesis we shall assume $p_0=10^5$ Pa.

The sound pressure caused by the propagating disturbance is the most important and useful quantity in acoustics. The perception of sound is caused by the sound pressure acting on the eardrum. The acoustic properties of spaces depend on the spatial and temporal distribution of sound pressure. Since the sound pressure is a scalar quantity, it can be contained in equations that have no vectors. The static pressure and density in the atmosphere is quite larger than the acoustic pressure transmitted by waves in air. Even some of the loudest sounds generated (e.g., close to a jet engine) produce pressure fluctuations that are of the order of 100 Pa, while in everyday life, acoustic pressure fluctuations

vary in their magnitude from about 10^{-5} Pa (about the smallest sound that can be detected) to around 1 Pa (typical of the pressure fluctuations generated in a noisy workshop).

The acoustic pressure is often symbolized by a logarithmic scale. Main reason for that is the extremely large range of acoustic pressure and the practicality of this approach. Sound pressure levels (SPLs) L_p in decibel (dB) are formed by the following equation:

$$L_p = 20 \log \frac{p_{rms}}{p_{ref}} \quad (2-2)$$

where $p_{ref} = 2 \cdot 10^{-5}$ Pa is the internationally standardized reference value for sound waves in the air. The p_{rms} is the square root of the arithmetic mean of the squares of the acoustic pressure.

2.1.2 Density, Particle Velocity, Particle Displacement

The air that surrounds us consist of tiny molecules which are about 0.33 nm in diameter, but are 3.3 nm apart, so they only occupy 0.1% of the space. Even so, at room temperature, a cubic meter weighs 1.18 kg [13]. Due to the fluctuations of the sound pressure, the medium density also varies. The total density ρ_t is then equal to:

$$\rho_T = \rho_0 + \rho \quad (2-3)$$

where:

- ρ_T Total density at a certain location
- ρ_0 Static density or Equilibrium density
- ρ Density increment due to the sound pressure

The ambient density of air is given by the formula:

$$\rho_0 = \frac{p_0}{287 \cdot T} \text{ Kg/m}^3 \quad (2-4)$$

T is the absolute temperature and p_0 is the static pressure. At a normal room temperature of $T=295^0$ K (22^0 C or 71.6^0 F), and for a static pressure $p_0=10^5$ Pa, the ambient density is $\rho_0= 1.18$ kg/m³ [14]. This value of ρ_0 will be used in this thesis unless otherwise stated.

The particles or molecules of the media vibrate with a particle velocity \vec{u} and particle displacement \vec{s} . These vectors are related as:

$$\vec{u} = \frac{\partial \vec{s}}{\partial t} \quad (2-5)$$

$$\vec{s} = \int_t \vec{u} \cdot dt \quad (2-6)$$

2.1.3 Speed of sound

The speed of sound is the distance travelled per unit time by a sound wave as it propagates through an elastic medium. The speed c of the fluctuations in the medium is a vector quantity. In many equations it is used as a scalar when the magnitude of the sound speed is needed. The propagation direction of this vector is perpendicular to the wave fronts. These are surfaces of the equal wave phase. The sound speed direction denotes the direction of energy propagation.

The speed of sound depends on several nonacoustic quantities. Temperature is the most common one which is associated. The international ISO 9613 [15] standard provides details for precise calculation of c . One of the significant effects on c has the medium temperature as given for air by:

$$c = 343.2 \sqrt{\frac{273.15 + T_{\circ C}}{293.15}} \text{ m/s} \quad (2-7)$$

Where T_c is the medium temperature in centigrade. As the earlier equation reveals, the speed of sound for 20°C is 343.2 m/s or 1,235 km/h. The constant 373.15 K is the absolute temperature of 0°C in Kelvin degrees. The speed has a weak dependence on frequency in air. In general we assume that the speed of sound is the same for every frequency. The speed of sound travels most slowly in gases has higher values in liquids and the highest in solids.

2.1.4 Impedance

The acoustic impedance at a given surface Z_A is defined as the complex ratio of sound pressure averaged over the surface to volume velocity through it [16]. The surface may be either a hypothetical surface in an acoustic medium or the moving surface of a mechanical device. The SI unit of acoustic impedance is the newton second per cubic meter ($N \cdot s/m^3$) or the rayl per square meter ($rayl/m^2$).

$$Z_A = \frac{p}{U} \quad (2-8)$$

The specific acoustic impedance Z_s is the complex ratio of the sound pressure at a point of an acoustic medium or mechanical device to the particle velocity at that point. The SI unit of specific acoustic impedance is the pascal second per meter ($Pa \cdot s/m$) or the rayl. That is:

$$Z_s = \frac{p}{u} \quad (2-9)$$

The characteristic impedance (r_0c) is the ratio of the effective sound pressure at a given point to the effective particle velocity at that point in a free, plane, progressive sound wave. It is equal to the product of the density of the medium times the speed of sound in the medium (r_0c). The unit is Newtons/m³ or rayls.

2.2 WAVE ACOUSTICS AND EQUATIONS

There are three main modeling approaches in acoustics that can be used to describe the complicated sound fields in spaces, which may be termed Wave acoustics, Geometrical acoustics, and Statistical (or Energy) acoustics. Wave acoustic is the most rigorous one and it is based on solutions of the wave equation. Geometrical acoustics is a simpler approach to modeling room acoustics and involves study of the propagation of sound rays throughout a room. Statistical acoustics discusses the acoustical properties of spaces in terms of the energy flow.

Modeling of a sound field as a discrete system is the goal for wave based acoustic analysis. Modeling can be performed in the frequency or the time domain. Wave acoustic modeling is essential especially in the low frequency range where the acoustic wavelength is comparable to the space dimensions. The reason for that is that wave interference that causes resonances in the room dominates the acoustic field. When using the wave equation, issues having to do with diffraction, diffusion, and reflections are automatically handled since the phenomena are assessed from a fundamental perspective without using geometrical simplifications.

Solving the wave equation allows for precise calculation of the acoustic pressure at any point in space. Appropriate boundary conditions and physical properties of the medium have to be defined. The materials that comprise the surfaces of a room can be defined in terms of their acoustic impedance. An analytical or a numerical approach can be used for solving the wave equation. High expectations have been placed for the field of wave acoustics for present and near future for solving problems that could not be resolved in the past.

2.2.1 Derivation of the wave equation

Wave equation dictates the propagation of acoustic waves through a medium. The form of the equation is a second order partial differential equation. The wave equation describes the evolution of acoustic pressure that was defined in

the previous chapter as a function of space and time. Presentation of the derivation of the wave equation allows for a better understanding of its different forms and allows for appropriate application for different cases.

The following derivation of the wave equation requires several things [17]:

- The medium is considered to be at rest.
- The sound pressure must be small enough compared to the static pressure for the medium to be considered linear. In practice, the maximum sound pressure is assumed to be less than 0.001 times the static pressure.
- There can be no heat exchange within the medium; that is, no heat flows into or away from the volume element. The process is said to be adiabatic.
- There should be no losses in the medium. The medium does not exhibit viscosity or other phenomena leading to damping.
- The medium is homogenous—the effects of gravitation are not considered.

Basic laws of mechanics and thermodynamics are applied for this derivation of the wave equation. Sound pressure, density, particle velocity, temperature and basic equations are going to be utilized and combined into one equation, the wave equation.

2.2.1.1 Euler's equation

The derivation for a one dimensional sound field will be presented. The waves and the medium particles will be considered to oscillate in one direction. At this point, we will not consider the generator of the field but will concentrate on the mathematical relationship in the free field [18]. Figure 2-1 shows a very small portion of the sound field of cross section S and length dx .

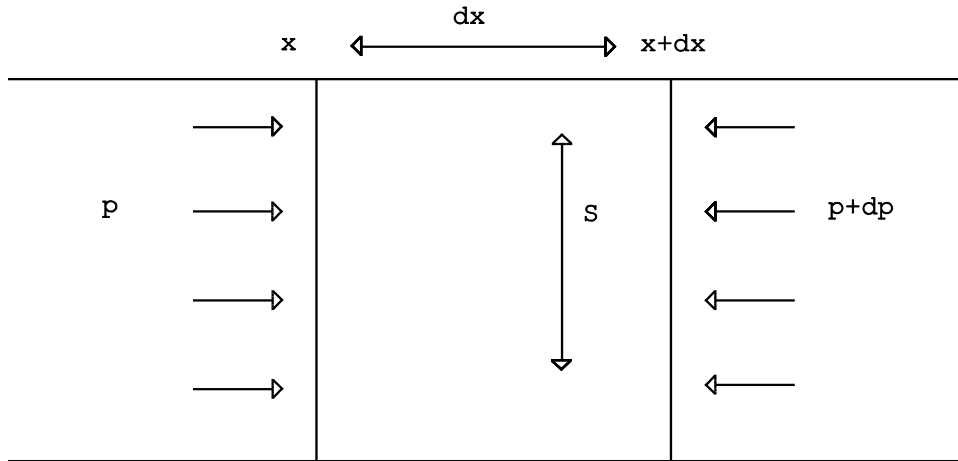


Figure 2-1 Sound pressure acting on a small volume

The two sides are considered perpendicular to the direction of the sound propagation. Different forces are applied to the sides so that the resulting force is equal to their differences:

$$S[p(x) - p(x + dx)] = -S \frac{\partial p}{\partial x} dx = F \quad (2-10)$$

For the next step Newton's law for force is used $F = m(du/dt)$. For the volume element the total mass is $m = (\rho + \delta)Sdx$ including the density change due to the sound δ . The Lagrangian description of acceleration is changed into an Eulerian using the equation:

$$\frac{du}{dt} = \frac{\partial u}{\partial t} + \frac{\partial u}{\partial x} \frac{\partial u}{\partial t} \approx \frac{\partial u}{\partial t} \quad (2-11)$$

The second term in this equation is much smaller than the first term [19] and is neglected so that Equation 2-9 becomes linear. We substitute into Equation 2-8:

$$-\frac{\partial p}{\partial x} = \rho_t \frac{\partial u}{\partial t} \quad (2-12)$$

This is the Euler's equation. It presents the relationship between the sound pressure and the particle velocity. Its main use is in the calculation of the particle

velocity u from the acoustic pressure p . The first term in Equation 2-10 is a part of the 3D gradient operator, that is:

$$\text{grad} \equiv \nabla = \frac{\partial}{\partial x} i + \frac{\partial}{\partial y} j + \frac{\partial}{\partial z} k \quad (2-13)$$

Equation (2-11) for a 3D field is:

$$\text{grad} p = -\rho_t \frac{\partial \vec{u}}{\partial t} \quad (2-14)$$

2.2.1.2 Equation of continuity

For this step the flux of the medium is going to be examined. The flux is defined by the product of medium density and velocity inside the considered volume at x in dt . This is shown in figure 2-2 where the flux moves into and out of a small volume element. The product of medium density and velocity defines the flux at position x in dt . It is given by:

$$S \rho_t(x) u(x) dt \quad (2-15)$$

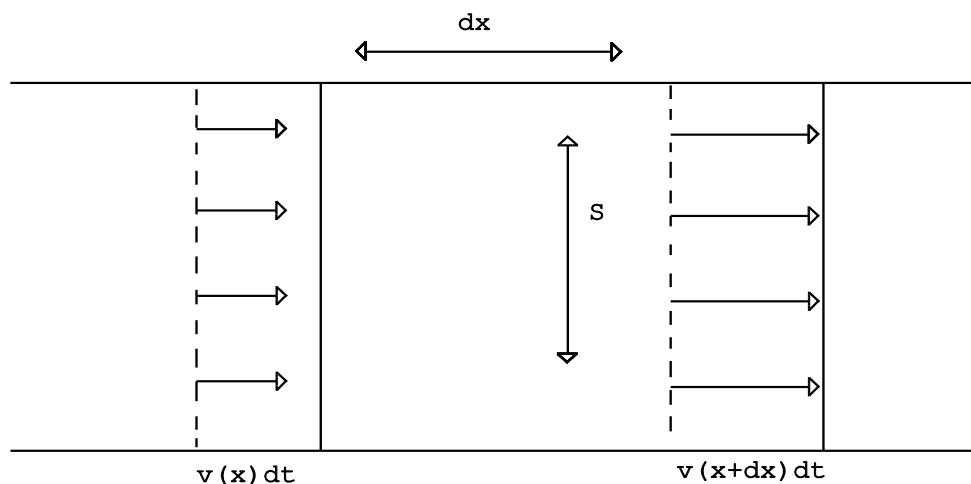


Figure 2-2 Medium flow through a small volume

The flux going through S at $x + dx$ is

$$\begin{aligned} S\rho_t(x + dx)u(x + dx)dt &= S\left[\rho_t(x) + \frac{\partial\rho_t}{\partial x}dx\right]\left[u(x) + \frac{\partial u}{\partial x}dx\right]dt \\ &= S\left[\rho_t u + \frac{\partial(\rho_t u)}{\partial x}dx + \frac{\partial\rho_t}{\partial x}\frac{\partial u}{\partial x}(dx)^2\right]dt \end{aligned} \quad (2-16)$$

For equation 2-14 the last term can be considered small so it will be neglected.

The medium flow from the volume now becomes:

$$S[\rho_t(x)u(x) - \rho_t(x + dx)u(x + dx)]dt = -S\frac{\partial(\rho_t u)}{\partial x}dxdt \quad (2-17)$$

The medium flow from the small volume is equal to the change of the matter $(\partial\rho_t/\partial t)dtSdx$. This now can be formulated by the equation of continuity:

$$\frac{\partial(\rho_t u)}{\partial x} = -\frac{\partial\rho_t}{\partial t} \quad (2-18)$$

The particle velocity in the earlier equation is an x component of the velocity vector $\vec{u} = \vec{u}_x i + \vec{u}_y i + \vec{u}_z i$. To proceed with the earlier equation, we will use the *div* operator:

$$div\vec{u} = \frac{\partial u_x}{\partial x} + \frac{\partial u_y}{\partial y} + \frac{\partial u_z}{\partial z} \quad (2-19)$$

The equation of continuity can now be written in the following form:

$$div\vec{u} = -\frac{1}{\rho c^2}\frac{\partial p}{\partial t} \quad (2-20)$$

2.2.1.3 Thermodynamic Law and Wave Equation

The sound field can be considered to consist of small volumes. Some volumes have positive acoustic pressure which results in an increased gas density and slightly higher temperature. Other volumes have negative acoustic pressure which results in a decreased gas density and slightly lower temperature. The temperature and density changes alternate very fast and hence it can be considered that there is no time for the heat to flow between those areas. This process can be called adiabatic.

For an adiabatic process, the relationship between the sound pressure and the density is given by $p = c^2\rho$ [20], where c is a constant equal to the speed of sound. We substitute in Equation 2-16 for ρ in $\partial\rho/\partial t$ and obtain for the equation of continuity and Euler's equation:

$$-\rho \frac{\partial u}{\partial x} = \frac{1}{c^2} \frac{\partial p}{\partial t} \quad (2-21)$$

$$-\frac{\partial p}{\partial x} = \rho_t \frac{\partial u}{\partial t} \quad (2-22)$$

We can combine the two equations after deriving the first equation by x and the second by t and making the mixed terms equal. We obtain:

$$\frac{\partial^2 p}{\partial x^2} - \frac{1}{c^2} \frac{\partial^2 p}{\partial t^2} = 0 \quad (2-23)$$

This is the one dimensional wave equation. There is not a source term in the equation so it applies for sound pressure-free waves. A similar equation can also be derived for acoustic quantities such as particle velocity and density. It is a fundamental equation that provides the spatial and temporal distributions of acoustic pressure.

In order to apply the equation in 3D problems, we replace $\partial^2 p / \partial x^2$ by a 3D Laplace operator Δ for a desired coordinate system. In Cartesian coordinates, the wave equation takes the form:

$$\Delta p - \frac{1}{c^2} \frac{\partial^2 p}{\partial t^2} = 0 \quad (2-24)$$

The equation states that the acoustic pressure at any given point in space must behave in such a way to ensure that the second derivative of the pressure fluctuation with respect to time is related to the second derivatives of the pressure fluctuation with respect to the three spatial coordinates [21]. Therefore this form of the equation does not require the existence of some form of source.

2.2.2 Other Forms of the Wave Equation

The classical wave equation derived in the previous section describes linear, non-dissipative sound wave waves in a homogeneous steady medium at rest without the presence of a sound source. In reality the wave equation can have many forms. Campo's comprehensive review gathered all forms of the wave equation [22, 23]. He stated that an extension of the classical wave equation may be required if any of the following four restrictions is lifted:

- linearity, i.e., perturbations of the mean state with small slope;
- neglect of dissipation, e.g., by shear and bulk viscosity and thermal conduction;
- steady homogeneous medium, e.g., medium with properties, such as mass density and/or sound speed dependent on position, inhomogeneous and/or on time unsteady
- medium at rest or in nonuniform motion, nonuniform flows, e.g., potential or vortical.

In the context of this thesis in the field of acoustics, the forms of the wave equation that are going to be presented and are relevant with this study, are the linearized inhomogeneous wave equation and the lossy wave equation.

2.2.2.1 Linearized inhomogeneous wave equation

The classical or linearized wave equation was previously derived on the assumption that the fluid element had no exchanges of heat or fluid mass. Also that it was not subject to any sound sources or external forces. The solutions of the equation therefore represent forms of sound waves that can exist, but tells us nothing about possible causes of their existence [24]. As a next step we proceed by modifying the linearized equation of mass conservation. The displacement of fluid volume is allowed hence the effect of sound sources can be included. For this reason the equation of motion and the equation of continuity that were combined for the formulation of the wave equation have to be modified.

Euler's equation does not require any extension. However, the equation of continuity that describes the fluid flux will be amended by a term ρQ that expresses generated mass per unit of volume flow Q [25]. The dimension of Q is $[\text{m}^3/\text{s}]$. The equation of continuity extended and modified, is:

$$\rho_0 \text{div} \vec{u} = -\frac{\partial p}{\partial t} + \rho_0 Q = \frac{1}{c^2} \frac{\partial p}{\partial t} + \rho_0 Q \quad (2-25)$$

We also need Euler's equation for three dimensions:

$$\text{grad} p = -\rho \frac{\partial \vec{u}}{\partial t} \quad (2-26)$$

In order to obtain the wave equation for the sound pressure, we eliminate from the earlier equations \vec{u} and obtain

$$\Delta p - \frac{1}{c^2} \frac{\partial^2 p}{\partial t^2} = -\rho_0 \frac{dQ}{dt} \quad (2-27)$$

Volume velocity of the source is represented by the right side of equation 2-25. External sources can be applied to the equation such as vibrating surfaces, musical instruments and loudspeakers. The sound radiation of a dodecahedral loudspeaker that was used for this thesis can also be applied with the use of this equation. An analytical solution to the inhomogeneous wave equation can be found in Lamb[26].

This linearized inhomogeneous wave equation is the form of the wave equation that will be used in the finite element method formulation of this thesis.

2.2.2.2 Lossy wave equation for propagation of sound in fluids

For the linearized wave equation and the linearized inhomogeneous wave equation that was presented before we assumed that there is no loss due to absorption of the medium. In reality when a sound source operates inside a room, the acoustic field which is created is governed not only by the absorbing characteristics of the boundaries but also by the absorption of the air filling the space.

In order to account for the effect of viscosity of the medium the Navier-Stokes equations must be used for the derivation of the lossy wave equation. For the general case the lossy wave equation which accounts also for the losses of the medium takes the following form [27]:

$$\begin{aligned} \nabla \left(\frac{1}{\rho_0} \nabla p \right) - \frac{1}{\rho_0 c^2} \frac{\partial^2 p}{\partial t^2} + \nabla \left[\frac{4\mu}{3\rho_0} \nabla \left(\frac{1}{\rho_0 c^2} \frac{\partial p}{\partial x} \right) \right] \\ = -\frac{\partial}{\partial t} \left(\frac{Q}{\rho_0} \right) + \nabla \left[\frac{4\mu}{3\rho_0} \nabla \left(\frac{Q}{\rho_0} \right) \right] \end{aligned} \quad (2-28)$$

where

c = speed of sound in fluid medium ($\sqrt{K/\rho_0}$)

K = bulk modulus of fluid

μ = dynamic viscosity

We can assume that the losses from the medium for the frequency range of this thesis (low frequencies) are negligible. However, if we want to apply wave acoustics at higher frequencies, we must also take into account the losses of the medium. In that case we must use the lossy wave equation for propagation of sound in fluids. The same equation should be utilized if we want to use wave acoustics for another medium, e.g. water.

2.2.3 Boundary conditions

The wave equation must be associated with boundary conditions. For that reason Neumann, Dirichlet or Robin conditions are assigned. These acoustic boundaries apply in the case of room acoustics where the domain is an enclosed space. In exterior problems where sound is radiated in unbounded media, the Sommerfeld radiation condition must be utilized. This condition ensures that the wave amplitude vanishes at infinity. A review of boundary conditions for the field of Acoustics can be found in Atalla [28].

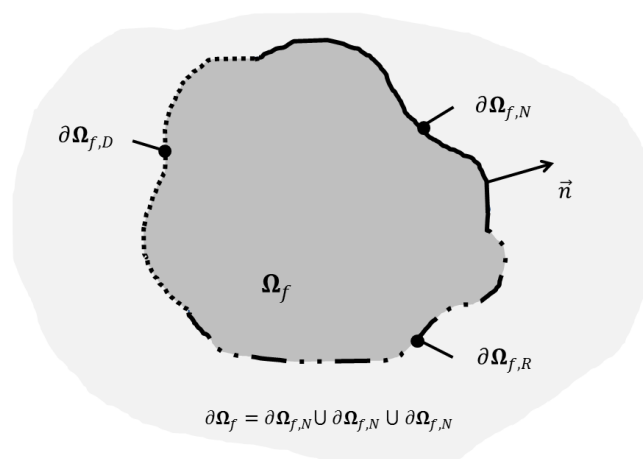


Figure 2-3 Boundary conditions [28]

2.2.3.1 Dirichlet boundary condition

Dirichlet boundary condition is also called the fixed boundary condition or first type condition. In mathematics when imposed on an ordinary or a partial differential equation, it specifies the values that a solution needs to take along the boundary of the domain. Dirichlet boundary condition on the field of acoustics specify the acoustic pressure on the part $\partial\Omega_{f,D}$ of boundary $\partial\Omega_f$ depicted in figure 2-3 as:

$$p = p_0 \quad (2-29)$$

2.2.3.2 Neumann boundary condition

Neumann boundary condition is also called natural boundary condition or second type boundary condition. In mathematics specifies the values of the derivative of a solution on the boundaries. For the field of acoustics the Neumann boundary condition is specified on the part $\partial\Omega_{f,N}$ of boundary $\partial\Omega_f$ depicted in figure 2-3 as:

$$\vec{n} \nabla p = 0 \quad (2-30)$$

2.2.3.3 Robin or impedance boundary condition

Robin boundary condition is also called third boundary condition. In acoustics it can also called impedance boundary condition. In mathematics when imposed on an ordinary or a partial differential equation, it is a specification of a linear combination of the values of a function and the values of its derivative on the boundary of the domain. For the field of acoustics the Robin boundary condition specifies the acoustic impedance on the part $\partial\Omega_{f,R}$ of boundary $\partial\Omega_f$ [29].

$$Z \frac{\partial p}{\partial n} + j\omega\rho_0 p = 0 \quad (2-31)$$

The symbol $\partial/\partial n$ denotes partial differentiation in the direction of the outward normal to the wall. For this thesis the Robin boundary condition is the one that was applied for the modeling of walls. Values of acoustic impedance can be measured or calculated for the application of the Robin boundary condition.

2.2.4 Helmholtz Equation

Apart from the wave equation, another equally important one in the field of acoustics is the Helmholtz equation named for Hermann von Helmholtz. The Helmholtz equation can result from the wave equation after applying the technique of separation of variables. If we assume that the time dependence of the sound pressure p is proportional to $\exp(j\omega t)$ [30] with ω denoting the angular frequency and $j^2=-1$, the linearized homogeneous equation transforms into the Helmholtz equation [31]:

$$\Delta p + k^2 p = 0 \quad (2-32)$$

where $K = \omega/c$ is the angular wave number. The Helmholtz equation represents a time-independent form of the wave equation. It can be applied to room acoustics or musical acoustics for identifications of resonant frequencies and modes of vibration for acoustic spaces and musical instruments respectively.

2.2.5 Eigenfrequencies, Eigenmodes, Eigenvalues

The Helmholtz equation supplemented by the boundary condition can only be solved for certain discrete values k_n of the angular wavenumber k , so-called eigenvalues. Then each eigenvalue is related to a characteristic angular frequency $\omega_n = ck_n$ and hence to a frequency called the resonant frequency or the eigenfrequency [31]. At resonance, the energy in the room will build up infinitely if there are no losses. This is called an oscillation mode of the room, an

eigenmode, or simply mode [32]. For each eigenfrequency, there is at least one eigenmode. For certain room dimensions, many eigenmodes may have identical eigenfrequencies.

In the common case of a rectangular room that is bounded by three pairs of parallel and rigid walls, the eigenfrequencies of the room are presented from the Eq. 2-33. Expressed in Cartesian coordinates x , y , and z , the room extends from $x = 0$ to $x = L_x$ in the direction of the x axis, from $y = 0$ to $y = L_y$ in y direction, and $z = 0$ to $z = L_z$ in z direction. For rigid walls, where $Z = \infty$, according to Eq. (2-31) the boundary condition transforms into $\partial p / \partial x = 0$ for $x = 0$ and $x = L_x$ along with two similar equations for the y and the z direction. The Helmholtz equation in Cartesian coordinates reads

$$\frac{\partial^2 p}{\partial x^2} + \frac{\partial^2 p}{\partial y^2} + \frac{\partial^2 p}{\partial z^2} + k^2 p = 0 \quad (2-33)$$

Its solutions satisfying the boundary conditions are given by [33]

$$p_{n_x n_y n_z}(x, y, z) = A \cos\left(\frac{n_x \pi x}{L_x}\right) \cos\left(\frac{n_y \pi y}{L_y}\right) \cos\left(\frac{n_z \pi z}{L_z}\right) \quad (2-34)$$

Here A is an arbitrary constant, and n_x , n_y , and n_z are integers. The associated eigenfrequency is

$$f_{n_x n_y n_z} = \frac{c}{2} \sqrt{\left(\frac{n_x}{L_x}\right)^2 + \left(\frac{n_y}{L_y}\right)^2 + \left(\frac{n_z}{L_z}\right)^2} \quad (2-35)$$

If two of n_x , n_y , n_z are zero, the waves are called axial waves because they propagate in the direction of one of the room axes. A wave with the wave fronts perpendicular to one of the room walls is called a tangential wave (tangential to a wall). These waves have one of the wave numbers equal to zero. If none of the wave numbers is a zero, the waves are called oblique waves.

2.2.6 Other modeling approaches

So far in this chapter we have presented elements of the field of wave acoustics where acoustical quantities can be defined as functions of space and time. For now, due to various reasons such as high computational costs, wave acoustics is not used in practical applications in the field of room acoustics. The most common methods that are applied are geometric and statistical acoustics. The statistical approach is the first scientific approach that has been implemented to architectural acoustics and is still in use today for the sake of easy implementation and simplicity. Geometric acoustics is the most widely used method for practical applications. The method provides satisfactory results down to the Schroeder frequency which is going to be presented in a following section (Sec. 2.2.7).

2.2.6.1 Geometrical acoustics

Geometrical acoustics is a conceptually simpler approach for estimating the sound field of a room than wave acoustics. Its basic concept is that it follows energy propagation in a room. It can be considered an energy based approximation and the wave nature of sound is disregarded. Existing software that applies concepts of geometrical acoustics apparently can predict impulse response of concert halls above a frequency limit. This frequency limit is the Schroeder frequency and it will be presented in the next section (Sec. 2.2.7). The method is widely used in practical acoustic design. Two methods are commonly used in geometrical acoustics for prediction of impulse response: the ray tracing method and the mirror image method.

Ray tracing method [34, 35] is based on the use of Fermat's principle that states that a wave travels by the quickest route and, in homogeneous air, sound follows straight lines, thought of as rays. The basis of ray tracing is that the sound power can be modeled as sound rays or particles that carry a part of the total power. A fraction of the power is carried by each ray and is emitted in the acoustic space in a straight line. When the ray reaches a surface or an object it is reflected or scattered. The software that is used emits the rays from different model sources

which emulate real life sources, e.g. monopole source (dodecahedron), loudspeaker source and follow its course in space. A source can be set to emit continuous rays in a large number (1,000–1,000,000) of uniformly spaced radial directions. According to the source the angular distribution of intensity is being specified according to source directivity. It is possible to simulate absorption from the air which is essential especially in the high frequency range since absorption increases with frequency. When a real source emits sound the intensity of the sound is decreased as the square of the distance travelled. In ray tracing modeling the divergence of rays automatically accounts for the decreasing of energy.

An alternative to ray tracing is mirror image method [36, 37]. The basic idea is that mirror images are created as a result of reflection by plane surfaces. Then sound is assumed to arrive from the mirrored sources. When the ray hits a mirror, whether plane or curved, it will be reflected. For a mirror, the incident and reflecting sound as well as the normal to the surface are in the same plane, and the angles of incidence and reflection are equal. When the mirrored copies of the source are established, sound rays can be drawn from the mirror images to the listening position. Mirror image analysis can provide the same result with ray tracing method if a large number of rays are studied.

In large and commercial scale mainly for large spaces, the impulse response is calculated by applying principles of geometric acoustics. The calculated impulse response will typically show some deviation from the actual measurements. The degree of this deviation depends on the acoustic characteristics of the space since geometrical acoustics neglect wave phenomena such as scattering and diffraction. However Schroeder and Antani [38, 39] implemented diffraction modules into simulation software for ray tracing and image sources. Still the method is not sufficient for accessing the acoustic field in the low frequency range below the Schroeder frequency. Nevertheless, the ray tracing method and mirror image method are important practical tools in analyzing the reflection paths of a room since both methods often give sufficient results for practical work in room acoustics.

2.2.6.2 Statistical acoustics

The field of statistical acoustics originated from the work of Sabine [40]. Sabine's empirical equation is still often used for an approximate calculation of reverberation time which is the most important acoustic parameter. Reverberation time is going to be presented in a following section (Sec. 2.4.1). Statistical acoustics, contrary to geometric or wave acoustics does not require utilization of a computer for its application. Through the years statistical acoustics has evolved by acquiring a solid mathematical foundation.

In statistical acoustic the sound field is considered to be diffused. A sound field is said to be diffuse if on average over some time interval the sound intensity (as a vector) in any field point is omnidirectional with constant magnitude for all directions [41]. The intensity of sound, is the time-averaged sound energy that passes through unit cross-sectional area in unit time [42]. The central concept of statistical acoustics is that of a sound field, which is considered to be diffused, consisting of a very large set of statistically unrelated (uncorrelated) elemental plane waves of which the propagation of direction is random with a uniform probability distribution [43]. This implies that there is an equal probability that sound will arrive from any direction[44].In reality the diffuse field model is not well suited to the representation of sound fields in enclosed spaces that are not highly reverberant, that have one or two principal dimensions much greater than other(s) or that have highly non-uniform distributions of sound absorption over the boundaries [45].

2.2.7 Schroeder Frequency

Schroeder frequency can be defined as a cross over frequency in the spectra of an acoustic room. It separates the low frequency area of the room, where separate modes dominate the spectrum, from the high frequency region where modes of the room overlap [46, 47]. A room mode is the characteristic distribution of the sound pressure amplitude of a resonant frequency of the room [31]. Every resonant frequency and hence every mode of a room has a specific bandwidth in the frequency response of the room. The transition is

considered to occur at a modal spacing of around three modes within a given mode's half-power bandwidth. The Schroeder frequency is defined as:

$$f_s = 2000 \sqrt{\frac{RT}{V}} \quad (2-36)$$

where V is the volume of the room and RT is the reverberation time.

The Schroeder frequency allows us to subdivide the room behavior into regions and indicates the techniques that can be used to calculate room response. Above the Schroeder frequency it is possible to analyze the room without having to take into account the behavior of its normal modes. Therefore geometrical or statistical acoustics can be applied. However below the Schroeder frequency these approaches will lead to significant divergences from the actual response of an acoustic space. Wave acoustics is the proper way for calculation of room response below Schroeder frequency.

2.3 IMPULSE AND FREQUENCY RESPONSE

Main motivation of this thesis is the precise calculation of the room impulse response. The frequency response of an acoustic space can be derived directly from the impulse response. Cumulative spectral decay which presents valuable information about the room resonances in the frequency and the time domain can also be extracted from the impulse response. The majority of the acoustic parameters can be calculated from the impulse response as it will be presented in the next section. Finally impulse response provides the ability of auralization of an acoustic space, a property that is particularly important for the field of architectural acoustics.

2.3.1 Impulse Response

The impulse response reveals the acoustic character of a room. It can be defined as the sound pressure as a function of time at the point of interest in the room for an impulsive source at some other point in the room [48].

In the field of room acoustics, the impulse response can be divided into three sections: the direct signal that arrives from the source, early reflections from walls and subsequent reverberation. The direct signal is traveling the most direct path (a straight line from the source to the microphone position) and usually is expected to be the loudest. Sound reflected by the walls is losing energy because of the absorption and arrives later in at lower levels. The subsequent reverberation consists of the large number of reflections to the walls which normally leads to a random signal. As reflected copies of the original sound keep arriving later and later, at lower and lower amplitude levels, they form an exponential decay slope. This reverberation typically looks like something close to a straight line when displayed on a graph with a logarithmic amplitude scale. A typical impulse response of a room where the three sections discussed before are identifiable is presented in figure 2-4.

All these sections contain a large number of information about the characteristics of a room. Except acoustic parameters and frequency responses that will be later discussed, also signal arrival times, direct sound and discrete reflections, decay characteristics, signal to noise ratio, clues about speech intelligibility can be measured. Even room shape and size can be estimated from the impulse response [49].

The impulse response is not only important in the field of room acoustic but also in many other fields. An impulse response is not only the time domain response of an acoustic space (time vs. amplitude) but also for a system in general. System not necessarily needs to be an acoustic space (room, concert hall, sports arena...). It can describe a filter, an equalizer, a loudspeaker, a microphone etc. So a more general definition is necessary. If the input signal to a Linear Time Invariant (LTI) system is the unit-impulse sequence $\delta(t)$, then the output signal is called

the impulse response of the system, $h(t)$. The unit impulse sequence, with only one nonzero value at $t = 0$, is defined as [50]:

$$\delta(t) = \begin{cases} 1 & t = 0 \\ 0 & t \neq 0 \end{cases} \quad (2-37)$$

In order to define a linear system we have to estimate the link between input and output of the system. The link between input $x(t)$ and output $y(t)$ is linear if the concept of superposition applies – i.e. if $y_1(t)$ is the response to $x_1(t)$ and $y_2(t)$ is the response to $x_2(t)$ then the response to $ax_1(t)+bx_2(t)$ is $ay_1(t)+by_2(t)$ [51]. The system is called time invariant if the output does not depend explicitly on time.

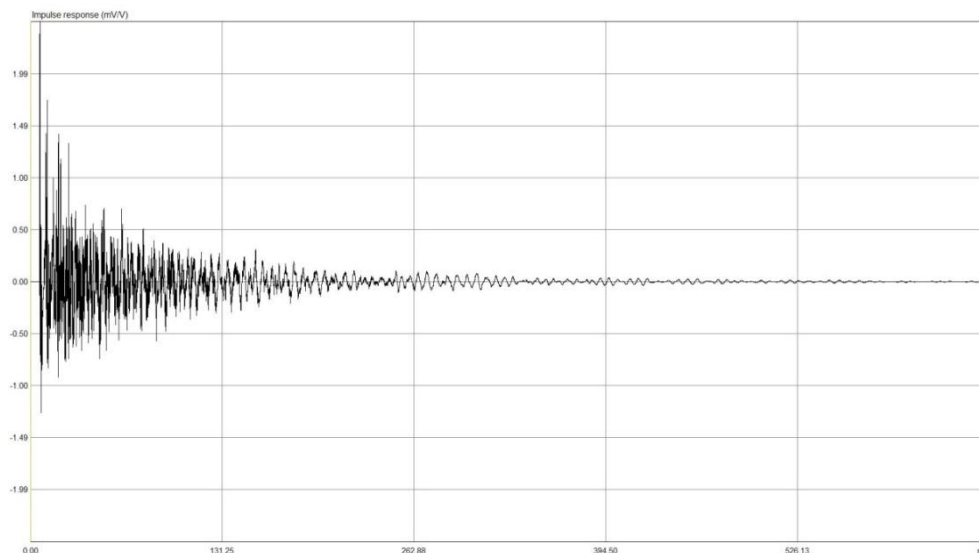


Figure 2-4 Impulse Response of a room

2.3.2 Frequency Response

The time domain behavior of a system (impulse response) can be displayed in the frequency domain as a spectrum and phase (transfer function) [52]. The classical Fourier analysis states that every time signal, with a finite energy, has a corresponding Fourier transform. The basic connection between the time domain and the frequency domain is the Fourier transform, with the following equation which transforms the time signal $h(t)$ into the frequency spectrum $H(f)$ [53].

$$H(f) = \int_{-\infty}^{\infty} h(t)e^{-i\omega t} dt \quad (2-38)$$

In a system analysis we assume that linear time-invariant system is excited with a signal $x(t)$ and on output has signal $y(t)$. Both signals $x(t)$ and $y(t)$ have corresponding Fourier transforms $X(f)$ and $Y(f)$.

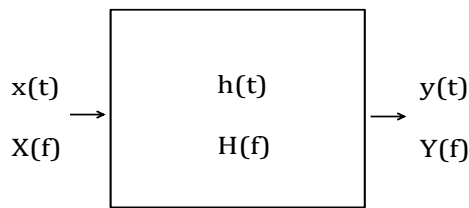


Figure 2-5 Linear Time Invariant System

The relationship between the input and the output of an LTI system, in the frequency domain, can be expressed as:

$$Y(f) = X(f)H(f) \quad (2-39)$$

where complex function $H(f)$ is called a frequency response:

$$H(f) = \frac{Y(f)}{X(f)} = |H(f)|e^{j\phi(f)} \quad (2-40)$$

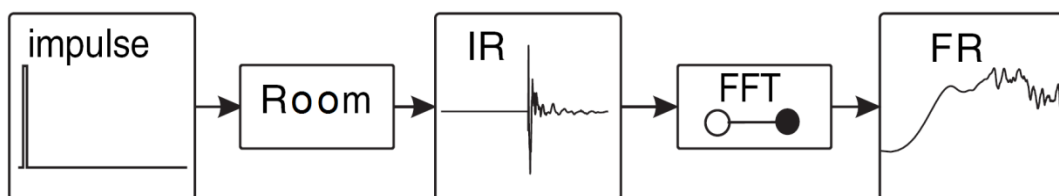


Figure 2-6 Relationship between Impulse Response and Frequency Response

$|H(f)|$ is termed a magnitude response, and $\varphi(f)$ is termed a phase response. The frequency response shows how the system changes the magnitude and phase spectrum of an input signal. The inverse Fourier transform of the frequency response is the impulse response.

The product $X(f)H(f)$ has a Fourier pair in the time domain defined by the convolution $x(t) \otimes h(t)$. This convolution is equal to the output signal $y(t)$:

$$y(t) = x(t) \otimes h(t) = \int_{-\infty}^{\infty} h(\tau)x(t - \tau)d\tau \quad (2-41)$$

It is obvious, as by analyzing the convolution $\delta(t) \otimes x(t)$, we get:

$$h(t) = \int_{-\infty}^{\infty} h(\tau)\delta(t - \tau)d\tau \quad (2-42)$$

The system frequency response is usually estimated by using the input-output cross-spectrum and the input auto-spectrum. By rewriting the expression for the transfer function in the following form:

$$H(f) = \frac{Y(f)}{X(f)} = \frac{Y(f)X^*(f)}{X(f)X^*(f)} = \frac{S_{xy}(f)}{S_{xx}(f)} \quad (2-43)$$

we can get the frequency response by dividing the input-output cross-spectrum with the input autospectrum (star denotes the complex conjugate value) [54]. This equation is usually called H1 estimator.

Fourier transform pairs of the cross-spectrum $S_{xy}(f)$ and the input auto-spectrum $S_{xx}(f)$ are the crosscorrelation $R_{xy}(t)$ and the auto-correlation $R_{xx}(t)$.

Using the H1 estimator for the frequency (and impulse) response estimation is important, as this estimator has good properties in reducing the influence of the

noise and distortions. The preceding theory is valid only for a noiseless environment and for an excitation signal that has infinite duration. In practice we always have some noise present and we can only analyze signals of finite duration.

2.3.3 Cumulative Spectral Decay

The cumulative spectral decay plot offers useful information about the behavior of the room, or for a system. It's basically a frequency response chart, but with the added time element. It shows how the frequency response develops, after the input signal has stopped. In the cumulative spectral decay some frequencies will decay slowly, and will show up on the graph as sustained frequencies in time. This will be an indicative of the room resonances. Since there is an extra axis, the plot will be 3D (waterfall graph).

Cumulative spectral decay is defined by Bunton and Small [55] as a time-frequency function:

$$C(t, \omega) = \int_{-\infty}^{\infty} h(\tau)u_0(\tau - t)e^{-j\omega\tau}d\tau \quad (2-44)$$

where $h(t)$ is the impulse response function and $u_0(t)$ is the unit step function. Theoretically $C(t, \omega)$ is a Fourier transform of the part of impulse response defined from the time t to infinity.

To better understand the significance of this function we multiply $C(t, \omega)$ with $e^{j\omega t}$.

$$C(t, \omega)e^{j\omega t} = \int_{-\infty}^{\infty} h(\tau)u_0(\tau - t)e^{j\omega(t-\tau)}d\tau \quad (2-45)$$

Next, we write the imaginary part of the equation only. We get:

$$|C(t, \omega)| \sin(\omega t + \text{arg}[C(t, \omega)]) = \int_{-\infty}^{\infty} h(\tau) u_0(\tau - t) \sin(\omega(\tau - t)) d\tau \quad (2-46)$$

The integral on the right side is a convolution of the system impulse response $h(t)$ and the excitation function

$$f(t) = u_0(-t)\sin(\omega t) \quad (2-47)$$

which is a sine function that exist for $t < 0$, and is zero from $t \geq 0$. As the linear system response to the sine function is also a sine function we can conclude that $|C(t, \omega)|$ is an envelope of the sine function response, after the excitation has been switched off. By a repeated application of the Fourier transform, each time for a part of an impulse response that is ahead in time by an interval dt , we get the time-frequency function.

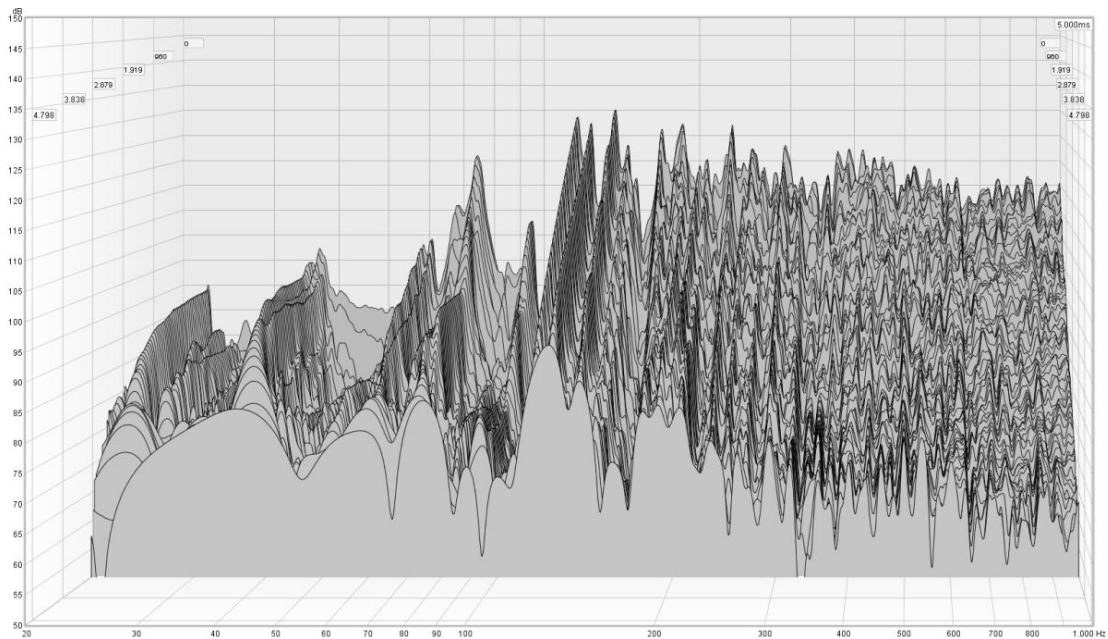


Figure 2-7 Cumulative Spectral Decay of a room

Figure 2-7 depicts a cumulative spectral decay of a typical room for frequencies up to 1000 Hz and for time up to 4 sec. Especially below 200 Hz the resonant frequencies of the room and their decay time can be observed. For this

characteristic, cumulative spectral decays are particularly important in the field of room acoustics and also in the field of loudspeaker design.

2.3.4 Auralization

An important application of calculating the impulse response of an acoustic space is the ability to ‘auralize’ the acoustic field of the particular space. Auralization is a term introduced to be used in analogy with visualization to describe rendering audible (imaginary) sound fields [56]. Architects, sound designers and acoustic engineers can replicate the way sound waves will behave in a structure through the use of computer software [57].

Once the room impulse response for the positions of the source and receiver in the room have been found, these can be appropriately convolved with the head-related impulse functions and with the impulse responses of the sound-reflecting surfaces—the impulse responses of the various reflection coefficients described previously. This yields the binaural room impulse responses. These impulse responses (one for each ear) can be convolved with anechoically recorded sounds such as music or speech. Then one can experience the recordings reproduced in the actual space. The convolution can be done using software in a general purpose computer or by a dedicated hardware convolver.

Auralization has a large number of interesting applications spanning information, education and entertainment. Its role in the near future will be enhanced especially in the field of virtual reality.

2.4 ACOUSTIC PARAMETERS AND ABSORPTION COEFFICIENT

The acoustic behaviour of a room can be characterized by values of acoustic parameters that define the space. The majority of acoustic parameters can be extracted from the impulse response of the space. Depending on the usage of a space e.g. music, speech, theatre, the appropriate acoustic parameters are chosen for the representation of the room.

A common way to estimate room acoustical characteristics is the standard ISO 3382 [58]. The ISO defines several room acoustical parameters as shown in Table 2-1. The standard also defines methods for the estimation of these parameters from the measured impulse response [59].

Quantity Symbol	Subjective Aspect
Reverberation time RT (s)	Reverberance, loudness, involvement
Early decay time EDT (s)	Reverberance, clarity
Clarity C_{80} (dB)	Clarity
Definition D_{50} (%)	Speech definition
Centre time T_s (s)	Clarity
Strength G (dB)	Relative sound level
Lateral energy fraction LF, LFC (%)	Spatial impression
Interaural cross-correlation IACC	Spatial impression

Table 2-1 Overview of General Room Acoustical Parameters (ISO 3382)

2.4.1 Reverberation time - RT

The most important room parameter is the Reverberation Time (RT). It is defined as a time interval required for the sound energy to decay 60 dB after an excitation in the room has stopped [60].

To estimate the reverberation time, measurement of the energy decay curve after the sound source is switched off is necessary. The energy decay curve is usually an irregular curve $r(t)$ that is approximated with a linear decay. The linear decay approximation is useful in the presence of background noise where the time interval required for the sound energy to decay 60 dB can still be calculated, as shown on Fig. 2-8

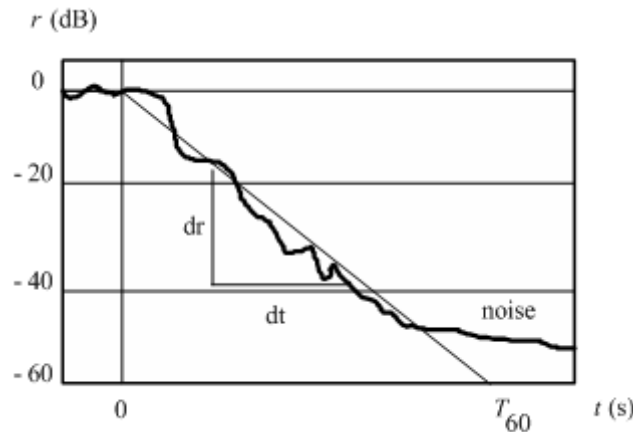


Figure 2-8 Energy decay curve for a sound that is switched off in time $t=0$

The reverberation time is determined from the slope of the estimated linear decay as:

$$RT = 60 \frac{dt}{dr} \quad (2-48)$$

Following the recommendation of the standard ISO3382, the energy decay slope can be estimated by the method of linear regression. The standard defines that measurement of the energy decay curve should be measured in standard octave bands 125Hz to 4kHz., or in third octave bands from 100Hz to 5kHz. The estimation of energy decay curve is obtained by the Schroeder integrated impulse response method [61]. Schroeder has shown by statistical analysis that the room averaged energy decay $r(t)$ can be obtained from the backward integrated squared impulse response $h(t)$:

$$r(t) \approx \int_t^{\infty} h^2(\tau) d\tau \quad (2-49)$$

The Schroeder expression can be used in more practical, normalized logarithmic form:

$$10 \log r(t) = 10 \log \left(\frac{\int_t^{\infty} h^2(t) dt}{\int_0^{\infty} h^2(t) dt} \right) \quad (2-50)$$

Note that in this expression the denominator represents the total energy. A typical energy decay curve of an actual room is depicted in figure 2-9.

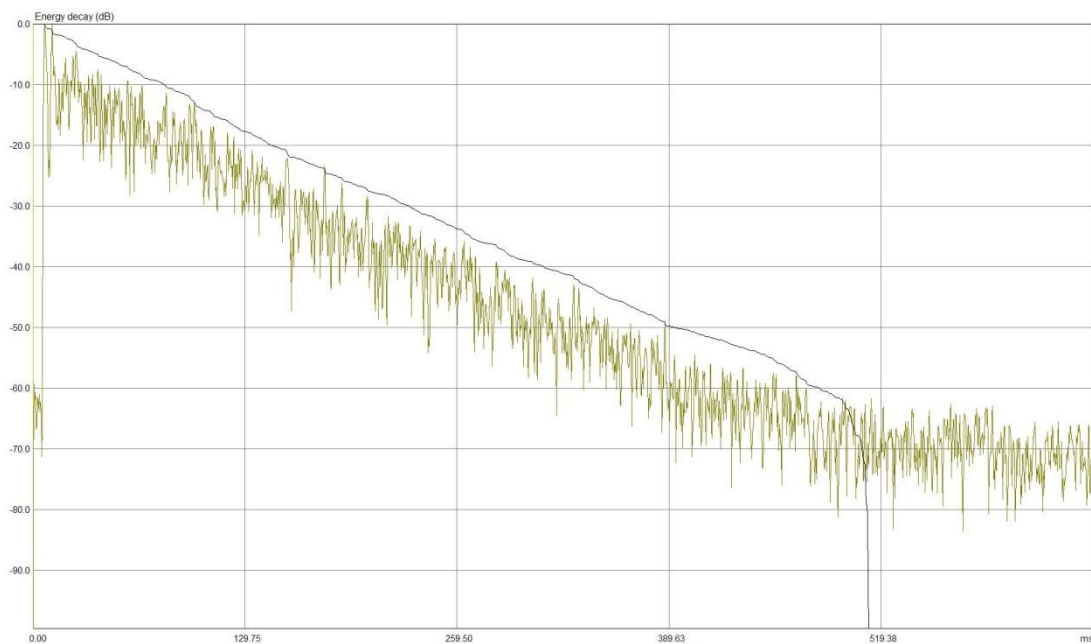


Figure 2-9 Energy Decay Curve of an actual Room

ISO3382 also defines the following notation which is similar to RT and can be used in acoustic measurements:

- T_{30} : reverberation time determined from the average slope of the energy decay curve obtained from part of the decay curve between -5dB and -35dB.
- T_{20} : reverberation time determined from the average slope of the energy decay curve obtained from part of the decay curve between -5dB and -25dB.
- T_{10} : reverberation time determined from the average slope of the energy decay curve obtained from part of the decay curve between -5dB and -15dB.

2.4.2 Early decay time - EDT

Early decay time (EDT) is defined as the time interval required for the sound energy level to decay 10 dB after the excitation has stopped [62]. To enable direct comparison with the reverberation time, the result is multiplied by a factor of 6. For an ideal exponential decay in a diffuse field, the expected value of the EDT equals reverberation time.

Early decay time is correlates better with the human perception of reverberation of a room than the reverberation time [63]. Hence it gives a better subjective evaluation of the reverberation of a room.

2.4.3 Clarity – C80, C50

Clarity or "early to late index" C_{80} (C_{50}) is defined as the logarithmic ratio of an impulse response's energy before time t_e , and its energy after t_e [64]. The value $t_e = 50$ ms is used to express the clarity of speech, whereas $t_e = 80$ ms is better suited for music.

$$C_{80} = 10 \log \frac{\int_0^{80ms} h^2(t) dt}{\int_{80ms}^{\infty} h^2(t) dt} \quad (2-51)$$

$$C_{50} = 10 \log \frac{\int_0^{50ms} h^2(t) dt}{\int_{50ms}^{\infty} h^2(t) dt} \quad (2-52)$$

Original German name for the clarity is "Klarheitsmaß". High values for the clarity indicate a large amount of the early energy, which corresponds to a subjective sensation of the clarity. On the contrary, a low clarity values indicate an unclear, excessively reverberant sound.

Subjectively, acceptable value for C_{80} is -3dB or higher. For a good speech or text intelligibility acceptable value of C_{50} is -2 dB or higher.

2.4.4 Definition - D_{50}

The Definition D_{50} or "early to total sound energy ratio" is a measure of the speech definition [65]. It is also known by its German name Deutlichkeit. It is defined as:

$$D_{50} = 100 \frac{\int_0^{50ms} h^2(t) dt}{\int_0^{\infty} h^2(t) dt} \quad (\%) \quad (2-53)$$

2.4.5 Centre time - T_s

The Centre time T_s corresponds to the centre of gravity of the squared impulse response:

$$T_s = \frac{\int_0^{\infty} t \cdot h^2(t) dt}{\int_0^{\infty} h^2(t) dt} \quad (2-54)$$

The upper integration limits are taken as the truncation point, or the end of the impulse response, according to the noise treatment option specified.

The subscript S in the name T_s stands for the German name “Schwerpunktzeit”. The value of T_s is expressed in milliseconds. Low T_s suggests a sensation of clarity, whereas high T_s suggests a reverberant sound. The centre time is very highly correlated with the EDT [66].

For an ideal system, the expected value of T_s is proportional to the reverberation time RT :

$$T_{s,expected} = \frac{RT}{13.6} \quad (2-55)$$

2.4.6 Strength - G

The sound strength G (or, relative sound level) is defined as the logarithmic ratio of the sound pressure exposure (squared and integrated sound pressure) of the measured impulse response $p(t)$ to that of the response $p_{10}(t)$ measured at a distance of 10m from the same sound source in a free field [67].

$$G = 10 \log_{10} \frac{\int_0^{\infty} p^2(t) dt}{\int_0^{\infty} p_{10}^2(t) dt} = L_{pE} - L_{pE,10} \quad (2-56)$$

Sound exposure is determined for each octave band as;

$$L_{pE} = 10 \log_{10} \frac{1}{T_0} \int_0^{\infty} \left(\frac{p(t)}{p_0} \right)^2 dt \quad (2-57)$$

where $p_0 = 20\text{uPa}$, $T_0 = 1\text{s}$.

The sound source must be omnidirectional, but this requirement is almost impossible to achieve in all frequency bands with real loudspeakers. To account for real loudspeaker directivity pattern, when making the measurement of $L_{pE,10}$ in a free field, or in anechoic room, it is necessary to make the measurement at every $12,5^\circ$ around the sound source and to calculate the energy-mean value of the sound pressure exposure levels in order to average the directivity of the sound source. This can be done by power averaging overlays of octave band smoothed frequency response curves. That curves can be saved (as overlay) and later used to estimate sound strength in different room positions. We get sound strength, or relative sound level, simply by subtracting values of overlay curve from the octave-smoothed frequency response.

The change of G over a distance in a room gives some indication of how diffuse the room's sound field is. The expected value in a room with diffuse sound field theory is given by:

$$G_{expected} = 10 \log \left(\frac{RT}{V} \right) + 45(dB) \quad (2-58)$$

where V is the volume of the room and T is its reverberation time.

2.4.7 Other acoustic parameters

There are many other acoustic parameters than can be calculated with the use of the impulse response. The calculation of these parameters requires the full spectrum measurement of the impulse response rather than octave band as the previous parameters. However, these parameters can be calculated by combining methods such as the finite element method (low frequency range), geometrical acoustics (mid and high frequency range).

IEC-60268-16 standard defines the method for the estimation of speech intelligibility and gives a rating called STI - Speech Transmission Index - that is close to the subjective intelligibility score. The same standard also defines a simplified method for the estimation of speech intelligibility called RASTI - Rapid Speech Transmission Index.

Besides STI ratings for male and female speech, an important parameter of speech intelligibility is $\%AL_{cons}$ (Articulation Loss of Consonants) that has been defined by Peutz experimental work. It is used in architectural acoustics with an equivalent subjective rating.

2.4.8 Absorption coefficient

The absorption coefficient is an important characteristic of acoustic materials. It also defines the absorption characteristics of the surfaces of a space. In this thesis the coefficient was used in the application of the finite element method. Modeling of acoustic boundaries was implemented with utilization of the absorption coefficient of walls. Also the coefficient of an acoustic panel was calculated by using the finite element method. For these reasons a definition of the coefficient follows.

When sound waves interact with real materials the energy contained in the incident wave is reflected, transmitted through the material, and absorbed within the material [68]. For this model the surfaces treated will be assumed

planar. Some curvature is tolerated for as long as the radius of the curvature can be considered large compared to the wavelength of the sound. The energy balance is illustrated in Fig. 2-10.

$$E_i = E_r + E_t + E_a \quad (2-59)$$

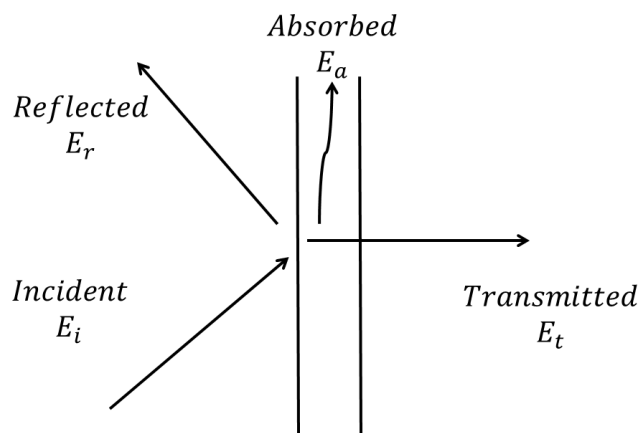


Figure 2-10 Interaction of sound waves with a surface [68]

This model involves the case of the interaction at the boundary of the material. We assume that the differences between absorption (conversion energy to heat) or transmission are not relevant. From the standpoint of the incident size we can assume that both mechanisms are absorptive since energy is not reflected. Because we are only interested in the incident side of the boundary, we can combine the transmitted and absorbed energies. If we divide Eq. (2-59) by E_i ,

$$1 = \frac{E_r}{E_i} + \frac{E_{t+a}}{E_i} \quad (2-60)$$

we can express each energy ratio as a coefficient of reflection or transmission. The fraction of the incident energy that is absorbed (or transmitted) at the surface boundary is the absorption coefficient:

$$a_{\theta} = \frac{E_{t+a}}{E_i} \quad (2-61)$$

Absorption coefficients of materials can be found in standard textbooks such as Kinsler and Frey [69].

Chapter 3

3. FINITE ELEMENT METHOD, ACOUSTICS AND FORMULATIONS



The chapter of Finite Element Method, Acoustics and Formulations is divided into four subsections. Those are: Introduction, Finite Element Method in Acoustics, Basic Steps of Finite Element Method and finally Finite Element Formulation of the Wave Equation. The first subsection serves as a general introduction to the method of finite elements. The section of Finite Element Method in Acoustics presents the method in the field of acoustics. Also, there is a reference to alternative wave based methods used in the field of room acoustics as well a comparison of the methods. The section of Basic Steps of Finite Element Method presents the general steps of the method along with a deeper presentation of the method with particular emphasis in the implementations in the field of acoustics. Finally the Finite Element Formulation of the Wave Equation section presents the formulation of the method that was applied for this thesis.

3.1 INTRODUCTION

The best way to solve any physical problem governed by a differential or partial differential equation is to obtain the analytical solution. Analytical solutions yield the values of a desired unknown quantity. They are given by a mathematical expression and are valid for a number of locations in a physical system, a body or a space. If the phenomenon is modeled using ordinary or partial differential equations, appropriate methods are required for the analytical solutions. Complicated boundaries, geometries and loadings often prevent us from obtaining analytical solutions. Irregularities of boundaries, for example, can be difficult or impossible to describe mathematically. Hence numerical methods, such as the finite element method, have to be employed, to obtain acceptable solutions.

Finite element method is one of the most widespread numerical methods for solving problems in a variety of fields. Typical problem areas of interest that are solvable by use of the finite element method include structural analysis, heat transfer, fluid flow, electromagnetic potential and acoustics. It is applicable to steady-state and time dependent problems as well as problems involving nonlinear material properties. Several mathematical concepts are combined under the finite element method. Finite element method has two primary subdivisions. The first utilizes discrete elements to obtain the joint displacements and member forces of a structural framework. The second uses the continuum elements to obtain approximate solutions to heat transfer, fluid mechanics and solid mechanics problems. The second approach is the true finite element method [70]. However finite element software is capable of solving both types of problems. The name finite element method is often used to denote both the discrete element and the continuum element formulations.

The basic idea of the finite element method is the modeling of a body by dividing it into an equivalent system of smaller bodies. A mesh is formed by dividing the space into a large number of non-overlapping elements, which are subfields of finite extent. The mesh can have an unstructured form in which the elements

can arbitrarily differ in size and position, provided the neighboring elements are hooked in a "compatible" way. This feature facilitates the automatic creation of meshes for arbitrary shapes, which gives great practical value to the method. The method can also be easily applied to objects composed of several different materials and having mixed boundary conditions. After the completion of a mesh instead of solving the problem for the entire body, equations are formulated for each finite element. An approximate solution can be developed for each of these elements. The equations are combined taking care to ensure continuity at the interelement boundaries. All the individual solutions are assembled together to obtain the solution of the whole body. This results in a system of algebraic equations that can be solved with a variety of methods.

For the application of the finite element method many general computer programs have been developed. User-assisting programs that generate a grid from a limited number of shape-defining points are available as well as programs that analyze the results and display them in graphic form for further study. The finite element method is the computational basis of many computer-assisted design programs. Dedicated software has helped widespread usage and dominance of the finite element method in many areas. The finite element method in the field of acoustics is presented in the following section along with alternative competitive methods.

3.2 FINITE ELEMENT METHOD IN ACOUSTICS

This section presents the use and utilization of the finite element method in the field of acoustics. In the end of the subsection the alternative wave based methods of Boundary Element and Finite Difference will be discussed in comparison with the Finite Element method.

3.2.1 Literature review-Applications of the Finite Element Method and the TDFEM in Acoustics

In the field of acoustics the first detailed study of the finite element method was presented by Gladwell in 1965 [71]. In the 1970s it was used for analysis of frequency responses and normal modes in ducts, cavities, and rooms [72, 73] and for optimization of room shape regarding modal distribution in the low frequency range [74]. From the early stage, it has been also applied to vibro-acoustic coupled systems and inhomogeneous sound fields [75, 76], which is currently useful for evaluation of sound insulation, floor impact noise, acoustic materials and components. Research developed to include the influence of sound absorbing materials [76, 77]. Later on the finite element method was used for the acoustic design of passenger car compartment [78, 79].

Because of the emergence of low-cost, high-speed computers finite element method is also being applied in the field of architectural acoustics mainly for estimation of room resonances and reverberation [80-82]. With the recent progress of iterative solvers for linear systems, the application of the finite element method to real life rooms and concert halls is being challenged [83]. Especially for the field of room acoustics some work that has to be mentioned in the field of finite element method and the finite element method in the time domain is the following:

Okuzono et al. [8] proposed a time domain finite element method for the calculation of the impulse response. Newmark time integration method was used and a COCG iterative solver. Also a hexahedral 27-node isoparametric element was used for this study.

Also Okuzono et al. [84] applied an explicit time domain method for room acoustics and compared it with an iterative one that he has previously used. The results showed that for higher impedances of walls the method performed better.

A finite element method was also recently used by Ayr et al [85], for the low frequency qualification of reverberation test rooms .

In his work Vorllander [57] discusses the application of measuring the impulse response in architectural acoustics towards virtual reality application uses.

Noh and Bathe proposed an explicit time integration scheme for the analysis of wave propagations [86]. The application of this scheme in the field of room acoustics seems to be quite promising.

Lam [87] discussed the issues for computer modeling of room acoustics in non-concert hall settings. Among others a good agreement was found between the FEM, BEM and the analytical solution in reverberant rooms.

3.2.2 Alternative Time Domain Methods

Besides FEM, the main time domain methods that can be applied in room acoustics problems are mainly the Boundary Element Method (BEM) and the Finite Difference Method (FDM) that will be discussed in the following subsections. Alternative time-domain methods that may be applied to acoustics are the Linearized Euler Equation (LEE) method, the Constrained Interpolation Profile (CIP) method, and the Time Domain Finite Volume Method (TDFVM). Review of these methods can be found by Oshima et al [88]. The LEE method is applicable to wave propagation phenomena under the influence of arbitrary background flows. The main application of the method is sound propagation simulations outdoors where wind effects are not negligible. The CIP method is characteristic in that the method is in principle free from numerical dispersion. The characteristic allows simulations with high phase accuracy. The TDFVM method is constructed on an unstructured grid system. The method thus has an advantage in modeling complex geometries compared to the TDFDM method where orthogonal structured grid is used.

3.2.2.1 Finite Difference Method in Acoustics

The Finite Difference Method is a numerical method for solving differential equations by approximating them with difference equations. In this approach instead of describing the surface with a mesh (as with the FEM, BEM), a grid is used and the algebraic equations [89] are solved at the points of the grid. Hence the volume of the medium is represented as a mesh of interconnected nodes, and the differential terms of the wave equation are replaced by finite-difference approximations between nodes in space and time. This creates many unknowns, but their interactions are simple and efficient to solve.

For transient phenomena the Time Domain Finite Difference Time Method (TDFDM) is a popular competing algorithm. It is a very efficient method in terms of computational speed and storage while also offering excellent resolution in the time domain. The explicit formulation makes computations efficient, and the computational effort increases linearly with the number of discretization cells. Especially in the field of room acoustics the TDFDM has been used for computing the impulse response in a space. It has been demonstrated [90] that the method can be used to effectively model low-frequency problems in room acoustics simulations.

However, the architectural space boundary shape is simulated by a staircase approximation which is a fundamental disadvantage for the finite difference method. Difficult boundary conditions will result in errors for the method. The room's shape is an important factor in determining acoustic behavior. Results from Sakamoto et al [91] were in good agreement in the middle-frequency bands but in the low-frequency range, large discrepancies were observed because of the difficulties in determining and modeling the boundary conditions. Sakuma states [92] that the simple discretization of the wave equation in which the method has its basis is not sufficient for modeling more complex wave propagation phenomena, high-accuracy simulations, or acoustic fields with complex geometries. Also dispersion is a critical cause for errors for the TDFDM [93].

3.2.2.2 Boundary Element Method in Acoustics

The Boundary Element Method is a numerical computational method for solving linear partial differential equations which have been formulated as integral equations. It can be applied in many areas of engineering and science such as fluid mechanics, fracture mechanics, electromagnetics and wave propagation [94].

In the field of acoustics the BEM is based on Green's theorem, according to which the pressure at a point can be calculated from knowledge of the acoustic conditions at the boundary [95]. The main difference between FEM and BEM is in the requirement in FEM for modeling of a closed acoustic space and its boundary, whereas BEM can be used for an open space and only requires modeling and meshing of the boundary. With the FEM, results are obtained for all nodes, whereas the BEM only gives one point at a time. In both methods, all physical effects such as surface scattering and diffraction are included, provided the boundaries can be correctly described.

Because BEM requires only meshing of the boundary in the case of homogeneous problems it can be said that it can produce a faster solution. Astley [96] states that the question of whether BE or FE methods are the more effective for acoustical computations remains an open one. BEM models that discretize only the bounding surface require fewer degrees of freedom but are nonlocal in space. FE models require many more variables but are local in space and time, which greatly reduces the solution time for the resulting equations. Research from Harati [97] suggests that, for interior problems, finite element methods are more economical on most practical configurations. Davies [98] states that the major advantage of the FEM is that it is significantly further advanced than the BEM and that there is a wide variety of easily available codes.

The general purpose applicability, robustness, mathematical structure and overall flexibility of finite element methods highlight their attractiveness and justify further developments of the methods. The strength of FE models lies in their ability to treat inhomogeneous media and difficult boundary conditions

that may arise in real life room acoustics problems. From all the methods mentioned above only the FEM has become sufficiently inexpensive and simplified in commercial software, for practical application in the field of acoustics.

3.3 BASIC STEPS OF THE FINITE ELEMENT METHOD

This section contains the basic steps of the finite element method. Although the particulars will vary, the implementation of the finite-element approach usually follows a standard step-by-step procedure [99, 100]. The following provides an overview of each of the finite element steps.

3.3.1 Definition of governing equations

Initially we define the problem which usually may be an ordinary differential equation or partial differential equation. In the field of acoustic common problems to be solved include some form of the wave equation (Eq. 2-24) or the Helmholtz equation (Eq.2-32).

For a more general approach to the finite element method let us consider the partial differential equation:

$$L[u(\vec{r})] = f(\vec{r}) \quad (3-1)$$

The PDE is defined in a domain Ω_F . $L[\cdot]$ represents a linear differential operator. $u(\vec{r})$ is the unknown function to be determined and $f(\vec{r})$ is the source function. The basic concept of the finite element method consists of discretizing the continuum problem so that an approximate solution can be found by solving an algebraic system of equations. The next step to that direction is to transform the governing equation into a weak integral formulation.

3.3.2 Weak Integral Formulation

In mathematics the weak formulation is a significant concept for the analysis of ordinary and partial differential equations. Its application allows the transfer of linear algebra concepts for the solution of problems in many fields. An equation after its weak formulation has solutions with respect to certain test functions. The concept of the weak formulation is utilized in the finite element method.

3.3.2.1 Derivation of the Weak Formulation

Derivation of the weak formulation of an ordinary or partial differential equation results from multiplying the equation with a function, called test function. As a next step an integral is applied on both sides of the equation. The test functions play a crucial role in the finite element method. A test function that solves the integral equation is a likely candidate for solving the original PDE or ODE problem.

The divergence theorem by Gauss or Green's formula (also known as integration by parts) can then be applied on second order derivatives. The boundary conditions are significant for the correct implementation of the weak formulation to the problem. The boundary integral is responsible for the correct modeling of the interactions with the surrounding.

Multiplying Eq. 3-1 by a test function $w(\vec{r})$, and integrating over the domain gives the following formulation:

$$\int_{\Omega_F} w(\vec{r}) L[u(\vec{r})] d\Omega = \int_{\Omega_F} w(\vec{r}) f(\vec{r}) d\Omega \quad (3-2)$$

By defining the symbol $(*,*)$ as:

$$(a, b) = \int_{\Omega_F} a(\vec{r}) b(\vec{r}) d\Omega \quad (3-3)$$

Eq. 3-2 can be written as:

$$(L[u], w) = (f, w) \quad (3-4)$$

3.3.2.2 Test Functions - Galerkin's method

There are many possible choices for test functions. More precisely, we consider not only one test function, but a whole class of test functions represented by w where each one corresponds to an equation. Of course, we could never consider all possible test functions as this would result in an infinite amount of equations. In practice, we need a finite number of well-chosen test functions.

A finite element method divides the domain into a mesh. The geometry is divided into a set of smaller volumes — elements. Test functions can then be defined using polynomials on each element. A requirement is that they are non-zero only on a small group of neighboring elements, and zero outside the group. The most common type of polynomials, constructed in this way, is known as Lagrange shape functions.

Galerkin's method uses the same functions that were used in the approximating equation. This approach is the basis of the finite element method for problems expanding in a variety of fields. This method yields the same result as the variational method [101] when applied to differential equations that are self-adjoint. Galerkin's method is used to develop the finite element equations for the field problems discussed in this thesis.

3.3.3 Discretization

This step involves dividing the solution domain into finite elements. A finite element mesh is a partition of a given domain into subdomains, which are called elements, such that every point of the domain is found in one of the elements. The entire domain has to be covered by the elements without overlapping, and the conditions of compatibility between finite elements on the boundary have to be satisfied as well. A finite number of nodes define the topology of each element. They are placed on the vertices, edges or on the surfaces of the elements or even inside them. The finite element method facilitates the use of an unstructured grid in which the elements can arbitrarily vary in size and position, provided the neighboring elements are hooked to a node in a "compatible" way. Locating and numbering of the node points, have to be included as well as specifying their coordinates values. This characteristic of the method gives great practical value and applicability in a variety of fields..

Two-dimensional domains can be discretized into triangular, quadrilateral or a mixture of triangular and quadrilateral elements. Over three-dimensional domains, tetrahedral and hexahedral elements can be used. Also in some cases wedges, pentahedral elements and pyramid elements could also be employed.. Figure 3-1 provides examples of elements employed in two and three dimensions. The points of intersection of the lines that make up the sides of the elements are referred to as nodes and the sides themselves are called nodal lines or planes.

To reduce discretization (numerical) error in a finite element analysis, the quality of the finite element meshes has to be optimized such that the element size is in compliance with the specified nodal spacing and that the shape of the elements ought to be as equilateral as possible. For conforming meshes, the boundary nodes of the finite element mesh have to lie on the boundary surface of the given domain, and for constrained meshes, apart from the geometrical requirements of a conforming mesh, additional topological requirements such as specified edges and faces have to be present in the mesh as well [102].

Furthermore, a higher-order curvilinear element can also be employed to fit domains with curved boundaries to reduce discretization error. More details about mesh creation and mesh requirements in the field of finite element in acoustics especially for the problem encountered in this thesis can be found in section 4.1.4.

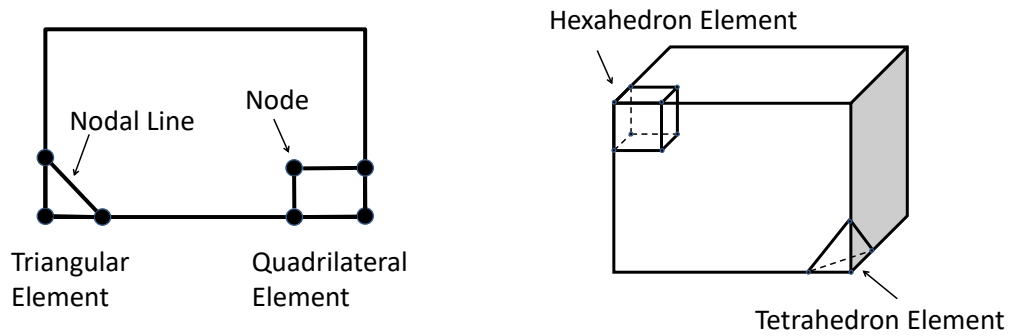


Figure 3-1 Examples of elements in two and three dimensions

For that reason the domain Ω_F is divided in a set of m elements T_1, T_2, \dots, T_m , which do not overlap, hence $\forall i \neq j: T_i \cap T_j = \emptyset$. The mesh now can be represented as:

$$T_h(\Omega_F) = \bigcup_{i=1}^m T_i \quad (3-5)$$

A set of P grid points, the nodes, have to be defined, with each point $p_k \in P$ being described by a global index $k=1,2,\dots,N$, where N is the total number of nodes in the mesh.

3.3.4 Approximation of variables and calculation of elementary matrices

An approximate solution for the unknown function $u(\vec{r})$ now has to be defined. The approximate solution is $u_h(\vec{r})$ and the unknown function $u(\vec{r})$ can be expressed as:

$$u_h(\vec{r}) = \sum_{i=1}^N u_i N_i(\vec{r}) \quad (3-6)$$

where $N_i(\vec{r})$ are the so called shape functions.

Now the approximate solution of Eq.3-4, is determined by the coefficients u_i which represent the value of the unknown function at the node i . At the node i where the point is given by the coordinates \vec{r}_i , the shape functions must satisfy the following conditions:

$$N_j(\vec{r}_i) = \delta_{ij}, \quad i, j = 1, \dots, N \quad (3-7)$$

For the next step we substitute Eq.3-6 into Eq. 3-4. For Galerkin's method we choose as a test function $w = N_j(\vec{r})$. We obtain:

$$\left(L \left[\sum_{i=1}^N u_i N_i \right], N_j \right) = (f, N_j), \quad j = 1, \dots, N \quad (3-8)$$

since $L[\cdot]$ is a linear operator and the coefficients u_i are constants we can write:

$$\sum_{i=1}^N u_i (L[N_i], N_j) = (f, N_j), \quad j = 1, \dots, N \quad (3-9)$$

The previous equation is a linear system of N equations with N unknowns, u_1, u_2, \dots, u_N . Eq.3-9 can now be written in a matrix formation:

$$\mathbf{Ax} = \mathbf{B} \quad (3-10)$$

$\mathbf{A} = (a_{ij})$ is called stiffness matrix. It is given by:

$$\mathbf{A} = (a_{ij}) = (L[N_i], N_j) = \int_{\Omega_F} L[N_i(\vec{r})] N_j(\vec{r}) d\Omega, \quad i, j = 1, \dots, N \quad (3-11)$$

$\mathbf{x} = (u_1, u_2, \dots, u_N)^T$ is the vector of unknown coefficients

$\mathbf{b} = (b_1, b_2, \dots, b_N)^T$ is the load vector given by:

$$b_j = (f, N_j) = \int_{\Omega_F} f(\vec{r}) N_j(\vec{r}) d\Omega, \quad j = 1, \dots, N \quad (3-12)$$

3.3.4.1 Shape functions

As a next step we have to define the shape functions for our formulation. It is common to use polynomials as shape functions for finite element formulations. A common approach for modeling in 3d is the use of tetrahedral. Hence shape functions must be defined for every tetrahedron of the mesh.

Let us consider the tetrahedron in a Cartesian system in the following picture.

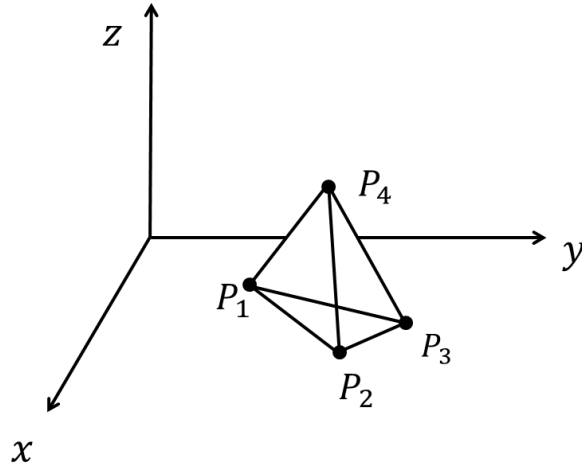


Figure 3-2 Tetrahedral Finite Element in Cartesian coordinates

The shape function of the node i has the following form:

$$N_i(x, y, z) = a_i + b_i x + c_i y + d_i z, \quad i = 1, \dots, 4 \quad (3-13)$$

If we consider the following condition the coefficients a_i, b_i, c_i, d_i can be calculated:

$$N_j(\vec{r}_i) = \delta_{ij}, \quad i, j = 1, \dots, 4 \quad (3-14)$$

For this element a system of four equations and the four coefficients is formed. The same has to be repeated for all the elements so that all the shape functions are determined. The next step is the solution of equation 3-10. This can be achieved after the shape functions have been derived and integrated.

In practice the above calculations are carried by a software implementation usually after a coordinate transformation has been applied. The main reason for this approach is the simplification of the calculations.

A tetrahedron in a transformed coordinate system can be shown in the following figure.

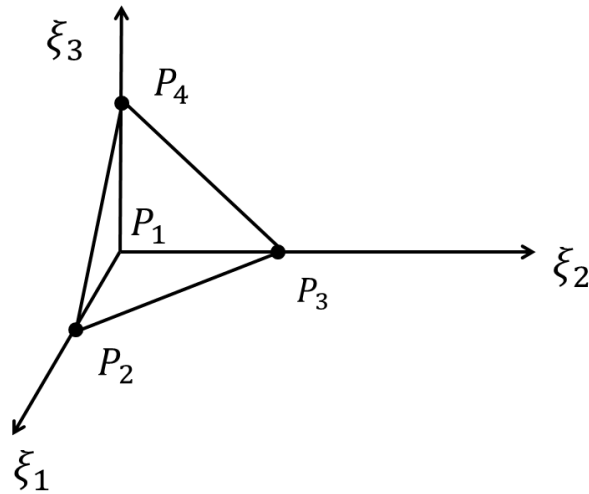


Figure 3-3 Tetrahedral Finite Element in a Transformed Coordinate system

The points in the original Cartesian coordinates (x, y, z) can now be transformed in corresponding points (ξ_1, ξ_2, ξ_3) as follows:

$$\begin{aligned}
 x &= x_1 + (x_2 - x_1)\xi_1 + (x_3 - x_1)\xi_2 + (x_4 - x_1)\xi_3 \\
 y &= y_1 + (y_2 - y_1)\xi_1 + (y_3 - y_1)\xi_2 + (y_4 - y_1)\xi_3 \\
 z &= z_1 + (z_2 - z_1)\xi_1 + (z_3 - z_1)\xi_2 + (z_4 - z_1)\xi_3
 \end{aligned}
 \tag{3-15}$$

The above transformation leads to the Jacobian matrix:

$$\mathbf{J} = \begin{bmatrix} x_2 - x_1 & x_3 - x_1 & x_4 - x_1 \\ y_2 - y_1 & y_3 - y_1 & y_4 - y_1 \\ z_2 - z_1 & z_3 - z_1 & z_4 - z_1 \end{bmatrix}
 \tag{3-16}$$

The new nodal basis functions for the tetrahedron in the transformed coordinate system are now [103]:

$$\begin{aligned}
N_1^t(\xi_1, \xi_2, \xi_3) &= 1 - \xi_1 - \xi_2 - \xi_3 \\
N_2^t(\xi_1, \xi_2, \xi_3) &= \xi_2 \\
N_3^t(\xi_1, \xi_2, \xi_3) &= \xi_3 \\
N_4^t(\xi_1, \xi_2, \xi_3) &= \xi_1
\end{aligned}
\tag{3-17}$$

3.3.5 Assembling – Imposition of constraints

After the individual element equations are derived, they must be linked together or assembled to characterize the unified behavior of the entire system. The assembly process is governed by the concept of continuity. That is, the solutions for contiguous elements are matched so that the unknown values (and sometimes the derivatives) at their common nodes are equivalent. Thus, the total solution will be continuous. When all the individual versions are finally assembled, the entire system is expressed in matrix form.

Before the element equations are assembled, a global numbering scheme must be established to specify the system's topology or spatial layout. This defines the connectivity of the element mesh. Once the topology is specified, the element equation can be written for each element using the global coordinates. Then they can be added one at a time to assemble the total system matrix

Finally the equations must be modified to account for the system's boundary conditions. These adjustments result in the final matrix form ready to be solved.

3.3.6 Solution and convergence study

3.3.6.1 Solution

Solutions of Eq. 3-19 can be obtained with techniques such as *LU* decomposition [104]. In many cases, the elements can be configured so that the resulting equations are banded. Thus, the highly efficient solution schemes available for such systems can be employed.

These quantities are usually related to the derivative of the parameter and include the stress components, and heat flow and fluid velocities.

3.3.6.2 Postprocessing

Upon obtaining a solution, it can be displayed in tabular form or graphically. In addition, secondary variables can be determined and displayed. Although the preceding steps are very general, they are common to most implementations of the finite-element approach.

3.3.6.3 Numerical Error

Finite element solutions of problems that can be encountered in acoustics may have errors [105] compared to the analytical solution. Possible errors that may arise are approximability error and pollution error. Astley [106] states that approximability error is a measure of the best approximation, which can be achieved for a given spatial interpolation while the pollution error is associated with the numerical representation of phase or dispersion.

The approximability error decreases as $(\lambda/h)^{-p}$ where λ is the smaller wavelength of a solution, h is the node spacing and p is the polynomial order of the shape functions. The approximability error will be smaller for higher order elements. Larger values of λ/h are essential for a better finite element method representation. This is achieved with smaller node spacing. An extensive review applicable to this thesis for problems in acoustics is presented in section 4.1.4.

For the finite element method the pollution error depends of the dimensions of the computational domain. For acoustical problems the pollution error is large when the wavelength of the disturbance is small compared to the dimensions of the space. This means that for higher frequencies the pollution error is also higher. The error may not be significant over a single wavelength but it may be accumulate over many wavelengths. This means that the pollution error may vary not only with the value of frequency but also with the size of the computational domain. The overall global error for a finite element solution for the Helmholtz equation takes the form [107]:

$$e \leq C_1 \left(\frac{hk}{2p}\right)^p + C_2 k \left(\frac{hk}{2p}\right)^{2p} \quad (3-18)$$

The first term represents the approximability error, the second the pollution effect. C_1 and C_2 are constants. For three dimensional problems considering the pollution error there are also considerations of element orientation with respect to wave direction.

In general the accuracy of a solution can be refined by two ways. By reducing mesh size for a fixed value of p . This is called h-refinement. The other way is by increasing the order of the elements. This is called p refinement. There are also combinations of the two techniques (h-p refinement). The most common method for better accuracy of solutions in the field of acoustics is the h refinement. Nevertheless higher order spectral elements ($p \sim 5$) have been applied for short wave problems with promising results [108].

3.4 FINITE ELEMENT FORMULATION OF THE WAVE EQUATION

The finite element formulation of the linearized inhomogeneous wave equation is presented [109-111]. This is the equation that will be mainly applied in this thesis.

The finite element formulation is obtained by testing wave Equation 2-25 using the Galerkin method. Equation 2-25 is multiplied by testing function w and integrated over the volume of the domain, which after some manipulation, yields the following:

$$\begin{aligned} \int_{\Omega_F} \frac{1}{\rho_0 c^2} w \frac{\partial^2 p}{\partial t^2} dv + \int_{\Omega_F} \nabla w \left(\frac{1}{\rho_0} \nabla p \right) dv - \int_{\Gamma_F} w \frac{1}{\rho_0} \hat{n} \nabla p ds \\ = \int_{\Omega_F} w \frac{1}{\rho_0} \frac{\partial Q}{\partial t} dv \end{aligned} \quad (3-19)$$

where:

dv = volume differential of acoustic domain Ω_F

ds = surface differential of acoustic domain boundary Γ_F

\hat{n} = outward normal unit vector to the boundary Γ_F

From the equation of momentum conservation, the normal velocity on the boundary of the acoustic domain is given by:

$$\frac{\partial v_{n,F}}{\partial t} = \hat{n} \frac{\partial \vec{v}}{\partial t} = -\frac{1}{\rho_0} \hat{n} \nabla p \quad (3-20)$$

Substituting 3-20 into Equation 3-19 yields the “weak” form of Equation 2-25 given by:

$$\begin{aligned} \int_{\Omega_F} \frac{1}{\rho_0 c^2} w \frac{\partial^2 p}{\partial t^2} dv + \int_{\Omega_F} \nabla w \left(\frac{1}{\rho_0} \nabla p \right) dv + \int_{\Gamma_F} w \frac{\partial v_{n,F}}{\partial t} ds \\ = \int_{\Omega_F} w \frac{1}{\rho_0} \frac{\partial Q}{\partial t} dv \end{aligned} \quad (3-21)$$

The normal acceleration of the fluid particle can be presented using the normal displacement of the fluid particle, given by:

$$\frac{\partial v_{n,F}}{\partial t} = \hat{n} \frac{\partial^2 \vec{u}_F}{\partial t^2} \quad (3-22)$$

where:

\vec{u}_F = the displacement of fluid particle

After using equation 3-22, equation 3-21 is expressed as:

$$\begin{aligned} \int_{\Omega_F} \frac{1}{\rho_0 c^2} w \frac{\partial^2 p}{\partial t^2} dv + \int_{\Omega_F} \nabla w \left(\frac{1}{\rho_0} \nabla p \right) dv + \int_{\Gamma_F} w \hat{n} \frac{\partial^2 \vec{u}_F}{\partial t^2} ds \\ = \int_{\Omega_F} w \frac{1}{\rho_0} \frac{\partial Q}{\partial t} dv \end{aligned} \quad (3-23)$$

3.4.1 Derivation of Acoustic Matrices

Equation 3-23 contains the fluid pressure p and the structural displacement components $u_{x,F}$, $u_{y,F}$, and $u_{z,F}$ as the dependent variables to solve. The finite

element approximating shape functions for the spatial variation of the pressure and displacement components are given by:

$$P = \{N\}^T \{P_e\} \quad (3-24)$$

$$u = \{N'\}^T \{u_e\} \quad (3-25)$$

where:

$\{N\}$ = element shape function for pressure

$\{N'\}$ = element shape function for displacements

$\{P_e\}$ = nodal pressure vector

$\{u_e\} = \{u_{xe}\}, \{u_{ye}\}, \{u_{ze}\}$ = nodal displacement component vectors

From equation 3-24 and 3-25, the second time derivative of the variables and the virtual change in the pressure can be expressed as follows:

$$\frac{\partial^2 P}{\partial t^2} = \{N\}^T \{\ddot{P}_e\} \quad (3-26)$$

$$\frac{\partial^2}{\partial t^2} \{u\} = \{N'\}^T \{\ddot{u}_e\} \quad (3-27)$$

$$\delta P = \{N\}^T \{\delta P_e\} \quad (3-28)$$

After substituting Equation 3-24 and 3-25 into Equation 3-23, the finite element statement of the wave Equation is expressed as:

$$\begin{aligned}
& \int_{\Omega_F} \frac{1}{\rho_0 c^2} \{N\} \{N\}^T dv \{\ddot{p}_e\} + \int_{\Omega_F} \frac{1}{\rho_0} [\nabla N]^T [\nabla N] dv \{p_e\} \\
& + \int_{\Gamma_F} \{N\} \{n\}^T \{N'\}^T ds \{\ddot{u}_{e,F}\} = \int_{\Omega_F} \frac{1}{\rho_0} \{N\} \{N\}^T dv \{\dot{q}\}
\end{aligned} \tag{3-29}$$

where:

$\{n\}$ =outward normal vector at the fluid boundary

$\{\dot{q}\}$ = the first time derivative of nodal mass source vector

Equation 3-29 can be written in matrix notation to create the following discretized wave equation:

$$[M_F] \{\ddot{p}_e\} + [K_F] \{p_e\} + \bar{\rho}_0 [R]^T \{\ddot{u}_{e,F}\} = \{f_F\} \tag{3-30}$$

where:

$$[M_F] = \bar{\rho}_0 \int_{\Omega_F} \frac{1}{\rho_0 c^2} \{N\} \{N\}^T dv = \text{acoustic fluid mass matrix}$$

$$[K_F] = \bar{\rho}_0 \int_{\Omega_F} \frac{1}{\rho_0} [\nabla N]^T [\nabla N] dv = \text{acoustic fluid stiffness matrix}$$

$$[R]^T = \int_{\Gamma_F} \{N\} \{n\}^T \{N'\}^T ds = \text{acoustic fluid boundary matrix}$$

$$\{f_F\} = \bar{\rho}_0 \int_{\Omega_F} \frac{1}{\rho_0} \{N\} \{N\}^T dv = \text{acoustic fluid load vector}$$

3.4.2 Acoustic Boundary Conditions

The Robin boundary condition on impedance boundary Γ_Z is given by:

$$v_{n,F}(\vec{r}) - v_{n,S}(\vec{r}) = Y(\vec{r})p(\vec{r}) \quad (3-31)$$

where:

$v_{n,F}(\vec{r})$ = normal velocity of fluid particle on the boundary

$v_{n,S}(\vec{r})$ = normal velocity of structure surface

Y = boundary admittance

Z (boundary impedance) = $1/Y$

Substituting Equation 3-31 into Equation 3-21 yields:

$$\int_{\Gamma_Z} w \frac{\partial v_{n,F}}{\partial t} ds = \int_{\Gamma_Z} w \left(Y \frac{\partial p}{\partial t} + \frac{\partial v_{n,F}}{\partial t} \right) ds \quad (3-32)$$

The matrix forms in are rewritten with a damping matrix:

$$[C_F] = \bar{\rho}_0 \int_{\Gamma_Z} Y \{N\} \{N\}^T ds \quad (3-33)$$

The acoustic fluid load vector is now:

$$\{f_F\} = \bar{\rho}_0 \int_{\Omega_F} \frac{1}{\rho_0} \{N\} \{N\}^T dv - \bar{\rho}_0 \int_{\Gamma_Z} \{N\} \{N\}^T ds \{ \dot{v}_{n,S} \} \quad (3-34)$$

More on the setup of the finite element method will be presented in the next section of this thesis. Alternative formulation of the finite element method based on the principle of minimum potential energy can be found in the Appendix.

Chapter 4

4. SETUP OF THE FINITE ELEMENT METHOD AND IMPLEMENTATIONS



The practical application of the finite element method, especially in the time domain, is the subject of this chapter. The method will also be applied in the frequency domain (finite element method for the Helmholtz equation). This chapter has two sections: the setup of the time domain finite element method and the implementation in three different cases. For the setup of the finite element method in the time domain, many considerations had to be taken into account for the right implementation of the method. Those were the proper selection of source, the accurate representation of the impedances of walls, the time scales, the finite element meshes, the stepping method, the modeling of the acoustic material, the solver and the type of elements. The method was implemented in the cases of a reverberant room and in a reverberant room with acoustic panels. Finally the finite element method (Helmholtz equation) was implemented in a reverberant room for the calculation of eigenfrequencies and eigenmodes.

4.1 SETUP OF THE FINITE ELEMENT METHOD

4.1.1 Source selection

For the calculation of the impulse response a sound source which is omnidirectional is needed. Also the use of a source with a finite frequency band is necessary since large frequency content may cause problems in the application of the finite element method due to frequency artifacts. For that reason the use of an initial pulse with high frequency content was not selected from the beginning of the study. The methods that were considered were a gaussian pulse point source and a filtered impulse with an Infinite Impulse Response (IIR) filter (Butterworth type band pass filter) that was used in similar studies [8, 112]. The gaussian pulse point source was selected due to superior characteristics in the time domain and ease of implementation. Gaussian pulse point source was also used in similar studies for the time domain modeling of room acoustics with the application of the time domain finite difference method [113-115].

4.1.1.1 Gaussian Pulse Point Source

A Gaussian Pulse point source was used in this study. The source is omnidirectional as can be seen in Figures 4-2 and 4-3 in 2d and 3d domain respectively. A Gaussian time profile is defined in terms of its amplitude A , its frequency bandwidth f_0 , and the pulse peak time t_p [116-118]. The spectrum of the pulse is similar to a low pass filter with the frequency bandwidth easily adjusted by controlling the width of the pulse. Hence the frequency bandwidth is limited so no frequency artifacts can be created for the finite element utilization of the source. The well-defined Fourier transform pair of the time signature and frequency spectrum equations also allows easy interpretation and postprocessing of the result. Considerations have to be made for the correct placement of the Gaussian source away from absorbing boundaries due to scattering effects [118].

The governing equations (Eq 4-1) were implemented in the Finite Element Analysis. Figure 4-1 shows the spectrum of the Gaussian Pulse Point Source. The non-linear frequency characteristics of the source were taken into consideration for the correct application of the method.

$$Q = -A2\pi^2 f_0^2 (t - t_p) e^{-\pi^2 f_0^2 (t - t_p)^2}$$

$$t_p - \frac{1}{f_0} < t < t_p + \frac{1}{f_0}$$
(4-1)

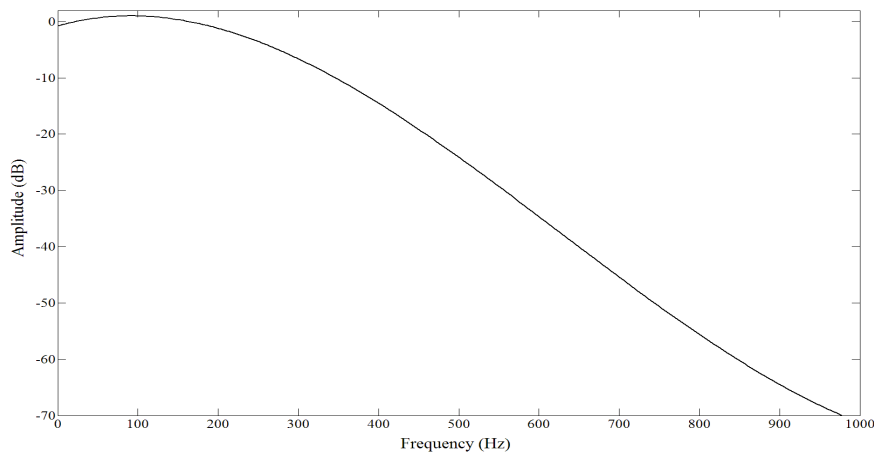


Figure 4-1 Spectrum of Gaussian Pulse Point Source

In figures 4-2 and 4-3, a Gaussian Pulse Point source is presented in small time increments (0.005 sec) for a 2d and a 3d space respectively. We can observe how the acoustic pressure spreads in space having the speed of the sound. The wave front is spherical. As expected, the amplitude of the acoustic pressure decreases as the pulse moves away from its original position. The same can be observed for the 2d and 3d depiction. The interaction with boundaries is presented in the following section.

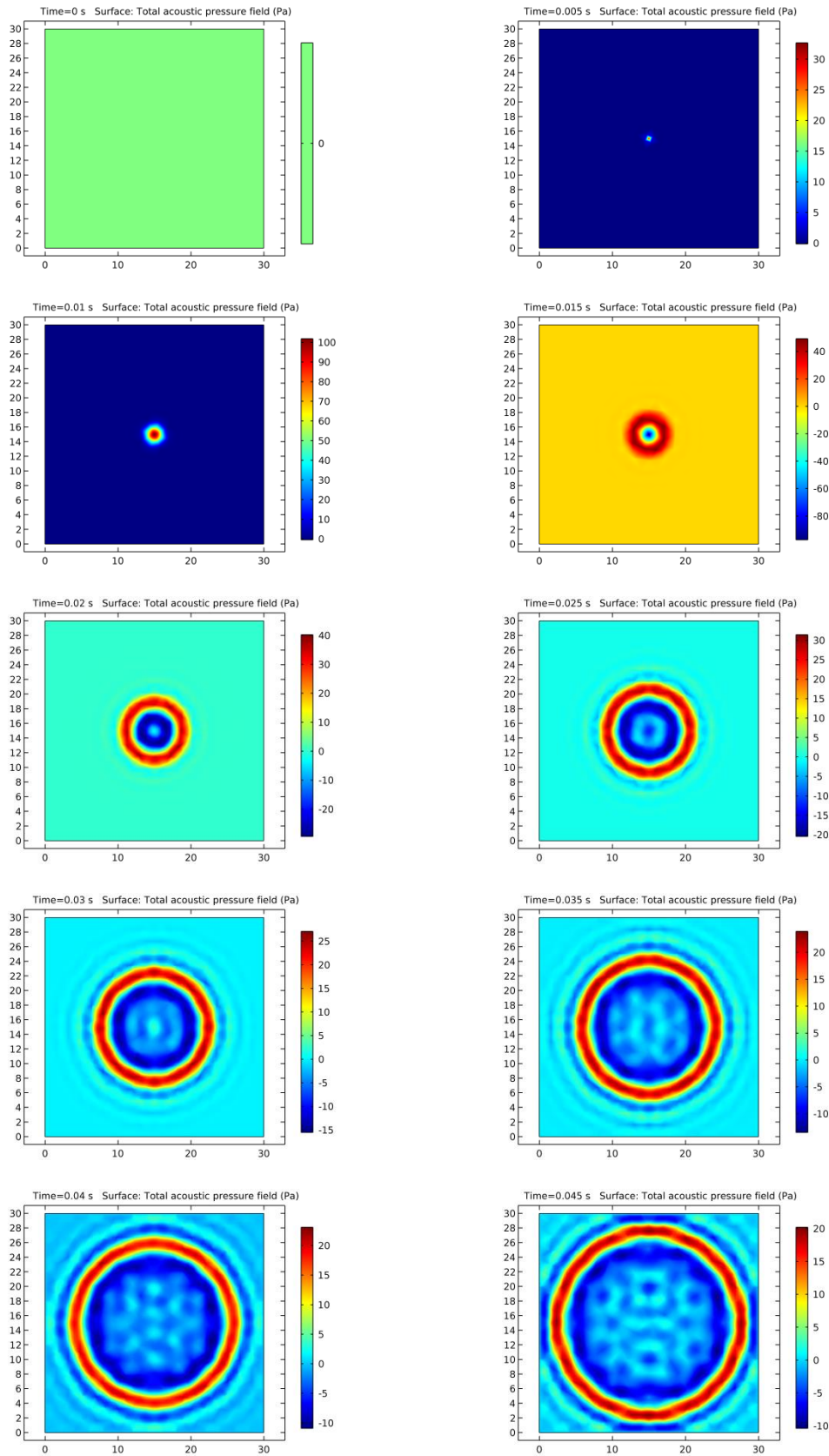


Figure 4-2 Gaussian Pulse Point Source in small time increments (2d)

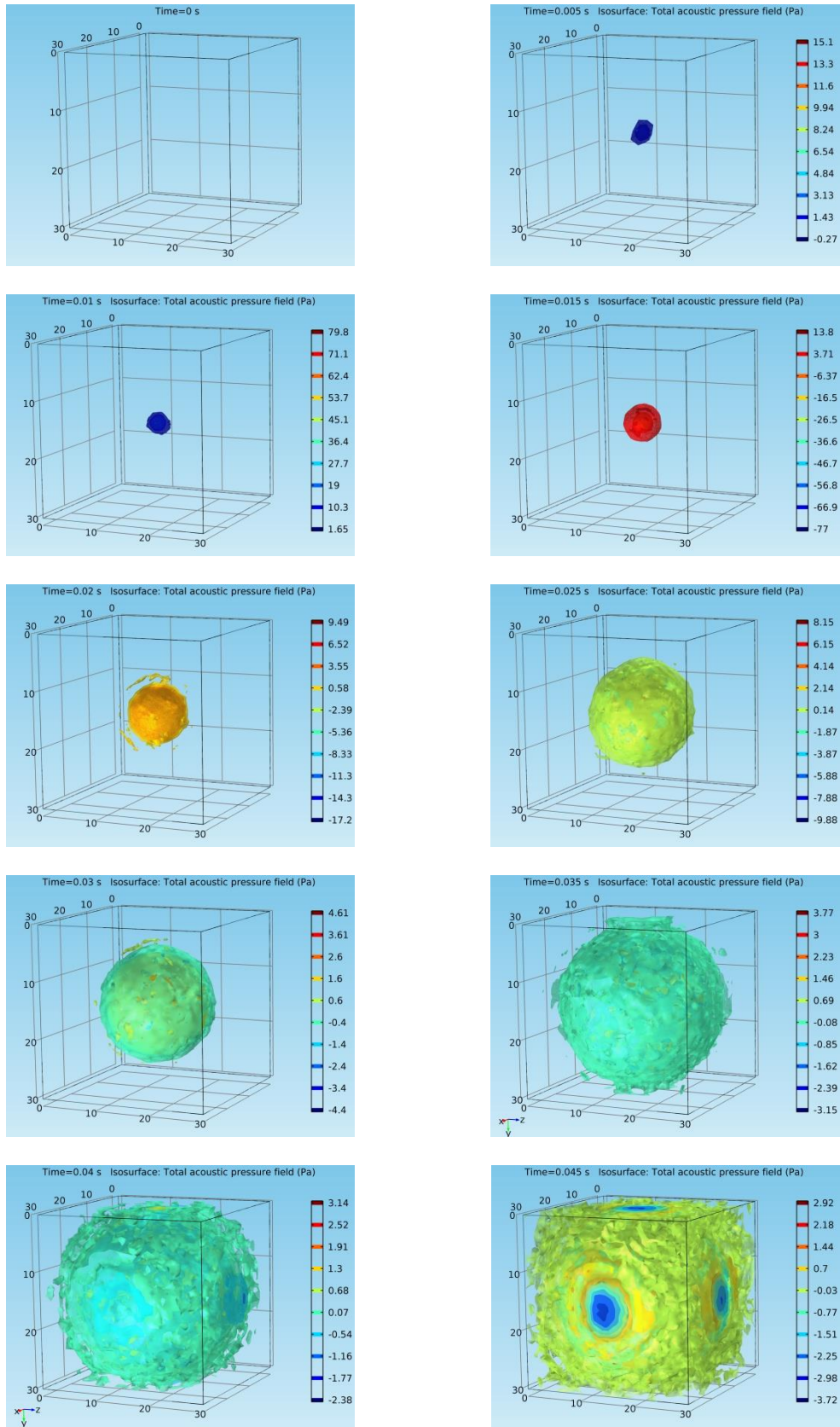


Figure 4-3 Gaussian Pulse Point Source in small time increments (3d)

4.1.2 Impedances of walls

One of the most important considerations for the accuracy of the finite element method modeling of an acoustic space is the correct implementation of wall modeling. The field of room acoustics deals with sound propagation mainly in enclosed spaces. The sound, hence the acoustic pressure is bounded on all sides by walls. The sound absorbing characteristics of the walls governs the way the acoustic pressure is distributed and decayed after an acoustic sound source radiates in the acoustic space. A fraction of the sound is reflected from the acoustic boundaries after impact. Another fraction of the sound is absorbed after impinging on the walls. The acoustic energy is either converted into heat or transmitted outside of the walls. It is this combination of numerous reflections and interaction in the acoustic boundaries of rooms that contributes to the complexity of the sound field in a space which is known as the acoustics of a room.

In the finite element formulation presented in the previous chapter, the modeling of the walls was carried out using the acoustic impedance. The wall impedance is a quantity which closely emulates the physical behavior of a wall. It is based on the particle velocity normal to the wall which is generated by a given sound pressure at the surface. Considering the incident condition of acoustic wave to the boundary surface, the normalized acoustic impedance of wall surfaces were calculated by substituting the random incidence absorption coefficient of the walls into the Eq. 4-2 [119, 120] with the assumption that the acoustic impedance is independent of the incidence angle.

$$Z = \rho_0 c \frac{1 + \sqrt{1 - \alpha}}{1 - \sqrt{1 - \alpha}} \quad (4-2)$$

Kuttruf [121] states that “a rigid wall ($\alpha = 0$) has impedance $Z = \infty$ and for a completely absorbent wall the impedance equals the characteristic impedance of the medium”. We can see that this statement is true if we replace the values of absorption coefficient ($\alpha = 0$ and $\alpha = 1$) into Eq. 4-2. For the derivation of the

Eq.4-2 we have assumed that the incident wave is a plane wave. In reality and in this study however the waves originate from a sound source and are therefore spherical. Hence the incident wave into a wall can arrive from any direction. However, it is necessary to note that the above selection affects correspondence between the computed and measured values. The effect may also be different for different room shapes and sizes. For this thesis we assumed that the sound source is not too close to the absorbing surface so that the curvature of the wave fronts can be neglected. We also took care that the actual placement of the source in the modeling process is as far away as possible from the walls. The extent of this influence is going to be investigated in future studies.

The absorption coefficient in reality is dependent on the angle of incidence (θ) [122-125]. Equation 4-3 presents the dependence of the acoustic impedance to the angle of incidence and the absorption coefficient [126]. Although this approach is more close to reality, it is difficult to be implemented in a finite element formulation. In fig. 4-4 the dependence of the absorption coefficient to the angle of incidence is depicted for different materials.

$$Z = \frac{\rho_0 c}{\cos \theta} \frac{1 + \sqrt{1 - \alpha}}{1 - \sqrt{1 - \alpha}} \quad (4-3)$$

Of special interest are surfaces, the impedance of which is independent of the direction of incident sound. This applies if the normal component of the particle velocity at any wall element depends only on the sound pressure at that element and not on the pressure at neighboring elements. Walls or surfaces with this property are referred to as 'locally reacting'.

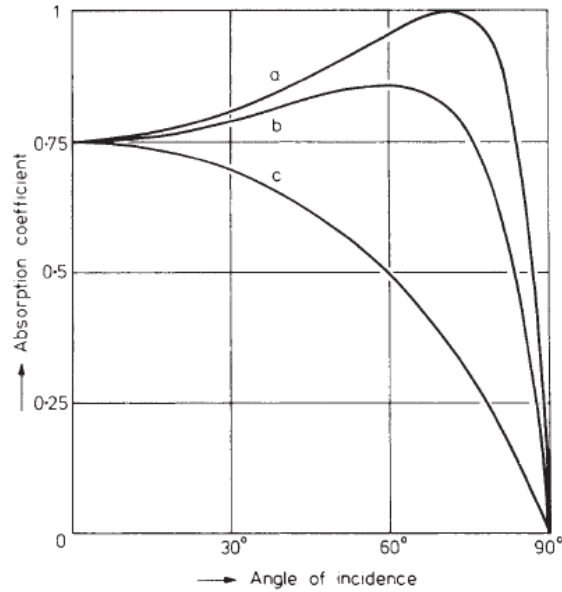


Figure 4-4 Dependence of the Absorption Coefficient of Materials to the angle of incidence (Materials with different Impedances) [127]

In order to present how the impedance of walls affects the incident wave in a finite element formulation in the time domain, examples follow for three different cases. In figures 4-5, 4-6 and 4-7 an acoustic space with a Gaussian Pulse Point source is presented in small time increments. In the first case (fig. 4-5) all the walls are fully reflective ($Z = \infty$). In the second case (fig.4-6) all walls are reflective but one which is fully absorptive ($Z=\rho c$). In this case the impedance of wall is equal with the impedance of the medium. In the final case (fig. 4-7) all walls are reflective but one which is slightly absorptive. The impedance of this wall is higher than the one of the medium.

For the first case (fig. 4-5) it can be seen that the walls are fully reflective and there is no decrease in the acoustic pressure after the impact of the sound wave in the wall as expected. In the second case (fig. 4-6) the sound wave and the acoustic pressure is eliminated after impact with the absorptive wall. It can be seen in the case of the room with a slightly absorptive wall (fig.4-7) that the acoustic pressure is decreased because of the absorptivity of the wall as expected in real life rooms. Naturally different absorption of the walls will also cause different impulse responses as it will be presented later.

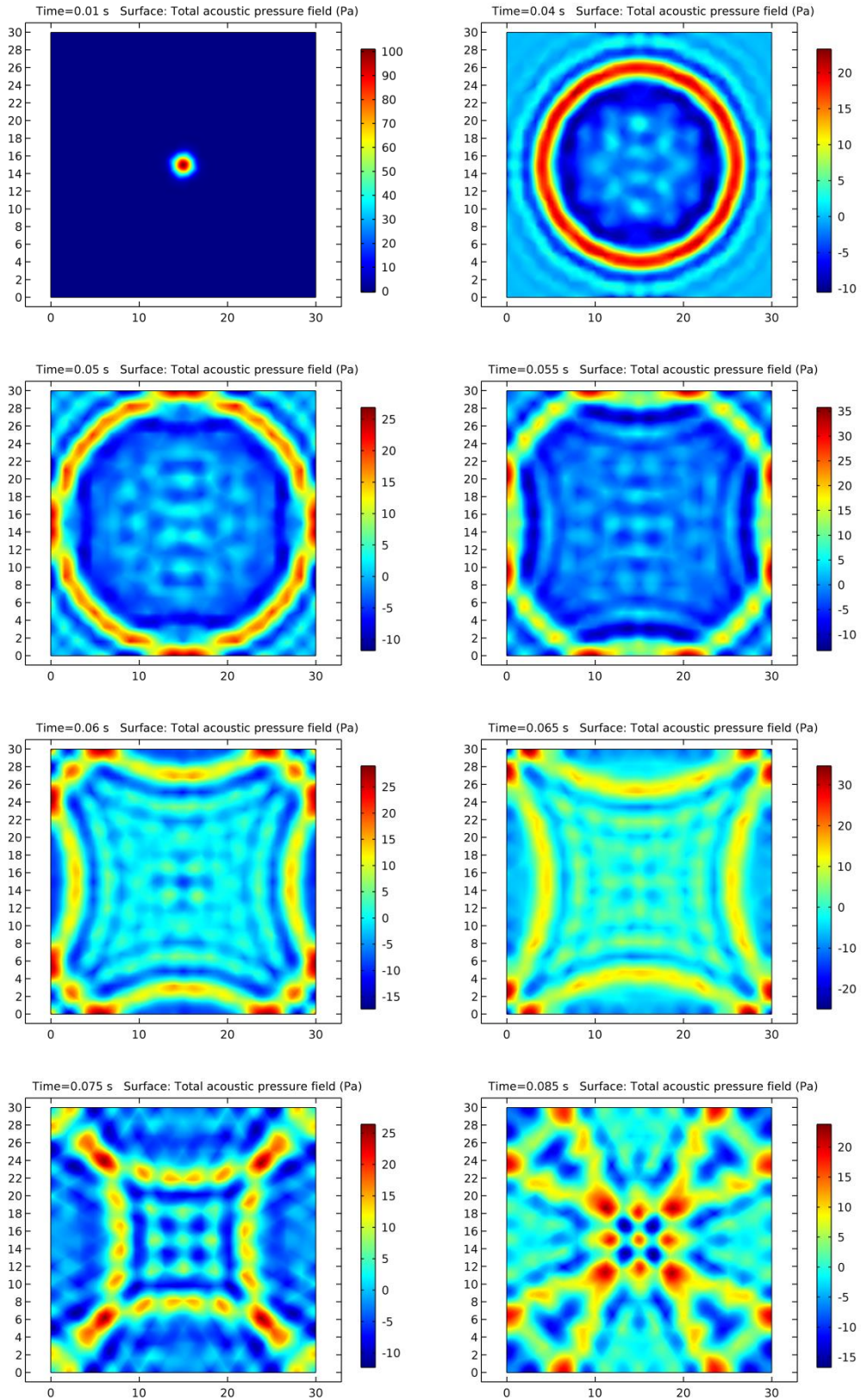


Figure 4-5 Gaussian Pulse Point Source in small time increments within a room with reflective walls (2d)

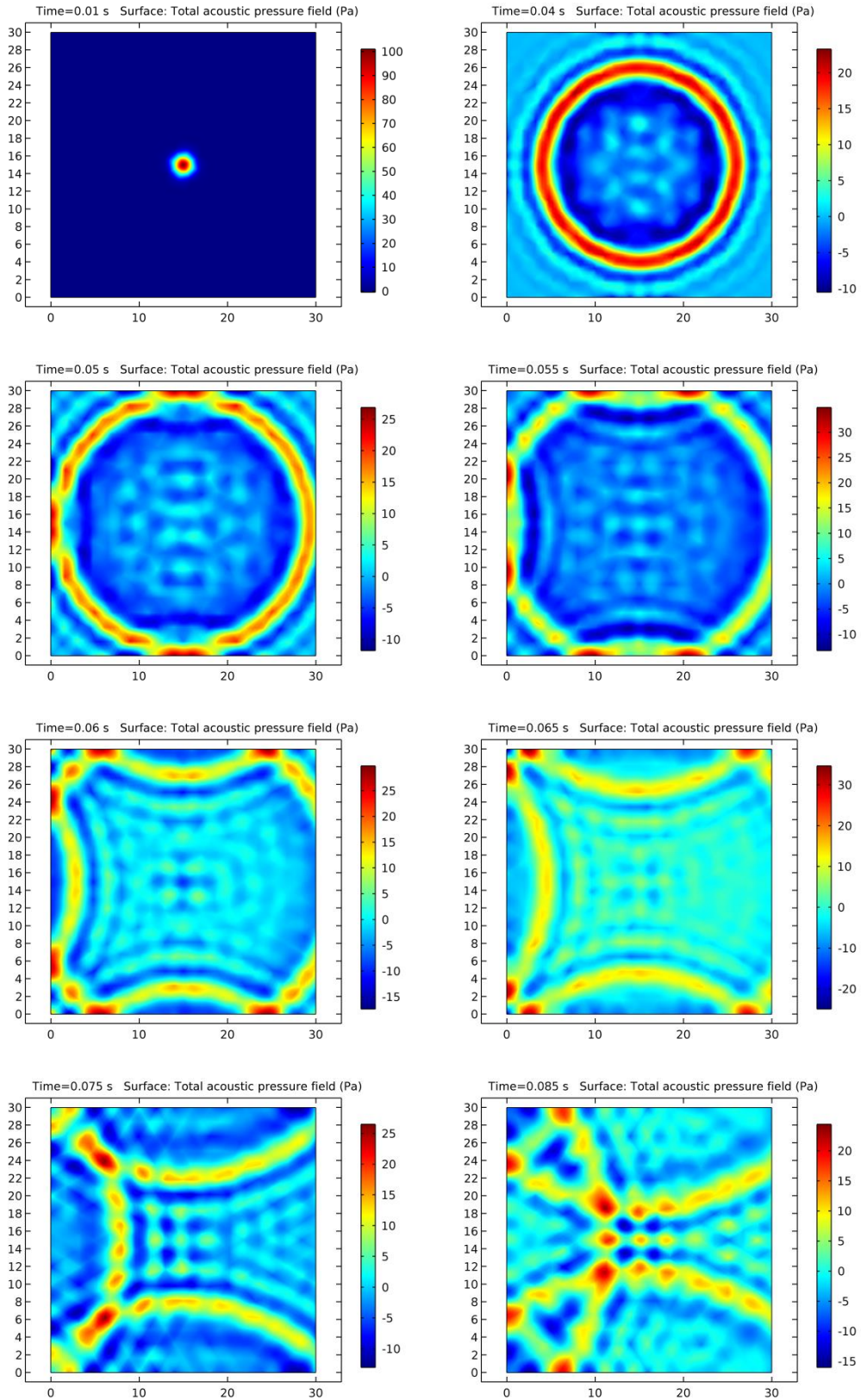


Figure 4-6 Gaussian Pulse Point Source in small time increments within a room with all walls reflective but the right which is fully absorptive (2d)

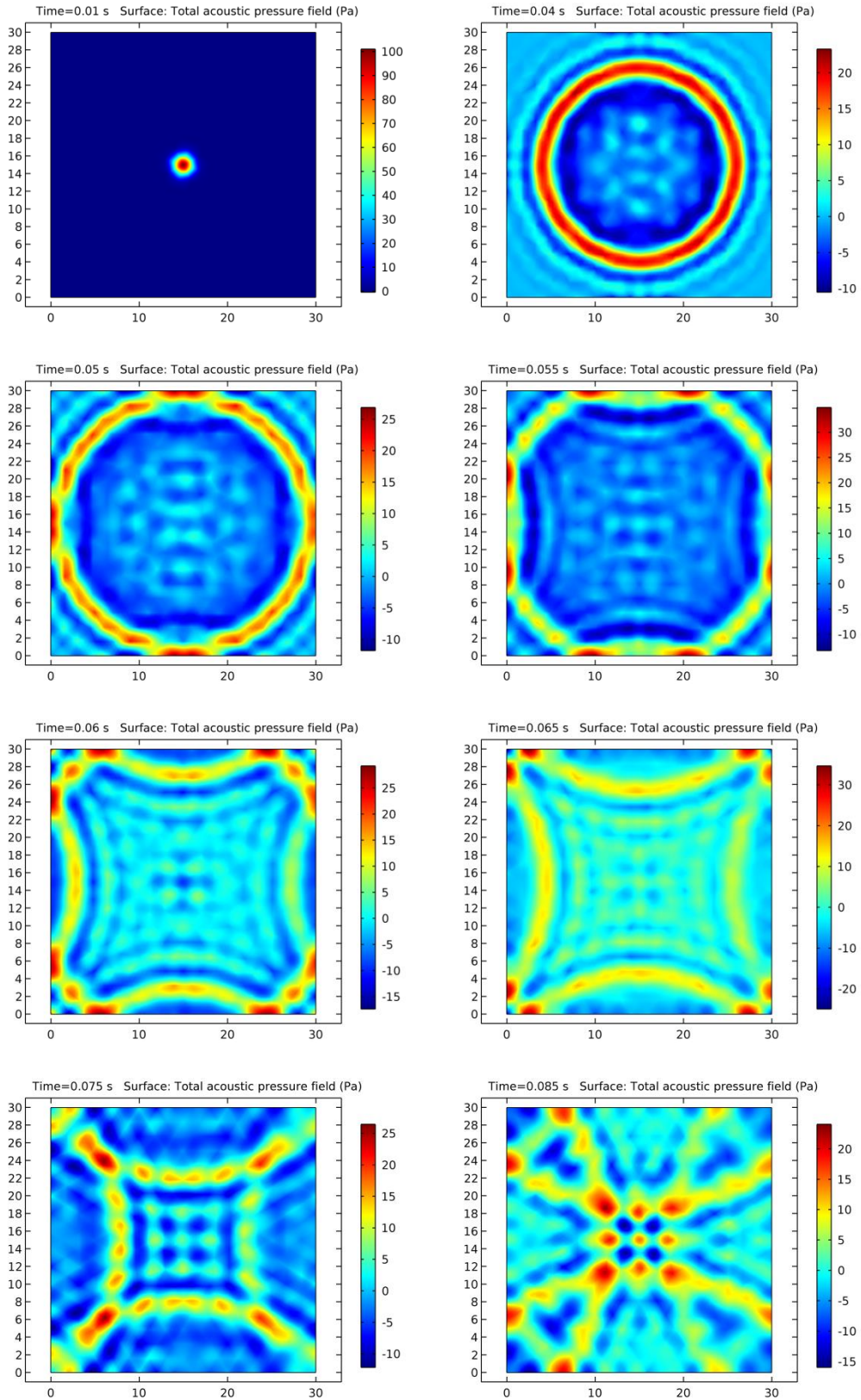


Figure 4-7 Gaussian Pulse Point Source in small time increments within a room with all walls reflective but the right which is lightly absorptive (2d)

For a direct comparison of the results, the same time increment for the three cases previously stated is presented in fig. 4-8. The differences in acoustic pressures can be better observed. Figure 4-9, presents an alternative depiction of the acoustic pressure (height depiction) for a different representation of the acoustic pressures.

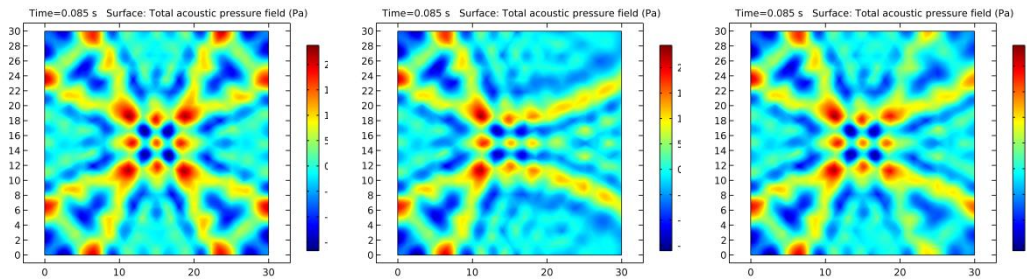


Figure 4-8 Comparison of the same moment in time of a room with all reflective walls, a room with all walls but right reflective (right wall absorptive) and a room with all walls reflective but right (right wall lightly absorptive)

The previous approach is used in the case where we want to apply the finite element method in an enclosed space, a room, a hall etc. In the case that we want to implement modeling with finite elements in an open space (e.g. external environment) we need to apply the Perfectly Matched Layer (PML)[128, 129] boundary conditions. The PML boundary condition is a domain or layer that is added to an acoustic model to mimic an open and non-reflecting infinite domain. It sets up a perfectly absorbing domain as an alternative to non-reflecting boundary conditions. The PML works with all types of waves, not only plane waves. It is also efficient at very oblique angles of incidence. The PML imposes a complex-valued coordinate transformation to the selected domain that effectively makes it absorbing at maintained wave impedance, and thus eliminating reflections at the interface.

The above can be implemented for the modeling of acoustic spaces with the use of the finite element method. For geometrical or statistical acoustics the absorption coefficient is used for the modeling of walls. The absorption coefficient is measured with the use of a reverberation chamber according to the

ISO 354 [130, 131]. It can also be measured with the use of an impedance tube [132, 133].

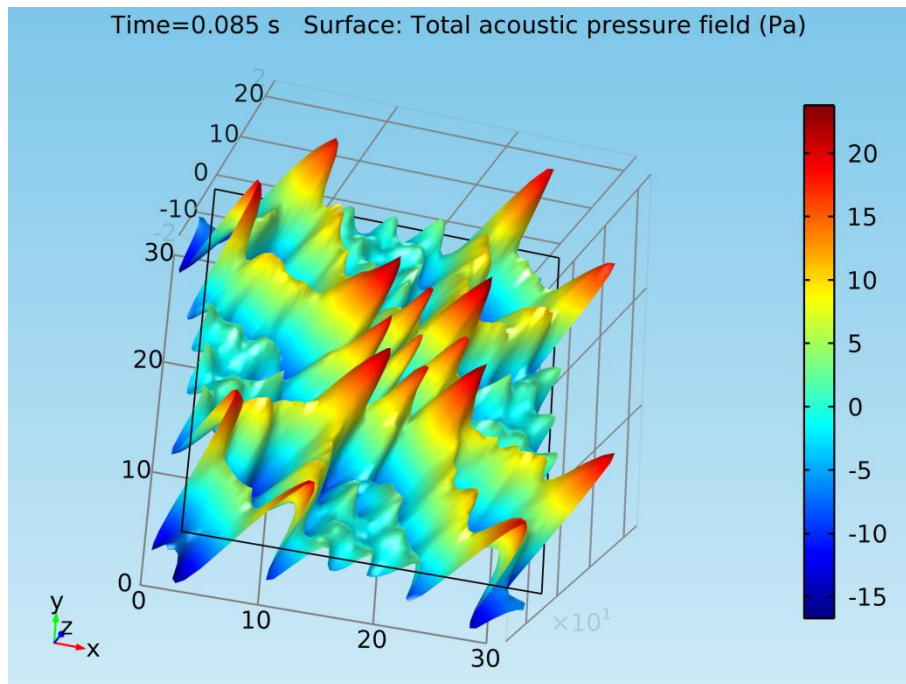


Figure 4-9 Acoustic Pressure of a room with reflective walls

4.1.3 Time step

For the application of the finite element method in the time domain an appropriate time step needs to be chosen. The time step is necessary for the utilization of the time stepping method that will be presented later in this chapter. The correct time step is the basis for calculating correctly the impulse responses and acoustic parameters since the impulse responses in essence are the acoustic pressure values in short time steps.

The time step is dictated by the Courant–Friedrichs–Lewy (CFL) condition. Richard Courant, Kurt Friedrichs, and Hans Lewy described the CFL condition [134, 135] investigating finite difference approximations. The condition was applied to prove existence of solutions to partial differential equations. The CFL condition was formed long before finite element applications and invention of

digital computers. Trefethen [136] states that the CFL paper laid the theoretical foundations for practical finite difference computations and in particular it identified a fundamental necessary condition for convergence of any numerical scheme that has subsequently come to be known as the CFL condition. The CFL condition is a necessary condition for the convergence of a numerical approximation of a partial differential equation linear or nonlinear. It has to be applied in the numerical analysis of explicit time integration schemes, when these are used for the numerical solution. The consequence of the CFL condition is that the time step must be less than a certain time in time-marching numerical simulations, otherwise the simulation will produce incorrect results.

The condition dictates that the time step must be kept small enough so that information has enough time to propagate through the space discretization. The principle behind the condition is that, for example, if a wave is moving across a discrete spatial grid and we want to compute its amplitude at discrete time steps of equal duration, then this duration must be less than the time for the wave to travel to adjacent grid points [137]. As a corollary, when the grid point separation is reduced, the upper limit for the time step also decreases. In essence, the numerical domain of dependence of any point in space and time (as determined by initial conditions and the parameters of the approximation scheme) must include the analytical domain of dependence (wherein the initial conditions have an effect on the exact value of the solution at that point) in order to assure that the scheme can access the information required to form the solution. The condition in numerical equation solving states that, given a space discretize on, a time step bigger than some computable quantity should not be taken. In the general case, the CFL has the following form:

$$C = \frac{u\Delta t}{\Delta x} \leq C_{max} \quad (4-4)$$

where the dimensionless number C is called the Courant number,

- u is the magnitude of the velocity (whose dimension is length/time)

- Δt is the time step (whose dimension is time)
- Δx is the length interval (whose dimension is length).

For application in the finite element method the time step depends on the frequency contents of the signal and by the desired maximal frequency resolution $T = 1/f_{max}$. The CFL number dictates the relation between the time step size and the minimal mesh size h_{min} . When solving transient models the maximal frequency we want to resolve is set as f_{max} . This frequency translates to a minimal wavelength $\lambda_{min} = c/f_{max}$ and in turn to a maximum element size $h_{max} = \lambda_{min}/5$, as will be discussed in the next section. The mesh resolution imposes a restriction on the time step size Δt taken by the solver. The relationship between mesh size and time-step size is closely related to the CFL number, which is now defined as

$$CFL = \frac{c\Delta t}{h} \leq C_{max} \quad (4-5)$$

where c is the speed of sound and h is the mesh size.

A CFL number around 1 would correspond to the same resolution in space and time if the discretization errors were of the same size, however, that is normally not the case. The value of C_{max} changes with the method used to solve the discretised equation, especially depending on whether the method is explicit or implicit. If an explicit (time-marching) solver is used then typically $C_{max} = 1$. Implicit (matrix) solvers are usually less sensitive to numerical instability and so larger values of C_{max} may be tolerated. The limiting step size, where the errors are of roughly the same size, can be found somewhere at $CFL < 0.2$. The implicit second-order accurate method generalized- α was used for this thesis for the transient acoustics problems. In reality a longer time step is permitted if the forcing does not make full use of the mesh resolution, that is, if high frequencies are absent from the outset. Generalized- α introduces some numerical damping of high frequencies.

Applying $CFL < 0.2=1/5$, and $h_{max} = \lambda_{min}/5$ into Eq.4-5, will result in a time step given by:

$$\Delta t < \frac{1}{5} \frac{h_{max}}{c} = \frac{\lambda_{min}}{25c} = \frac{1}{25} \frac{1}{f_{max}} \quad (4-6)$$

Another issue that affects the choice of time step is the sampling rate of the actual measurements on the reverberant room. The measurements were performed in the typical 44.1 KHz sampling rate which means that there were a time step of 1/44100 sec for every sample measurement. The process of conversion between sampling rates [138] can have effects on the quality of the impulse response. So a time step for the finite element method equal to the time step of the actual measurements was chosen for a direct comparison. The time step size that was chosen for this finite element study is $T=1/44100$ sec.

The following figure (Fig. 4-10) presents images from the acoustic pressures in a 2d space. The walls are slightly absorptive. The time step for this modeling is 1/44100 sec. Figures 4-11, 4-12, 4-13 present the impulse responses for three different points in the space. The points and dimensions of the space are presented in figure 4-15. The Gaussian pulse point source is located in point 1. It can be seen that the impulse responses are different for different points. This can be explained by the different reflections from the walls and the different distance from the source. A comparison of the different impulse responses can be seen in figure 4-14. This is also true for real life rooms. The impulse responses inside the room are different for every measuring point.

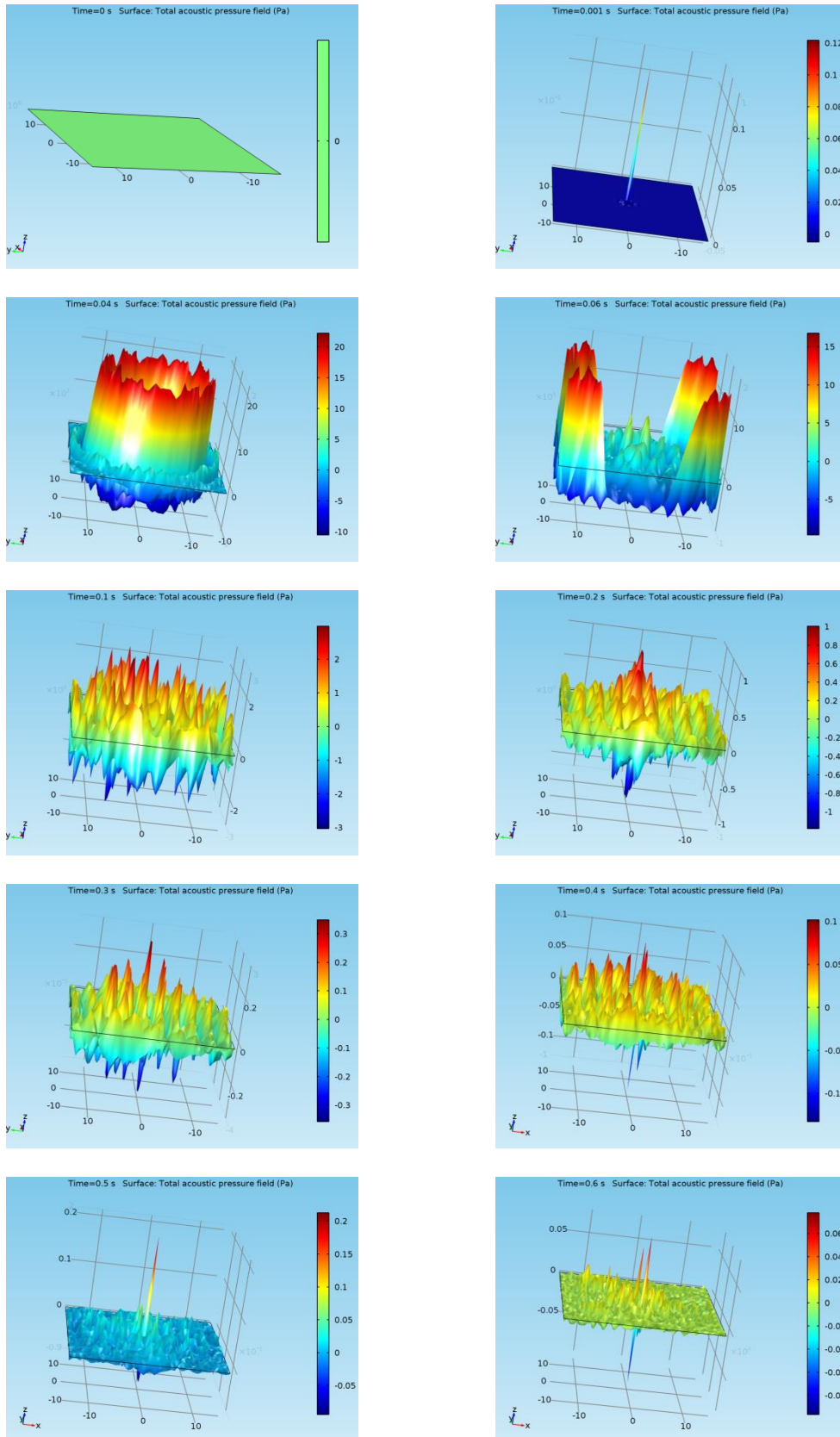


Figure 4-10 Acoustic Pressure in a room with absorptive walls (t=0 sec to t=0.6 sec)

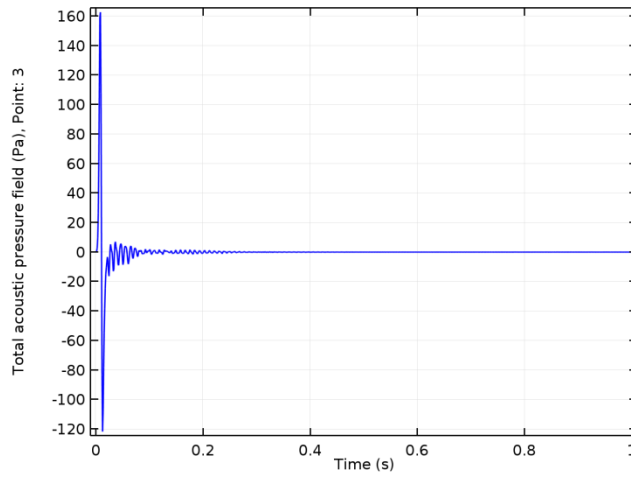


Figure 4-11 Impulse Response (Point 1)

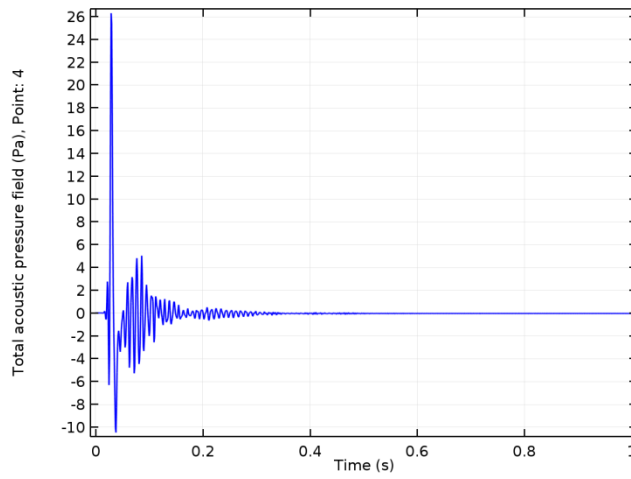


Figure 4-12 Impulse Response (Point 2)

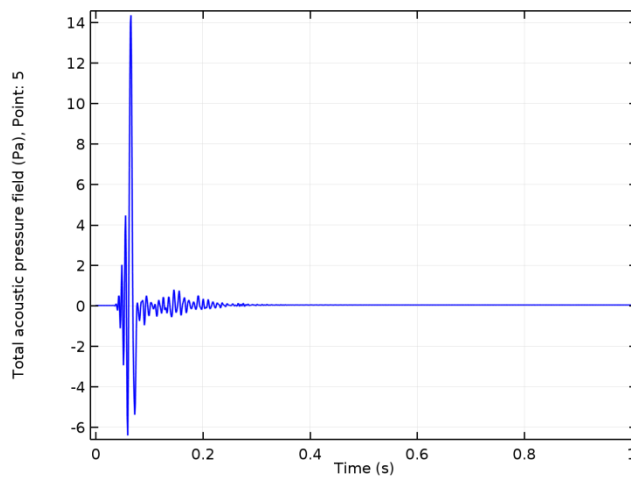


Figure 4-13 Impulse Response (Point 3)

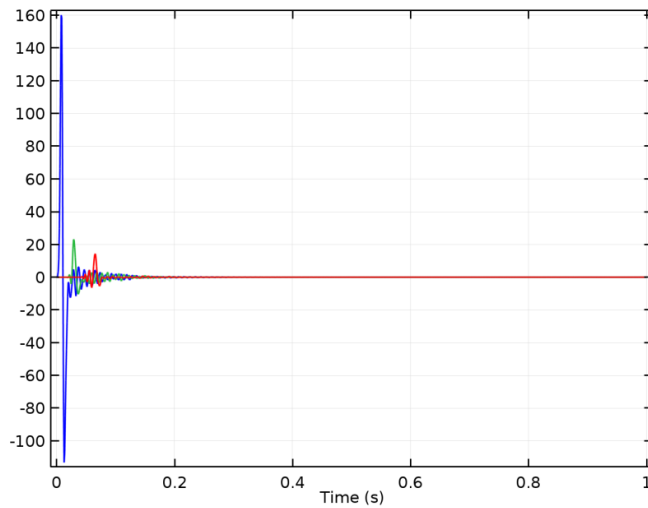


Figure 4-14 Comparison of the Impulse Responses

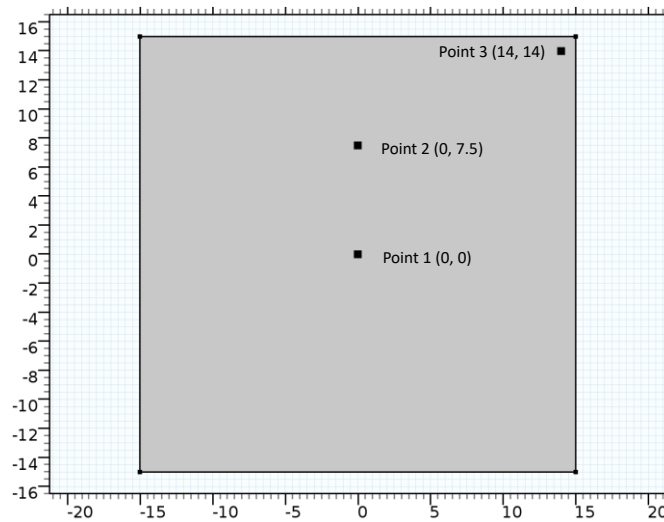


Figure 4-15 2d space dimensions and Points

4.1.4 Finite element meshes

Another important consideration for this thesis was the correct implementation of meshes for the finite element method formulations. Solutions to acoustic problems are wavelike. The waves are characterized by a wavelength λ in space, whose value depends on the frequency and speed of sound c in the medium according to $\lambda = c/f$. This wavelength has to be resolved by the mesh. To represent a wave on a discrete grid (the mesh), it is obvious that the mesh

elements must be smaller than the wavelength in order to resolve the wave. That is, there needs to be several degrees of freedom per wavelength in the direction of propagation.

The smallest element side length that can be used is determined by the shortest wavelength, that is, highest frequency, to be analyzed. Typically five or six elements are used [139, 140]. Schmiechen [141] states that two points per wavelength are strictly sufficient, but would not lead to accurate mode shapes so a factor of three to five is advised. Wojcik et al. [142] report computational results with five percent error using nine and two percent error using 18 linear elements per wavelength. Harari [143] proposes 10 nodes per wavelength or more similar to Thompson [144]. In Zienkiewicz [145] it is stated that 'a rule of thumb' which has been used for some time, is that there should be 10 nodes per wavelength. Marburg found that six elements per wavelength can provide acceptable accuracy [146] similar to Ihlenburg's comprehensive study on finite element error analysis [147].

In a similar fashion Otsuru tested the accuracy for the meshes in the field room acoustics for different elements [148]. The FE meshes were created for different requirements for λ/h . Here, λ and h respectively denote wavelengths of upper limit frequencies of the octave band and the maximum nodal distance. He found that on the condition $\lambda/h > 4$ successful interpolation of peaks in mode shapes assures small errors in the eigenfrequency approximation.

For this thesis the requirement that $\lambda/h > 5$ was followed. Assuming the frequency range between 20 and 500 Hz to be of interest, the distance between the nodes in the FEM mesh should not exceed 0.1 m.

Equally important is also the form of the mesh. Unstructured meshes are generally better than structured meshes for wave problems where the direction of wave propagation is not known everywhere in advance. The reason is that in a structured mesh, the average resolution typically differs significantly between directions parallel to the grid lines and directions rotated 45 degrees about one of the axes. Because the direction of propagation is generally not known

beforehand, it is good practice to aim for an isotropic mesh independently of the direction.

The generation of a suitable FEM 3D mesh to describe the room by volume elements used to be a tedious process, but modern software has removed much of the effort needed to mesh small rooms such as a control room or studio. Sometimes, it is useful to manually design a finite element mesh in 2D (such as over its floor surface) and then expand it (automatically) vertically at uniform intervals, to create a 3D mesh of the room volume.

The two most popular techniques for automatic mesh generation are the Delaunay triangulation [149-151] and the Advancing Front Technique (AFT) method [152-154]. Other techniques exist also such as the Octree method, the adaptive refinement, the medial surface method, the plastering method, the whisker weaving method and the H-morph algorithm [155]. For this thesis the Delaunay triangulation was used. 'The defining property of a Delaunay triangulation in the plane is that no vertex of the triangulation lies in the interior of any triangle's circumscribing disk—the unique circular disk whose boundary touches the triangle's three vertices. In three dimensions, no vertex is enclosed by any tetrahedron's circumscribing sphere'[156].

In the following figure (Fig. 4-16) impulse response calculations are presented in a 3d space with different meshes. The meshes for the first two cases were created with the restriction that $\lambda/h < 5$. For the third case with the restriction that $\lambda/h = 5$. Finally in the last case the restriction was $\lambda/h > 5$. From comparison of the results it can be seen that in cases 3 and 4, the impulse response is the same. In the first two cases the impulse responses have differences if compared with cases 3 and 4. This is a clear indication that the restriction $\lambda/h > 5$ should be followed for an accurate calculation of the impulse response.

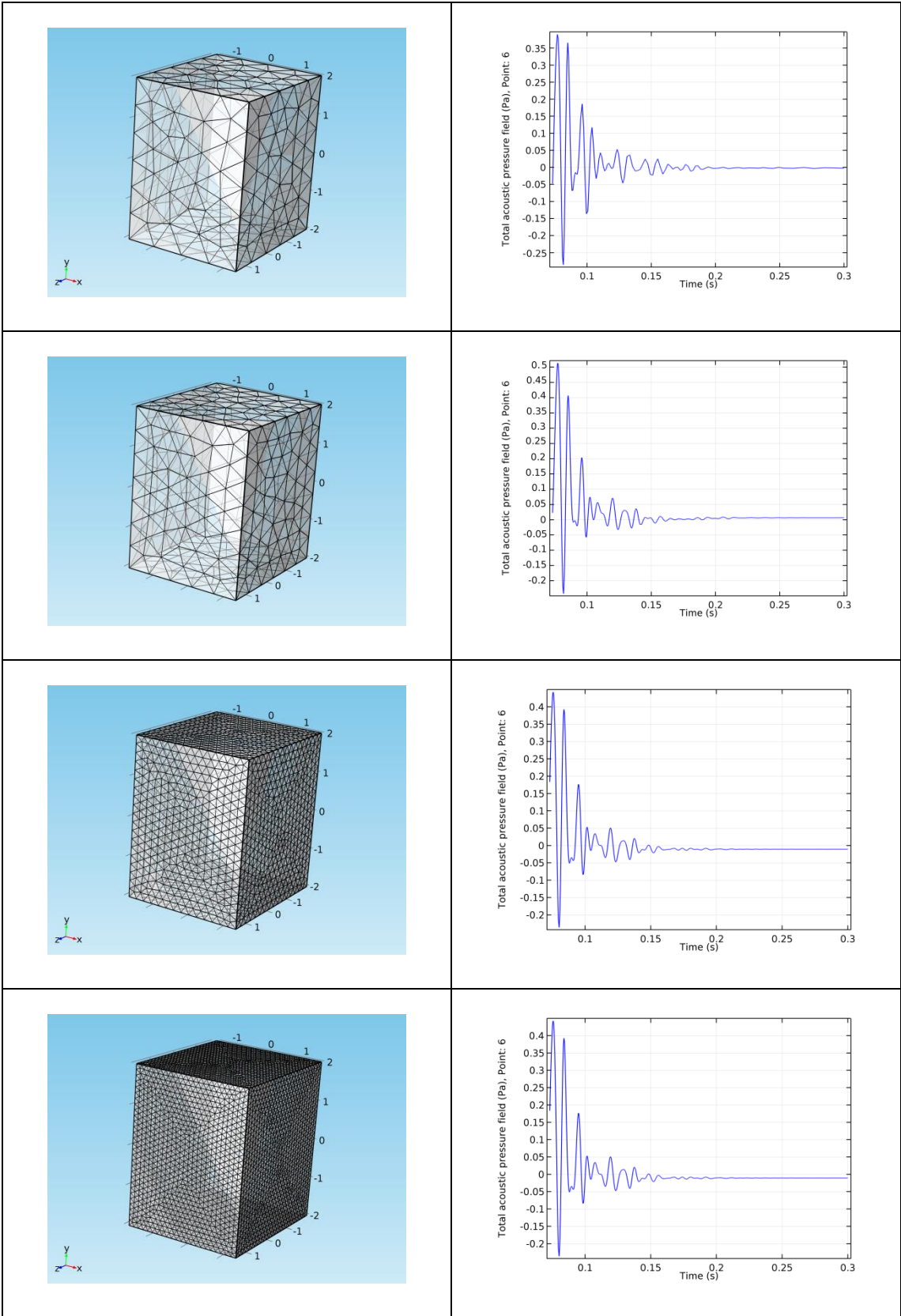


Figure 4-16 Impulse Response calculations in a 3d space with different meshes (Mesh 1,2: $\lambda/h < 5$, mesh 3: $\lambda/h = 5$, mesh 4: $\lambda/h > 5$)

The wall impedances were selected in the previous case so that the room's impulse response is small, less than 0.3 sec, and allows for rapid calculations. While the restriction $\lambda/h > 5$ seems to be adequate for the calculation of impulse responses presented in figure 4-16, this does not seem to be the case in every situation.

Experimental data from this thesis, however, suggests that in rooms where the impulse response has a longer duration there are differences in the impulse responses and indeed they are increasing over time. This is presented in section 6.1.1 of this thesis where experimental and calculated impulse responses for a reverberant space are compared. The results showed that the cross correlation coefficient between calculated and impulse response has a decreasing step over time. For those measurements and calculations the reverberant room impulse response is greater than 3 sec. This shows us that for acoustic spaces with longer time impulse responses, the restriction $\lambda/h > 5$ will provide good correlation between measured and calculated impulse responses in the early region of the impulse response but with an accuracy that is decreasing over time. Acoustic spaces that have a longer impulse response are rooms with a larger volume, rooms that have less absorptive walls or a combination of the previous ones.

In order to test the above, the wall impedances were altered in the same space that was used in the previous calculations (Fig. 4-16), resulting in less absorptive walls and with a room with longer impulse response. Impulse responses were then calculated for two different cases of meshes. The new calculations are presented in figure 4-17. Comparing the impulse responses for the two different cases (Fig. 4-16, Fig. 4-17) will show that in the second case the time duration of the impulse responses is about twice as long and allows for a better comparison.

Comparison of the impulse responses that were obtained for different meshes (depicted in Fig. 4-17) is presented in figure 4-18. We notice that while the impulse responses in the initial stages are identical, the differences are increasing over time. This is a clear indication that the effect of the mesh size on

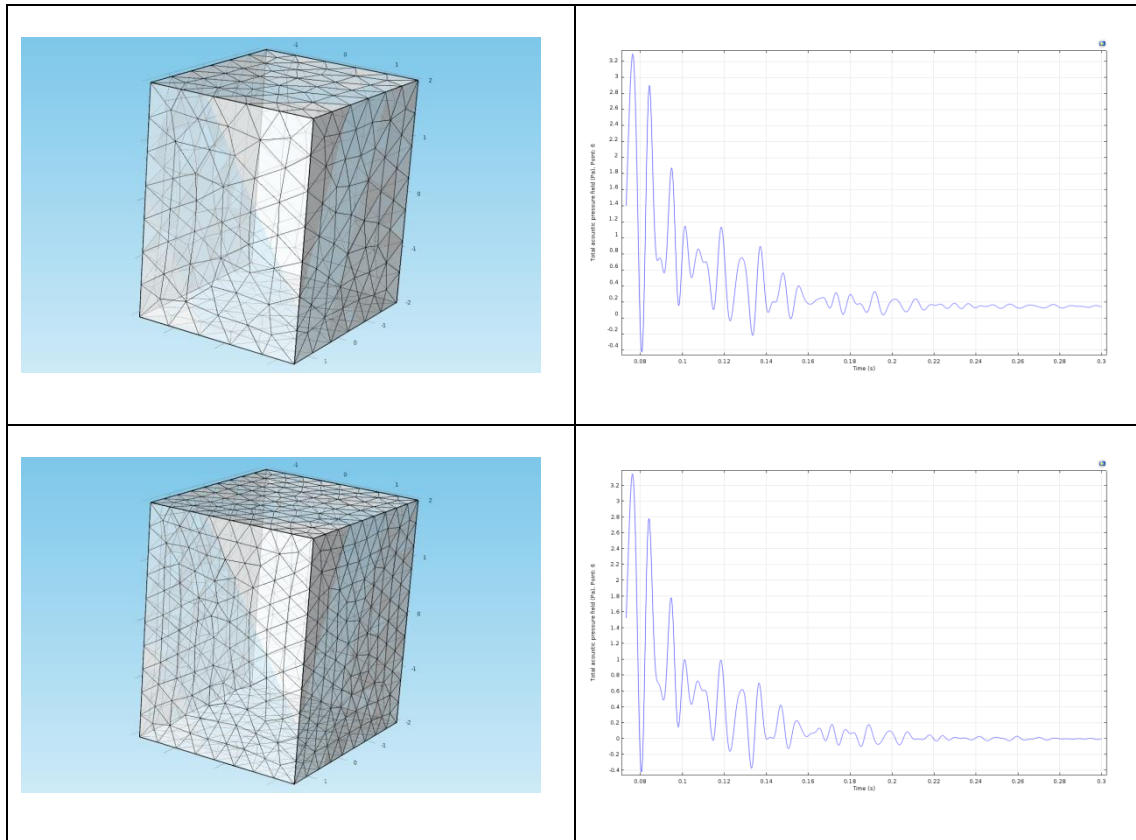


Figure 4-17 Impulse Response calculations in a 3d space with different meshes (Mesh 1: $\lambda/h < 3$, mesh 2: $\lambda/h = 3$)

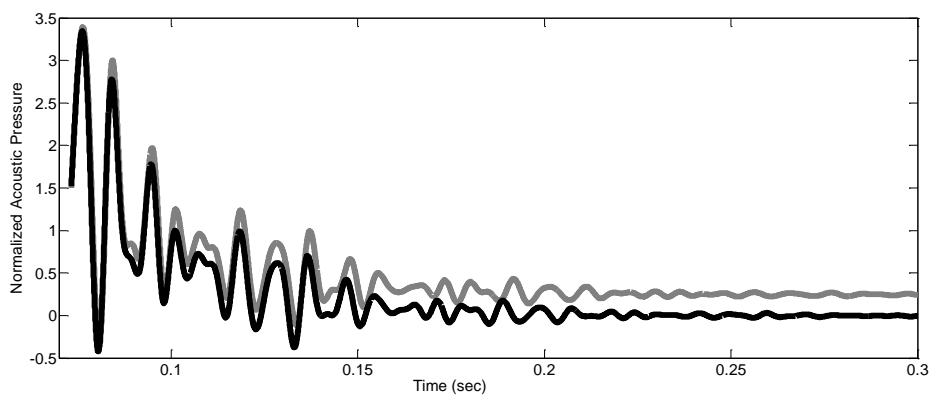


Figure 4-18 Comparison of the Impulse Responses for different meshes (Gray: Mesh 1, $\lambda/h < 3$, Black: mesh 2, $\lambda/h = 3$)

the time domain finite element method creates these effects on the impulse response. As Astley states [106] ‘small phase differences between the exact and computed solution may not contribute significantly to numerical error over a

single wavelength but accumulate over many wavelengths to give a large global error'. The importance of these findings is significant. Mesh restrictions imposed so far for the field of acoustics, are reasonable and provide good results but mainly for calculation in the frequency domain. For calculations in the time domain it appears that mesh restriction requirements depends on the time duration of the impulse response. Longer impulse responses require smaller mesh size than the current restrictions proposed for more accurate calculations.

4.1.5 Modeling of the acoustic material

Absorptive materials used in architectural applications tend to fall into three categories: porous absorbers, panel absorbers, and resonant absorbers. The most common category is the one of porous absorbers. This includes fiberglass, mineral fiber products, fiberboard, carpet, pressed wood shavings, cotton, felt, open-cell neoprene foam, sintered metal, and many other. Panel absorbers are nonporous lightweight sheets, solid or perforated, that have an air cavity behind them, which may be filled with an absorptive material such as fiberglass. Resonant absorbers can be lightweight partitions vibrating at their mass-air-mass resonance or they can be Helmholtz resonators or other similar enclosures, which absorb sound in the frequency range around their resonant frequency. They also may be filled with absorbent porous materials. Extended review of acoustic materials referring to their acoustic impedances can be found in Long [157].

For the modeling of the acoustic material for this thesis the Delany-Bazley-Miki model was used [158]. It is an empirical model used to describe fibrous materials such as fiberglass, cotton wool and rock wool with great accuracy. The model can be used for materials with porosity close to one. The Delany-Bazley-Miki model is an equivalent fluid model that mimics the bulk losses in certain porous-fibrous materials. The model represents a porous medium with complex propagation constants. For a highly porous material with a rigid skeleton, the model estimates the complex wave number k_c and complex impedance Z_c as functions

of frequency and flow resistivity. Using the original coefficients of Delany and Bazley, the expressions are:

$$k_c = k_a \left(1 + 0.098 \left(\frac{\rho_a f}{R_f} \right)^{-0.7} - i \cdot 0.189 \left(\frac{\rho_a f}{R_f} \right)^{-0.595} \right) \quad (4-7)$$

$$Z_c = Z_a \left(1 + 0.057 \left(\frac{\rho_a f}{R_f} \right)^{0.734} - i \cdot 0.087 \left(\frac{\rho_a f}{R_f} \right)^{-0.732} \right) \quad (4-8)$$

where R_f is the flow resistivity and $k_a = \omega/c_a$ and $Z_a = \rho_a c_a$ are the free-space wave number and impedance of air, respectively. Measurements of the flow resistivity of rock wool can be found in bibliography [159].

4.1.6 Stepping method

For the solution of the wave equation in the time domain with the use of finite elements, a time stepping method is necessary. The time stepping method that was used in this study is the Generalized- α [160, 161]. A viable alternative which is commonly used in structural problems is the Newmark β method [162]. More about this method for acoustics problems can be found in Otsuru [163]. An analysis and comparison of the method for the time integration algorithms of the finite element solutions can be found in Dettmer [164].

The Method solves for a discrete time step n and the equations can be expressed as presented below.

$$\mathbf{p}_{n+1} = \mathbf{p}_n + h\dot{\mathbf{p}}_n + h^2 \left(\frac{1}{2} - \beta \right) \ddot{\mathbf{p}}_n + \beta \ddot{\mathbf{p}}_{n+1} \quad (4-9)$$

$$\dot{\mathbf{p}}_{n+1} = \dot{\mathbf{p}}_n + h((1 - \gamma)\ddot{\mathbf{p}}_n + \gamma\ddot{\mathbf{p}}_{n+1}) \quad (4-10)$$

$$\mathbf{F}(t_{n+1-a_f}) = M\ddot{\mathbf{p}}_{n+1-a_m} + C\dot{\mathbf{p}}_{n+1-a_f} + K\mathbf{p}_{n+1-a_f} \quad (4-11)$$

Where h is the time step:

$$h = t_{n+1} - t_n \quad (4-12)$$

Also:

$$\mathbf{p}_{n+1-a_f} = (1 - a_f)\mathbf{p}_{n+1} + a_f\mathbf{p}_n \quad (4-13)$$

$$\dot{\mathbf{p}}_{n+1-a_f} = (1 - a_f)\dot{\mathbf{p}}_{n+1} + a_f\dot{\mathbf{p}}_n \quad (4-14)$$

$$\ddot{\mathbf{p}}_{n+1-a_m} = (1 - a_m)\ddot{\mathbf{p}}_{n+1} + a_f\ddot{\mathbf{p}}_n \quad (4-15)$$

$$t_{n+1-a_f} = (1 - a_f)t_{n+1} + a_ft_n \quad (4-16)$$

The parameters a_f, a_m, γ, β are:

$$a_f = \frac{\rho_\infty}{\rho_\infty + 1} \quad (4-17)$$

$$a_m = \frac{2\rho_\infty - 1}{\rho_\infty + 1} \quad (4-18)$$

$$\gamma = \frac{1}{2} - a_m + a_f \quad (4-19)$$

$$\beta = \frac{1}{4}(1 - a_m + a_f)^2 \quad (4-20)$$

4.1.7 Solver

After the system of linear equations is formed by the finite element method a solver must be applied. There are two main categories of solvers: the ones that use a direct elimination process (direct solvers) and the ones that use an iterative method (iterative solvers).

The MULTifrontal Massively Parallel sparse direct solver (MUMPS) [165, 166] was used in this thesis. The basis of the direct solvers involves a direct elimination process. Decomposition of the matrix $[K]$ is performed into lower and upper triangular matrices, $[K] = [L][U]$. Forward and back substitutions are performed for the computation of the solution. The MUMPS works on general systems of the form $[K]\{u\} = \{F\}$ and uses several reordering algorithms to permute the columns and thereby minimize the fill-in. MUMPS is multithreaded on platforms that support multithreading and also supports solving on distributed memory architectures. A practical aspect of MUMPS, is that it has the capability to store the LU factors on the hard drive. This minimizes the internal memory usage. The PARDISO [167] direct solver was also tested with similar results in computational time.

The iterative solvers are similar to a conjugate gradient method. Variations include the generalized minimum residual method and the biconjugate gradient stabilized method. A typical iterative method involves an initial guess and successive steps of iteration leading. This leads to the calculation of the unknown variable from one or two of the previous iterations. A specified tolerance can be defined for the solver convergence. The advantage of the iterative solvers is the smaller memory usage, but the performance is not always robust. Some iterative solvers are the GMRES (generalized minimum residual)[168], FGMRES (flexible generalized minimum residual)[169] and the BiCGStab Iterative Solver (biconjugate gradient stabilized)[170]. More about the iterative methods applied in acoustics can be found in Otsuru [171].

4.1.8 Type of Elements

The Lagrange 2nd-order tetrahedral elements were used for this thesis in the finite element formulation. The shape functions for the tetrahedral elements are presented in table 4-1. Shape functions for the two and three dimensional tetrahedron, hexahedron and prism element can be found in Atalla [103]. Figure 4-19 presents the Lagrange 2nd-order tetrahedron element.

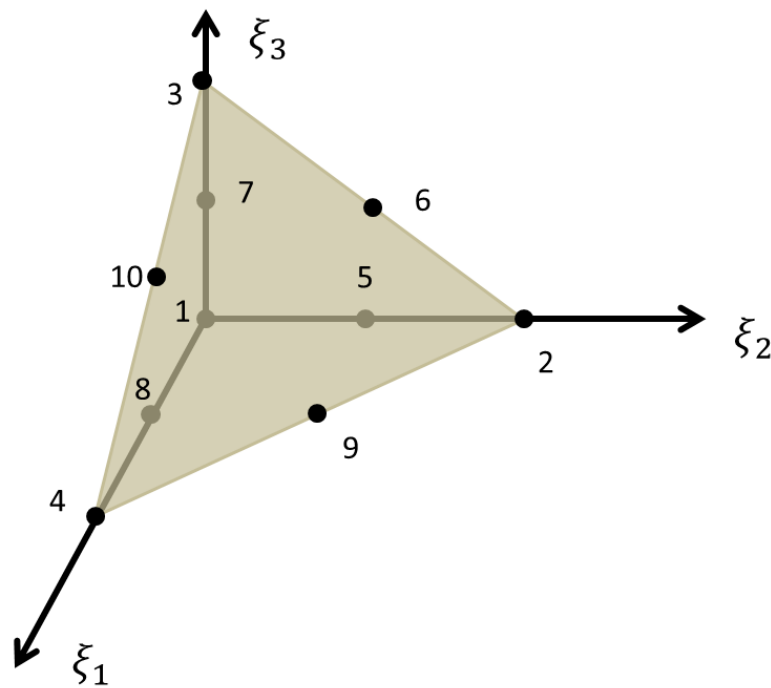


Figure 4-19 Lagrange 2nd order tetrahedron element [103]

The accuracy of the finite element method depends on the shape functions used in the formulation. Different elements have been studied by Otsuru for acoustic applications [148] in the frequency domain. Differences were found, especially after mesh manipulation. Different elements cause different convergence of results. The study with the different elements was applied for the calculation of eigenfrequencies. A significant area of improvement for the time domain finite element method lies in this area and is reserved for future work.

Node id	Coordinates	Shape functions
1	(0,0,0)	$N_1 = (2\xi_4 - 1)\xi_4$
2	(0,1,0)	$N_2 = (2\xi_2 - 1)\xi_2$
3	(0,0,1)	$N_3 = (2\xi_3 - 1)\xi_3$
4	(1,0,0)	$N_4 = (2\xi_1 - 1)\xi_1$
5	(0, 1/2, 0)	$N_5 = 4\xi_4\xi_2$
6	(0, 1/2, 1/2)	$N_6 = 4\xi_2\xi_3$
7	(0,0, 1/2)	$N_7 = 4\xi_3\xi_4$
8	(1/2, 0, 0)	$N_8 = 4\xi_1\xi_4$
9	(1/2, 1/2,0)	$N_9 = 4\xi_1\xi_2$
10	(1/2, 0, 1/2)	$N_{10} = 4\xi_1\xi_3$
		$\xi_4 = 1 - \xi_1 - \xi_2 - \xi_3$

Table 4-1 Shape functions for Lagrange 2nd order three dimensional element [103]

4.2 IMPLEMENTATIONS OF TIME DOMAIN FINITE ELEMENT METHOD

The finite element method was implemented in the time domain for the cases of a reverberant room and a reverberant room with absorptive material. Finally the finite element method was implemented in the frequency domain for the reverberant room.

4.2.1 Reverberant room Modeling

For the first implementation the goal was the calculation of impulse responses in a reverberant room. Acoustic parameters, frequency responses and cumulative spectral decays were going to be extracted from the impulse responses for later comparison with measured results.

For the application of the finite element method in the time domain a reverberant room in the Technical University of Crete was used due to its simple shape and uniformity of absorption characteristics of walls. The reverberant room is depicted in Fig. 4-20. The volume and the surface area of the room are, respectively, 38.71 m³ and 71.17 m². Inner walls of the room are made of concrete.

A Gaussian Pulse Point Source was used in this study. The source was placed at a height of 1.5 m for all calculations, as depicted in the figure 4-20. Considerations were taken so the source was not near the walls due to scattering effects. Measuring positions are depicted as points in figure 4-20.

Considering the incident condition of acoustic wave to the boundary surface, the normalized acoustic impedance of wall surfaces were calculated by substituting absorption of the walls into the Equation 4-2 of the random incidence absorption coefficient with the assumption that the acoustic impedance is independent of the incidence angle. The absorption coefficients that were used in the finite element formulation were measured during the experimental procedure that is

presented in section 5.2.1 of this thesis. Table 5-1 contains the values of the absorption coefficients.

The time step size that was chosen for this study is $T=1/44100$ sec.

The FE meshes were created to satisfy the requirement that $\lambda/h > 5$. Here, λ and h respectively denote wavelengths of upper limit frequencies of the octave band and the maximum nodal distance. Figure 4-21 presents the mesh of the reverberant room.

The Lagrange 2nd-order tetrahedral elements were used in the finite element formulation.

The MULTifrontal Massively Parallel sparse direct solver (MUMPS) was used for solving the system of equations that arose from implementing the finite element method.

After the computation, the pressures at 60 points were extracted. The impulse responses were constructed from the extracted pressures for each time step by using the Generalized- α time stepping method. From the calculated impulse responses acoustic parameters were derived. Also frequency responses and cumulative spectral decays were extracted. Derivation methods for acoustic parameters, frequency response and cumulative spectral decays are presented in sections 2.3 and 2.4 of this thesis. Calculated impulse responses, frequency responses and cumulative spectral decays are compared with the ones measured with the MLS technique in the sixth chapter of the study.

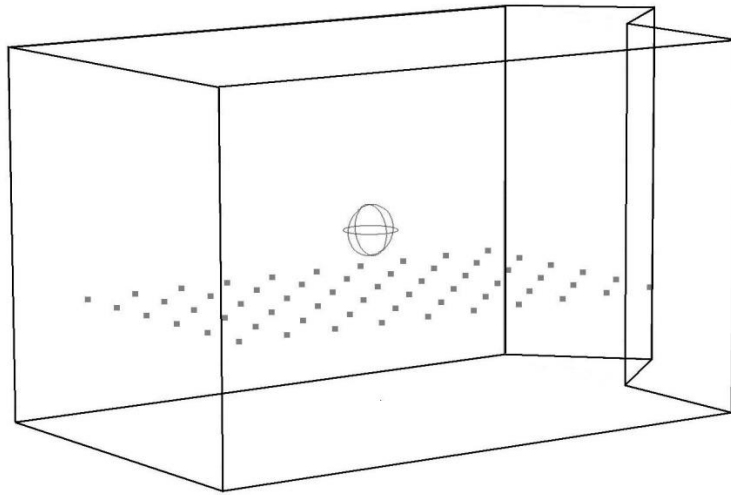


Figure 4-20 Reverberant room with computed points

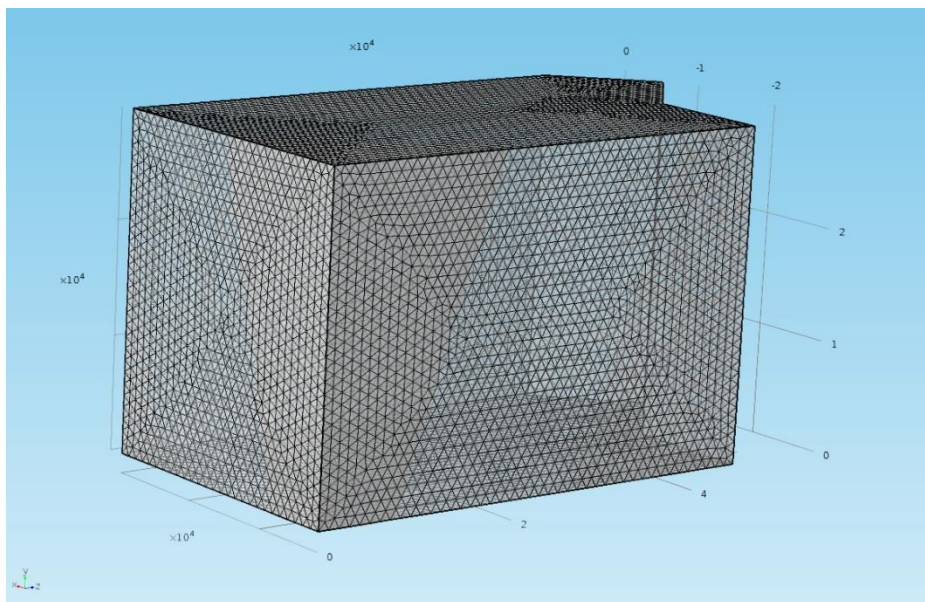


Figure 4-21 Meshing of the Reverberant room

4.2.2 Reverberant room with Acoustic Material Modeling

For this implementation, a ‘virtual reverberation chamber’ method was applied [6]. A description of the method and the actual setup are presented in the following section.

4.2.2.1 ‘Virtual reverberation chamber’ method

In room acoustics the knowledge of the absorption coefficient of the materials that cover the surface of a space is necessary for predicting the majority of the acoustic parameters that define a space. For the measurement of the absorption coefficient the reverberation chamber method [130, 131] and the impedance tube method [132, 133] are commonly used. The impedance tube method can measure the absorption coefficient of a plane material but not in the case when an acoustic panel has a variant shape (e.g. pyramidal). The most common method that can measure the absorption coefficient if a material has a variant shape is the reverberation chamber method.

The utilization of a ‘virtual reverberation chamber’ method that could be used for the prediction of the absorption coefficient of acoustic panels could be of great use. An applicable ‘virtual reverberation chamber’ could predict the absorption coefficient of an acoustic panel prior to its manufacturing and it would help reducing the cost of development. It could also lead to new shapes and variations of acoustic panels.

The goal of this implementation was the application of a ‘virtual reverberation chamber’ method for the measurement of the absorption coefficient of an acoustic panel. For that cause a virtual replication of the reverberation chamber method with the use of the time domain finite element method was performed. The reverberation chamber method is presented in ISO 354 [130]. It consists of two separate sets of impulse response measurements in a reverberant chamber. On the first one impulse responses of the empty reverberant room are measured. On the second one impulse responses are measured with the presence of an acoustic panel. The presence of the acoustic panel, because of its absorption,

causes changes in the measured impulse responses. Reverberation time is extracted from the impulse response as presented in section 2.4.1. The presence of the acoustic panel results in a lower reverberation time. From the differences in the reverberation time between the two measurements, the absorption coefficient of the material can be measured. The absorption coefficient can be calculated according to equation 4-21 as the ISO 354 suggests.

The same procedure was followed for the ‘virtual reverberation chamber’ with the use of the time domain finite element method. Impulse responses in the reverberant room were calculated in two different cases. In the first one impulse responses of the empty reverberant room are calculated. In the second one impulse responses are calculated with the presence of an acoustic panel that was modeled in the finite element method. Reverberation times are extracted and the absorption coefficient is calculated for the ‘virtual reverberation chamber’ method according to equation 4-21.

Absorption Coefficients (α_s) of the acoustic panel can be calculated using the following formula:

$$a_s = 55.3 \frac{V}{S} \left(\frac{1}{c_2 T_2} - \frac{1}{c_1 T_1} \right) - 4V(m_2 - m_1) \quad (4-21)$$

- V is the volume of the empty reverberation chamber (m^3)
- S is the area of the test specimen (m^2)
- T_1 is the mean reverberation time of the empty reverberation chamber (seconds)
- T_2 is the mean reverberation time of the reverberation chamber with the test specimen installed (seconds)
- c_1, c_2 are the velocity of sound calculated from the following formula:
 $c = 331 + 0.6t$ m/s
- t is the air temperature of the reverberation chamber (Celsius)
- m_1, m_2 are the power attenuation coefficient at T_1 and T_2 calculated according to ISO 9613:1993 [15]

4.2.2.2 Setup of the calculation for the ‘virtual reverberation chamber’ method

The time domain finite element method was used for the application of a ‘virtual reverberation chamber method’. The same reverberant room in the Technical University of Crete that was presented in section 4.2.1 was used. The volume and the surface area of the room are, respectively, 38.71 m³ and 71.17 m². Inner walls of the room are made of concrete.

A Gaussian Pulse Point Source was used in this study. The source was placed at two different points as presented in table 4-2. The sound sources can be seen in figure 4-23 as spheres. Considerations were taken so the source placement was not near the walls due to scattering effects. The source positions were at least 3 m apart as the ISO suggests.

Considering the incident condition of acoustic wave to the boundary surface, the normalized acoustic impedance of wall surfaces were calculated by substituting absorption of the walls into the Equation 4-2 of the random incidence absorption coefficient with the assumption that the acoustic impedance is independent of the incidence angle. The absorption coefficients that were used in the finite element formulation were measured during the experimental procedure that is presented in section 5.2.1 of this thesis.

The placement of the acoustic material is depicted in figure 4-22 and 4-23. For the modeling of the acoustic material the Delany-Bazley-Miki model was used. It is an empirical model used to describe fibrous materials such as fiberglass, cotton wool and rock wool with great accuracy. The Delany-Bazley-Miki model is an equivalent fluid model that mimics the bulk losses in certain porous-fibrous materials. The acoustic material that was modeled is that of rock wool. The acoustic material was laid directly over the floor so that no part was closer than 0.63 m to any edge of the boundary of the room.

The time domain finite element method was applied for two sets of calculation as presented in section 4.2.2.1. The first calculation was without the modeled acoustic panel and the second one with the presence of the acoustic panel.

The time step size that was chosen for this study is $T=1/44100$ sec.

The FE meshes were created to satisfy the requirement that $\lambda/h > 5$. Here, λ and h respectively denote wavelengths of upper limit frequencies of the octave band and the maximum nodal distance. Meshing of the room with the acoustic material is presented in figure 4-24.

After the computation, the pressures at 6 receiving points were extracted for each of two source positions. A total of 12 impulse responses were calculated. The placement of the receiving points is presented in table 4-2. The receiving points can be seen in figure 4-23 as points.

The impulse responses were constructed from the extracted pressures for each time step. From the calculated impulse responses, the mean reverberation times and finally the absorption coefficient were derived and will be discussed and compared with the ones measured with the MLS technique in the results and discussion of this study.

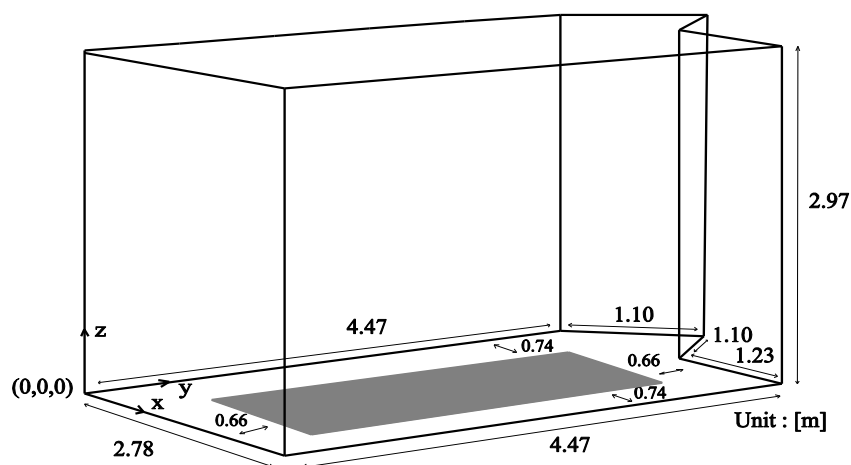


Figure 4-22 Reverberant room with acoustic material

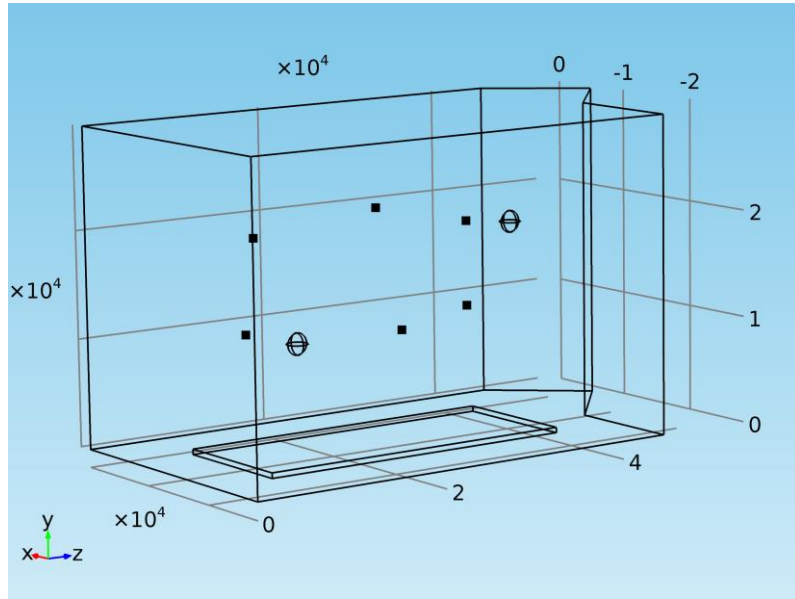


Figure 4-23 Placement of Sources (spheres) and Calculation Points (points)

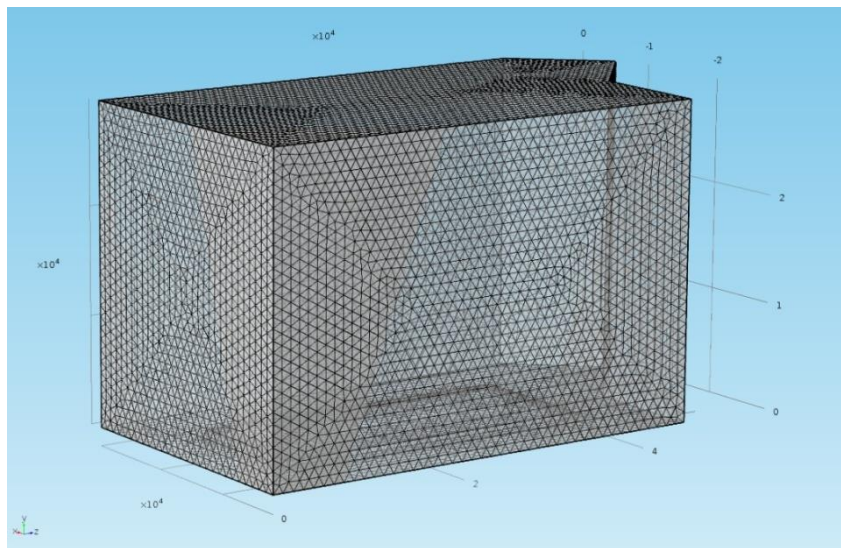


Figure 4-24 Meshing of the reverberant room with the acoustic material

Receiving Points	Source Points
R1 (1.10,1.00,1.10)	S1 (1.78,1.10,1.10)
R2 (1.10,1.00,1.97)	S2 (1.78,3.47,1.97)
R3 (1.78,2.24,1.10)	
R4 (1.78,2.24,1.97)	
R5 (1.10,3.47,1.10)	
R6 (1.10,3.47,1.90)	

Table 4-2 Source Placement and Points of Calculation

4.2.3 Reverberant room Modeling (Frequency Domain)

The goal of this implementation was the calculation of the eigenfrequencies and eigenmodes of the reverberant space. The finite element method for the Helmholtz equation was used. Finite element formulation of the Helmholtz Equation can be found in Atalla [172], Fahy [173] and Astley [174].

Since the formulation of the Helmholtz equation was utilized for this implementation there is not a source in the finite element formulation. Also because modeling is in the frequency domain a time step was not set.

Considering the incident condition of acoustic wave to the boundary surface, the normalized acoustic impedance of wall surfaces was calculated by substituting absorption of the walls into Equation 4-2 of the random incidence absorption coefficient with the assumption that the acoustic impedance is independent of the incidence angle. The absorption coefficients that were used in the finite element formulation were measured during the experimental procedure that is presented in section 5.2.1 of this thesis. Table 5-1 contains the values of the absorption coefficients.

The FE meshes were created to satisfy the requirement that $\lambda/h > 5$. Here, λ and h respectively denote wavelengths of upper limit frequencies of the octave band and the maximum nodal distance.

Eigenmodes and eigenfrequencies were extracted in the frequency area between 100 and 200 Hz. The purpose of these calculations was the comparison of the results for the resonant frequencies from the TDFEM, the finite element method in the frequency domain (Helmholtz equation) and the analytical solution. The comparison will be presented in the following chapter.

Chapter 5

5. ACOUSTIC MEASUREMENTS



In order to compare the results obtained using the finite element method, acoustic measurements were performed in the same reverberant room that was modeled for the application of the method. The acoustic measurement process is presented in two parts. For the first part the setup of the acoustic measurements is presented along with the considerations that have to be taken into account for precise measurements. Those were the appropriate choice of measurement method, the correct application of the method, calibration of the dodecahedral loudspeaker and calibration of the microphone. The second part includes the implementations in the reverberant room for two different cases. For the first case impulse response measurements were performed in the reverberant room. In the second case impulse response measurements were performed in the reverberant room with the presence of an acoustic material.

5.1 SETUP OF ACOUSTIC MEASUREMENTS

Major part of this thesis deals with the subject of correct calculation of the impulse response of an acoustic space. Hence the correct and precise measurement of the impulse response is important for the experimental confirmation of the method. The necessary considerations that led to the best possible measurement of the impulse responses are presented in the following sections.

5.1.1 Impulse Response Measurements

Appropriate measurement of the impulse response of an acoustic space is a particularly important process. As mentioned previously, the precise impulse response measurement is crucial because the majority of the acoustic parameters that characterize a space can be derived from it. Choosing the right method should be done with care. Room conditions are the ones that affect the choice of appropriate measuring method. Every acoustic space can be defined as a linear invariant system. Hence for the assumption of source and receiver immobility an impulse response $h(t)$ can characterize the space and the specific source and receiver points of measurement in that space. The measurement process involves the transmission of a signal from the source (input) and its recording from the receiver (output). For acoustic measurements the source is usually a dodecahedral speaker and the receiver is an omnidirectional microphone. The choice of the excitation signal is extremely important for the best possible impulse response measurements. The excitation signal should have some specific features for that purpose. The signal to noise ratio of the deconvolved impulse response must be the maximum. Signal to noise ratio can be improved if the excitation signal and measurement technique allow multiple averages of the measured output signal before the impulse response deconvolution process is started. Also reproducibility of the excitation signal is essential. Nonlinear artifacts also should be avoided in the impulse response measurements.

Setup and fundamentals for impulse response measurements are detailed in Ballou [175]. Those are:

- The sampling rate must be fast enough to capture the highest frequency component of interest. 44.1 kHz or 48 kHz are more than sufficient for acoustic measurements.
- The time length of the measurement must be long enough to allow the decaying energy curve to flatten out into the room noise floor.
- The measurement must have a sufficient signal-to noise ratio to allow the decaying tail to be fully observed. This often requires that the measurement be repeated a number of times and the results averaged.
- Repeatability of the results.

5.1.2 Impulse Response Measurement Techniques

The most common excitation signals are the Maximum Length Sequence (MLS), the Inverse Repeated Sequence (IRS), the Logarithmic Sine Sweep (LSS) and the Time-stretched pulses. The ones most used are the MLS and the LSS excitation signals. The acoustical impulse response measurements using the MLS technique were first proposed by Manfred Robert Schroeder and have been used with success in the field of acoustics. Shortly after the publication of MLS technique the IRS method was developed as an alternative theoretical option of the MLS for reducing distortion peaks [176]. The disadvantage of this method is the longer time needed for the calculation of the deconvolution by using high order FFT and IFFT filters [177]. The time-stretched pulses were introduced from Aoshima for the measurements of impulse responses [178]. This method aims at increased sound to noise ratio with the purpose of diminishing the peak distortions. Finally the logarithmic sine sweep method was first proposed and developed by Farina and Ugololli [179-181]. The method intended to overcome most of the limitations encountered in the other measurement techniques.

5.1.3 Choice of Measurement technique

The most prominent and widely used measurement techniques for the impulse response are the logarithmic sine sweep and the maximum length sequence. Studies by Farcas [177], Mateljan [182] and especially Stan [183] present a thorough comparison of the different impulse response measurement techniques.

The swept-sine is an optimal excitation signal for the fast measurement of an acoustical impulse response, without the averaging. It gives a better estimation than other excitation signals in acoustical time-variant environments and slightly nonlinear systems. Also in a noiseless environment the logarithmic sine sweep method seems to be the most appropriate. The swept-sine is not good excitation signal if the environment generates a large level of the colored or impulsive noise. It also gives a bad estimation in a system that has the frequency sensitive automatic gain control or automatic noise suppression. In those cases periodic noise excitation signals as the maximum length sequence give a better estimation.

In the presence of a nonwhite stationary noise the MLS technique outperforms the other methods. In a nonrandom noisy environment, where specific source is responsible for the noise, MLS method provides the best results and has better reproducibility. Same results can be obtained with the IRS technique, but the MLS method is more practical, faster and commonly used.

For this thesis at the beginning of the measurement procedure the methods were tested thoroughly in the reverberant room. After many measurements, it has been observed that both methods have very close results. However, it was obvious that the MLS method had greater stability and repeatability of results. This may be due to small background noise in the room. Therefore, it was preferred to follow the MLS method throughout the experiments.

5.1.4 Maximum Length Sequence (MLS) Measurement Technique

The acoustical impulse response measurements using the MLS technique were first proposed by Schroeder [184] and have been used in the field of room acoustics and loudspeaker design. Many papers discussed the theoretical and practical advantages and disadvantages of their technique. The MLS method presents great immunity in distortion [185]. Bleakley and Scaife [186] have shown that the signal-to noise ratio for the MLS sequence increases by 3 dB when the period length of the MLS sequence is doubled. Some practical aspects are discussed by Vanderkooy and Vorlander [187, 188].

A Maximum Length Sequence (MLS) [189] signal is a pulse signal with quasy-randomly exchanging states: +1 and -1. It can be analyzed as a binary sequence of N zeros or ones, that is periodic with a period $N = 2^m - 1$. The MLS can be generated with shift registers connected in a feedback.

Feedback connections are defined with some primitive polynomial of m -th order. For example, Fig. 5-1 shows generation of one MLS sequence with the polynomial $b(x) = x^4 + x^3 + 1$.

This is fourth order polynomial and the generated MLS sequence has length (period) $N = 2^4 - 1 = 15$.

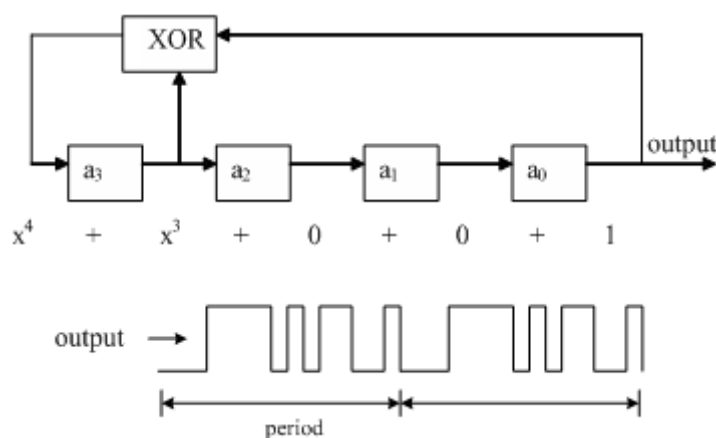


Figure 5-1 MLS sequence generation with shift registers

Every MLS sequence has following characteristics:

1. The autocorrelation function is constant $R_k^{xx} = \begin{cases} 1, & k = 0 \\ -1/N, & k \neq 0 \end{cases}$
2. DC value is equal to $1/N$
3. The crest factor is 1 (0dB)

For large N, a DC value ($1/N$) approaches zero. Then, the autocorrelation is equal to 1 for $k=0$, else it is equal to the zero. The power spectrum S_n and the autocorrelation R_k are Fourier pair:

$$S_n^{xx} = \sum_{k=0}^{N-1} R_k^{xx} e^{-j2\pi nk/N} = 1 \quad (5-1)$$

This power spectrum is a constant, which means that MLS sequence has a white spectrum. When system excitation has a white spectrum then cross-correlation of an output signal with an input signal is proportional to the system impulse response ($h_k \approx R_k^{xy}$).

The most important reason for the MLS popularity is the simple instrumentation necessary. A sound generator and a computer with fast correlation can compute the impulse response of an acoustic space. The correlation can be performed with an FFR algorithm or a Hadamard transform.

Another important aspect of MLS measurements is the low crest factor. In theory this can be the lowest among the other techniques. In practice this is not true due to the slight changes of an MLS signal through the output of the D/A converter "antialiasing" filter and passing through any other filter. Nevertheless a crest factor from 6dB to 9dB is common measurement for the MLS method on typical PC configuration.

The biggest problem with the MLS method seems to be the measurement of nonlinear systems. Sequences that are created from the MLS can generate

distortions that alter the impulse response of a nonlinear system. This problem is not so prominent for the measurement of acoustic spaces. In the case of nonlinearities the logarithmic sine sweep is better for measuring the frequency response of systems.

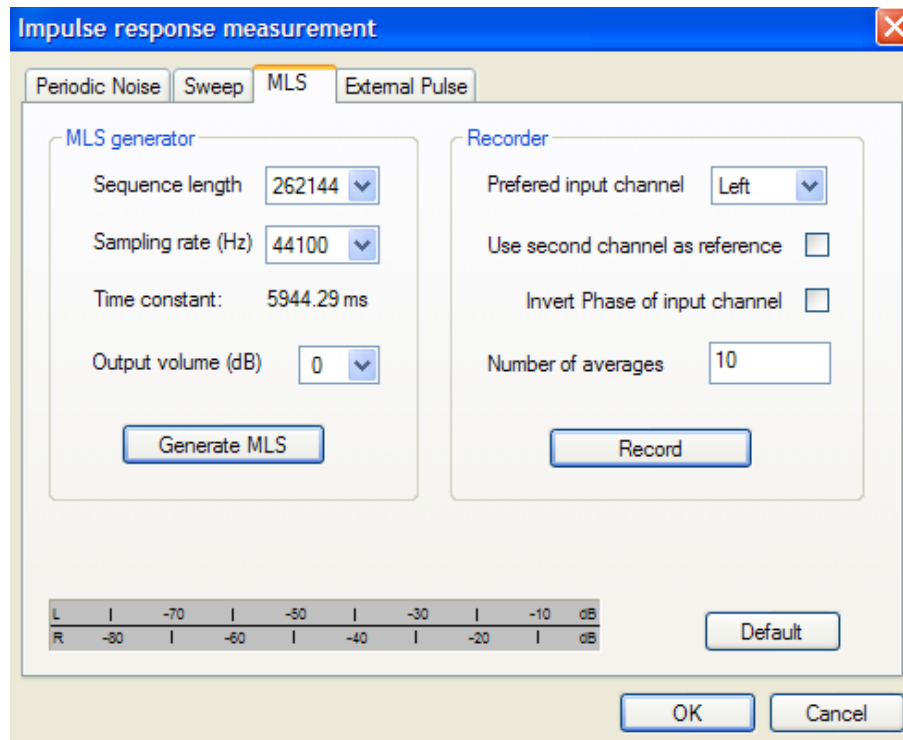


Figure 5-2 Dialog box for the measurement of the impulse response using MLS

5.1.5 Calibration of the loudspeaker

In order to measure the impulse response of a space, a point source is necessary which has to be omnidirectional. For this purpose a dodecahedral speaker is commonly used. There are also other techniques [190-192] for measuring the impulse response without the use of a dodecahedral loudspeaker but they are less precise.

The evaluation of a loudspeaker in the low frequency range usually requires measurements of distortion, frequency response and power output. A large and expensive anechoic chamber or a costly open-field outdoor testing site is

necessary for these measurements. Methods also exist with the use of a semi-anechoic and a reverberation room [193-195].

Small [196] pointed out that valid measurements could be made at low frequencies in any reasonable environment by sampling the pressure inside the enclosure. Keele [197] proposed a similar technique for loudspeaker assessment and calibration that was followed in this thesis. This loudspeaker test technique depends only on near field pressure measurements made in a nonanechoic environment. The necessary measurements of frequency response, distortion and power output can be measured in an easy and simple measurement. The relationship between near and far sound pressures depends only on two length constants and is independent of frequency. Therefore, Keele states, that low-frequency response can be measured quite simply by plotting the nearfield pressure (in dB) versus frequency. Total acoustic power output versus frequency can then be derived. The supporting experimental measurements show that loudspeaker system piston-range characteristics can easily be measured by sampling the nearfield pressure with a test microphone held close to the acoustic radiator. Valid nearfield measurements may be taken in any reasonable environment without the use of an anechoic chamber or large outdoor test site. Experimental measurements using the nearfield technique show excellent agreement with more traditional test methods.

For this thesis the dodecahedral speaker frequency characteristics were measured by sampling the nearfield pressure with a test microphone. The spectrum levels were extracted. A dedicated software was used for applying the frequency compensation. The following equation was used for the loudspeaker:

$$\text{Corrected level (dB)} = \text{Measured level (dB)} - \text{Compensation level (dB)}$$

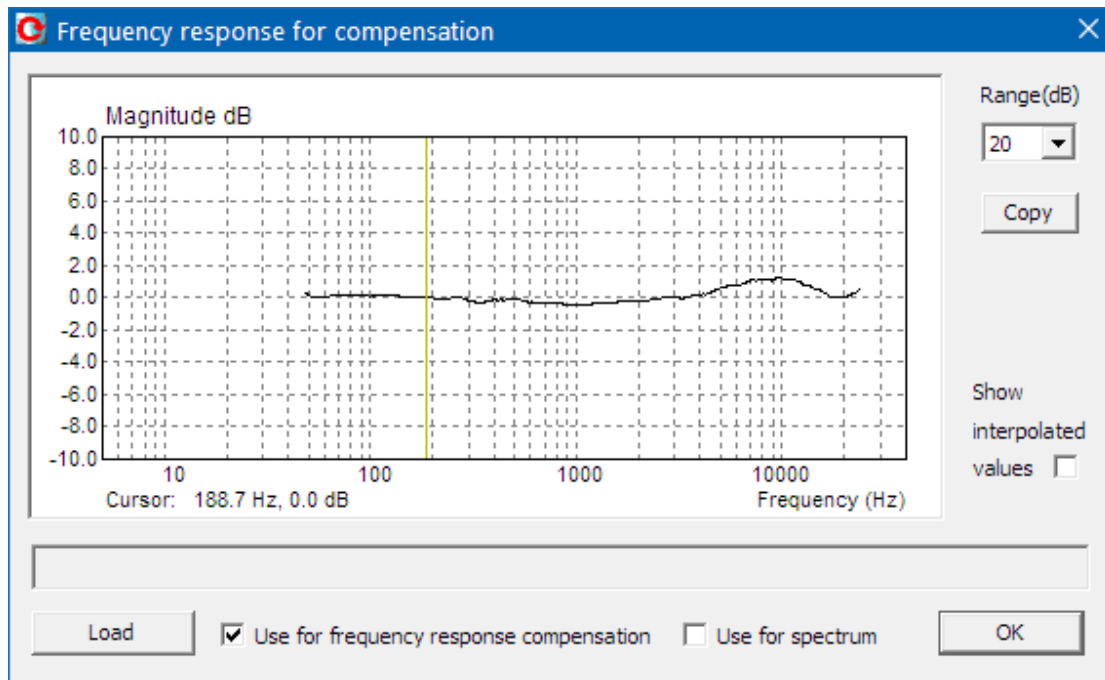


Figure 5-3 Frequency Response for Compensation (Loudspeaker Calibration)

5.1.6 Calibration of the Microphone

Many are the methods used for the correct calibration of the microphone for the impulse response measurements. Frederiksen [198] states that, ideally, the frequency response of a microphone should be measured with a sound pressure that is either known as a function of frequency or known to be constant over the frequency range of interest. This specific requirement is very difficult to implement with an acoustic source.

An alternative option is to use an electrostatic actuator which can produce a force, or say an electrostatic pressure, directly on a microphone diaphragm that is independent of the frequency. For this thesis frequency response calibration performed with the use of an electrostatic actuator. The actuator method is relatively cheap and easy to perform. The method is described in detail in the standard IEC61094-6 [199] and in the AIP Microphone Handbook [200]. The actuator can simulate a sound pressure on the microphone diaphragm, if this is electrically conducting. An actuator is usually a flat and very stiff metallic plate

with holes or slits that make it acoustically transparent. During the operation, the actuator is placed close to and in parallel with the microphone diaphragm. Typically, 800V DC and 30V AC are applied between the actuator and the diaphragm. These voltages will, with the most commonly used models of actuators, generate an equivalent sound pressure of about 1 Pa (94 dB).

For this thesis a cylindrically shaped condenser microphones was used with good acoustic properties, such as high stability of sensitivity and an influence of ambient conditions that is relatively small and predictable. The microphone was connected with the microphone preamplifier to the soundcard input. The sound actuator was attached on the microphone for the calibration process.

5.2 IMPLEMENTATIONS

For the first case impulse responses were measured in a reverberant room for the calculation of acoustic parameters and frequency responses. For the second case impulse responses were measured in a reverberant space with the use of acoustic panels for the calculation of the absorption coefficient of the material.

5.2.1 Reverberant room Measurements

The sound field in a reverberant space with a lightly damped wall was measured in this study with the use of a Maximum Length Sequence (MLS) signal. The reverberant room to be computed and measured here is depicted in Fig. 5-4. The volume and the surface area of the room are, respectively, 38.71m^3 and 71.17m^2 . Inner walls of the room are made of concrete.

The impulse responses at 60 receiving points were measured as depicted in Fig. 5-4. The sampling frequency of the measurement was 44.1 kHz. An appropriate sequence length (262144 samples) and time constant (approximately 6 seconds) for the MLS signal was chosen according to the expected reverberation time. Ten

iterations were performed for each of the sixty measurement points. The settings are depicted in Figure 5-2. Averaging was used for better signal to noise ratio and to reduce the temperature fluctuation effect. Averaging several measurements performed at one microphone/loudspeaker position in order to reduce the measurement uncertainty caused by statistical deviations.

The variations of temperature and hence the sound velocity with time and position cannot be entirely avoided but the effects which are caused by these inhomogeneities can be considered to be small for frequencies below 1 kHz.

An omnidirectional dodecahedral loudspeaker (Type D012; 01 dB-Stell) was placed at a height of 1.5 m, as depicted in Fig. 5-4. The assessment and calibration of the dodecahedral loudspeaker was achieved after near field sound pressure measurements of the impulse response were performed. The frequency range of this study is such that the method that was used is adequate for calibration.

In addition, a microphone (Type 4190; Earthworks) was placed 1.2 m above the floor for each of the 60 measurements.

Table 5-1 lists the average measured reverberation times and average absorption coefficients of the room surfaces for octave bands with center frequencies of 125, 250 and 500 Hz. The reverberation times are spatial average values of 60 receiving points calculated using the maximum length sequence method. The values of the absorption coefficient were calculated by substituting measured reverberation times into the Sabine equation on the assumption that the sound field in the room is sufficiently diffuse. However, the Schroeder frequency of the reverberant room is approximately 550 Hz. This indicates that the sound field in the reverberation room is insufficiently diffuse below 500 Hz. The average absorption coefficient is going to be used in the section of the setup of TDFEM for the calculation of the impedance of the walls.

From the measured impulse responses, acoustic parameters were derived and will be discussed and compared with the ones calculated from the TDFEM later in this study.

	125 (Hz)	250 (Hz)	500(Hz)
RT (sec)	5.16	3.11	2.65
SD (sec)	0.70	0.42	0.21
\bar{a}	1.70×10^{-2}	2.82×10^{-2}	3.30×10^{-2}

Table 5-1 Average Measured Reverberation times, standard deviations and average absorption coefficients of room surfaces

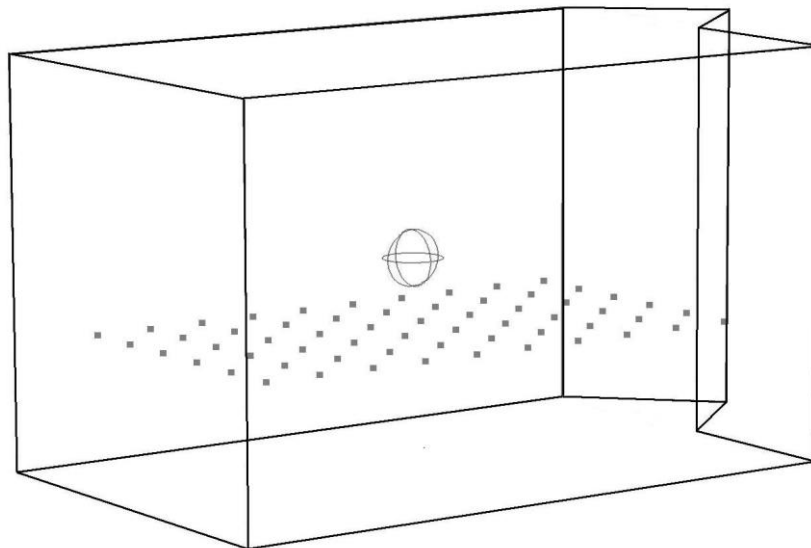


Figure 5-4 Reverberant room with measured and computed points



Figure 5-5 Maximum Length Sequence Impulse Response Measurements

5.2.2 Reverberant room with Absorptive Material Measurements

The measurements were carried out in a reverberant room of the Technical University of Crete, Greece (Fig. 5-6) with a volume and surface area of respectively, 38.71 m³ and 71.17 m². Inner walls of the room are made of concrete.

The specimen comprised of five acoustic panels covering an area of 315 x 130 cm, which for testing purposes were laid directly over the floor so that no part was closer than 0.63 m to any edge of the boundary of the room. The specimen comprised of rock wool (measured thickness 50 mm), which was overlaid synthetic open weave facing fabric. The perimeter edges of the specimen were shielded for test by a 50 x 25 mm timber batten framework. The test was conducted with the specimen installed within the chamber and also in the

absence of the specimen and any associated framework. The test specimen reached equilibrium with respect to temperature and relative humidity in the room before tests were carried out.

The measurements were made with the use of a Maximum Length Sequence signal in accordance with ISO 354. The sampling frequency of the measurement was 44.1 kHz. An appropriate sequence length and time constant for the MLS signal was chosen according to the expected reverberation time. Ten iterations were performed for each of the measurement points. Averaging was used for better signal to noise ratio and to reduce the temperature fluctuation effect. Same as the previous measurement, as the ISO suggests, several measurements performed at one microphone/loudspeaker position in order to reduce the measurement uncertainty caused by statistical deviations.

The variations of temperature and hence the sound velocity with time and position cannot be entirely avoided but the effects which are caused by these inhomogeneities can be considered to be small for frequencies below 1 kHz.

Six microphone positions were used for each of two loudspeaker positions to obtain a good average at each of the one-third octave intervals from 100 Hz to 500 Hz as prescribed in the Standard. A microphone (Type 4190, Earthworks) was placed for each of the measurements. An omnidirectional dodecahedral loudspeaker (Type DO12, 01 dB-Stell) was placed at two loudspeaker positions which were at least 3 m apart. The assessment and calibration of the dodecahedral loudspeaker was achieved after near field sound pressure measurements. The frequency range of this study is such that the method that was used is adequate for calibration. Absorption Coefficients (α_s) of the specimen were calculated using equation 4-21 according to ISO 354.

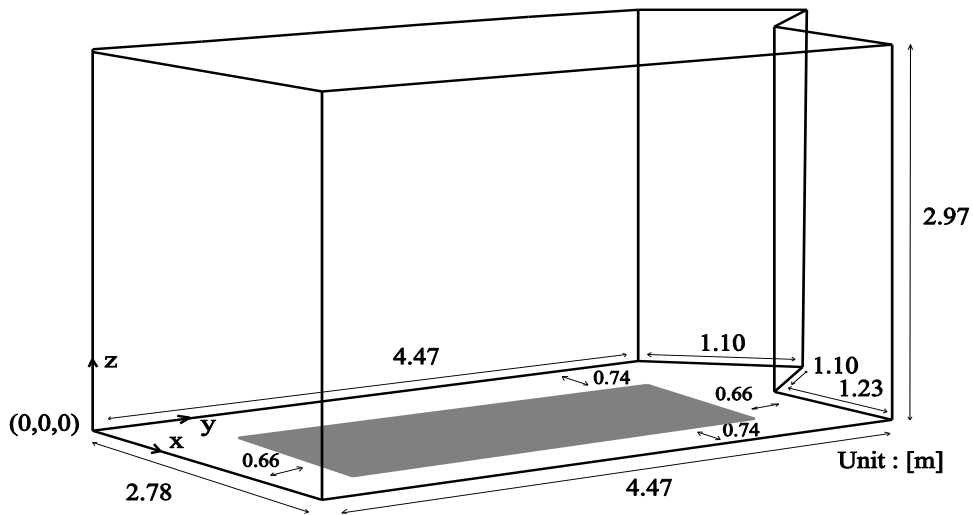


Figure 5-6 Reverberant room with acoustic material

Reverberant Room Conditions	Air Temperature	Relative Humidity	Air Pressure
Empty Room	18°C	78%	765 mmHg
Room with Specimen	18°C	77%	765 mmHg

Table 5-2 Reverberant Room Conditions

Receiving Points	Source Points
R1 (1.10,1.00,1.10)	S1 (1.78,1.10,1.10)
R2 (1.10,1.00,1.97)	S2 (1.78,3.47,1.97)
R3 (1.78,2.24,1.10)	
R4 (1.78,2.24,1.97)	
R5 (1.10,3.47,1.10)	
R6 (1.10,3.47,1.90)	

Table 5-3 Receiving and Source Points



Figure 5-7 Reverberant Room with Acoustic Material

Chapter 6

6. COMPARISON OF FEM MODELING AND MEASUREMENTS



Comparison of the results of the finite element method and the actual measurements in a space will be presented for three different cases. In the first case the comparison for measurements and calculations made in a reverberant room will be displayed. The impulse responses, acoustic parameters, frequency responses and cumulative spectral decays will be presented and discussed. In the second case, the measurements and calculations made in the reverberant room with the presence of absorbent material will be used for the extraction of the absorption coefficient of the material. The results will be presented along with a discussion of the findings. Finally the eigenfrequencies and eigenmodes of the room will be presented with the use of finite element method (Helmholtz equation). A comparison will be presented for the finite element method (Helmholtz equation), the time domain finite element method and the analytical results.

6.1 IMPULSE RESPONSES, FREQUENCY RESPONSES AND ACOUSTIC PARAMETERS

After the modeling, the pressures at 60 points of the reverberant room were computed. The impulse responses were calculated from the extracted pressures for each time step with the use of the finite element method in the time domain. From the calculated impulse responses, acoustic parameters were derived and will be discussed and compared with the ones measured with the MLS technique.

6.1.1 Impulse Response

The precise calculation of the impulse response is the prime goal of the thesis. Accurate modeling will enable accurate representation of the frequency responses and cumulative spectral decays and also precise calculation of the acoustic parameters. In order to evaluate the quality of modeling, the results of the calculation will be compared with the actual measurements in the reverberant room [1].

Comparisons of the computed and the measured impulse responses at three arbitrary receiving points at times up to 0.4 s are portrayed in Figure 6-1. The fine structures of the computed impulse responses correspond closely to those of the measured ones, irrespective of receiving point. Similar results were obtained for the other points in this investigation.

The cross-correlation coefficient between the measured and calculated impulse responses was assessed in order to quantify the accuracy of the results. The coefficient is calculated and averaged with 0.05 sec steps at all receiving points. The values of the coefficient are 0.89 for 0.1 sec and 0.82 for 0.5 sec with a decreasing step over time. The value of the coefficient and hence the accuracy of the TDFEM is high but further improvement of the method is necessary. Although high correlation coefficients are obtained in the early time region of the impulse responses, the value decreases gradually over time. This is a sign that there might be a factor which accumulates over time and affects the

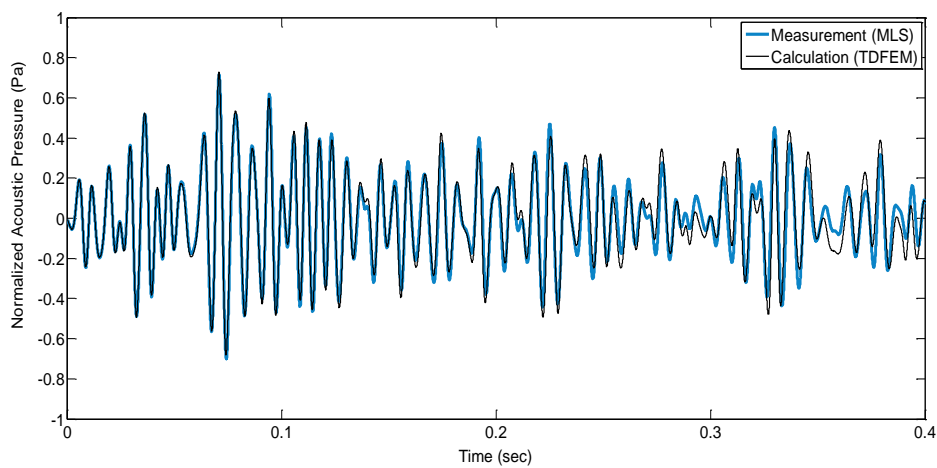
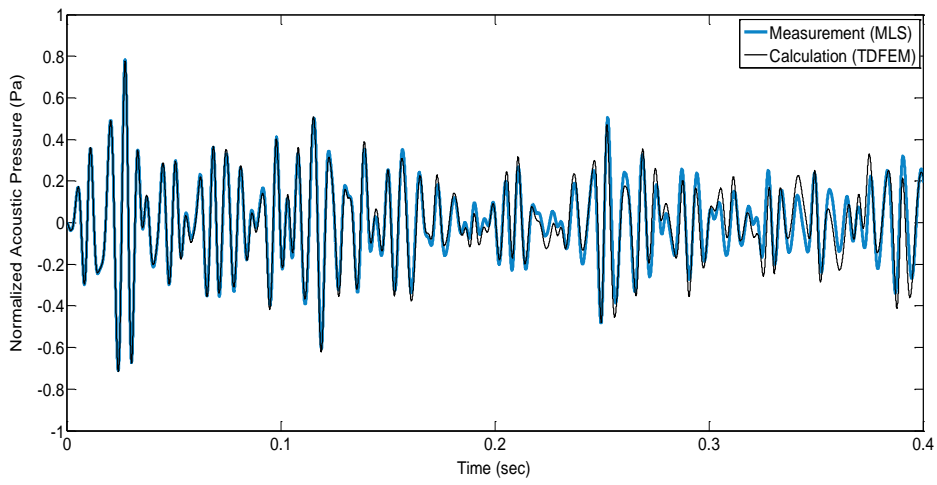
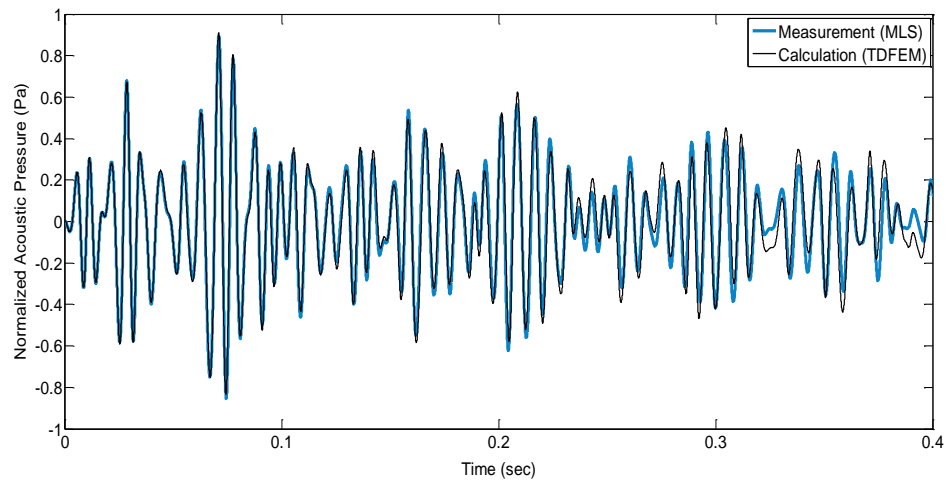


Figure 6-1 Measured and Computed Impulse Responses for three points in the Reverberant Room

correspondence between measured and calculated impulse responses. A review of the probable causes of this inaccuracy follows in the next chapter.

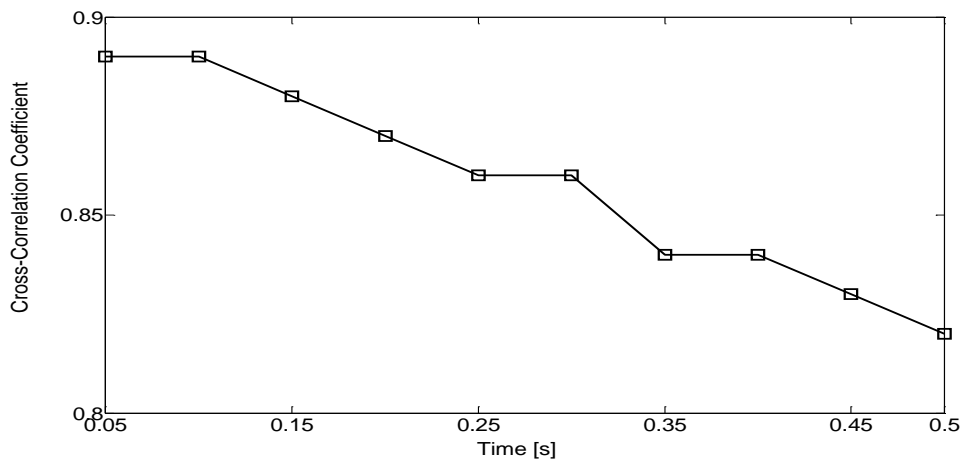


Figure 6-2 Averaged cross-correlation coefficients for Measured and Calculated impulse responses

6.1.1.1 Probable causes for differences between measured and calculated impulse responses

Although the convergence between the results is satisfactory, it is important to investigate the reasons for the differences between measured and calculated impulse responses in order to find ways to improve the modeling method. Initially, there were some hypotheses about the decrement of the correlation coefficient over time for the impulse responses. A probable cause for the decrement of the coefficient was assumed to be the insufficient modeling of the impedance of the boundary conditions. As it was discussed earlier the normalized acoustic impedance of wall surfaces were calculated by substituting the random incidence absorption coefficient into Equation 4-2 with the assumption that the acoustic impedance is independent of the incidence angle.

Later on, comparison of the impulse responses that were obtained for different meshes (presented in section 4.1.4) showed that while the impulse responses in the initial stages are identical, the differences are increasing over time. This is a clear indication that the effect of the mesh size on the time domain finite element

method creates these effects on the impulse responses. This seems to justify the gradually decreasing cross correlation coefficient of the impulse response. There is an error that accumulates over because of the insufficiency of the mesh size.

Another cause of uncertainty may also be due to the measurement process. The dodecahedral loudspeaker simulates a point omnidirectional source. This is not always the case and uncertainties are caused by source directivity in room acoustics investigations [201]. Martin [202] states that most of the commercial dodecahedron loudspeakers comply with the maximum allowed directional deviations of the source specified in the standard. While this requirement is adequate for the derivation of reverberation times, for the detailed investigation of the room impulse response time structure, however, the directivity of the source becomes more important. This problem has been addressed in the finite difference method in the time domain [114, 203]. An improvement of the measurements is proposed by Martellotta [204] who suggest a stepwise rotation of dodecahedron sound source to improve the accuracy of room acoustic measure. Also Kleiner [205] states that diffraction of the dodecahedral loudspeaker edges plays a role for the measurement of an accurate impulse response. In conclusion, we can say that there will always be a slight difference in the results between measurements and calculations because of the influence of the source.

Another cause of uncertainty may be because of the measurement software. There have been measured variations between standard room acoustic measures for impulse response measurements [206]. There is also might be a variation for calculating acoustic parameters between software implementations [207]. Hence there seems to be a limit to measurement accuracy of impulse responses due to the measurement process.

Finally, another cause of variations might also be a background noise that existed in the reverberant room during the measurements. The effect of background noise is also shown in the frequency response measurements to be presented in the next section.

6.1.2 Frequency responses- Cumulative Spectral Decays

Frequency responses and Cumulative Spectral Decays of the space were chosen to be presented in this study as the most important graphs for room acoustic analysis. These graphs are important for a representation of a room or an enclosed space of any dimensions. Frequency responses and Cumulative Spectral Decays of the space were derived from the measured and calculated impulse responses [2]. The results are presented in the following figures both for the TDFEM and MLS measurement for frequencies up to 200 Hz. The frequency responses are depicted for three arbitrary points of measurement in the reverberant room. Similar results were obtained for the other points of measurement and calculation.

Comparing the measured and calculated frequency responses shows that TDFEM modeling has managed to accurately predict the resonant frequencies at the measurement points. There is also a strong correlation with the relative levels in the resonant frequencies in the measurement points. At low frequencies there is a difference that is probably due to background noise that existed in the room. In general there are small variations due to differences observed in impulse responses measurements and calculations as previously stated.

As a second step the cumulative spectral decays were extracted from the measured and calculated impulse responses. In essence the cumulative spectral decays are a representation of the frequency response in the time domain. This is particularly important in the field of room acoustics because it serves as an additional indication for the problematic resonant frequencies in the room. As a result the appropriate acoustic treatment can be chosen to improve these problematic frequencies. The results are compared in Figure 6-4 for frequencies up to 200 Hz and in the time domain. The results are presented in different graphs for better comparison. There is a good correlation of the resonant frequencies between the measured and computed results. There is also a strong correlation with the relative levels in the resonant frequencies in the measurement points. Similar with the frequency responses at low frequencies

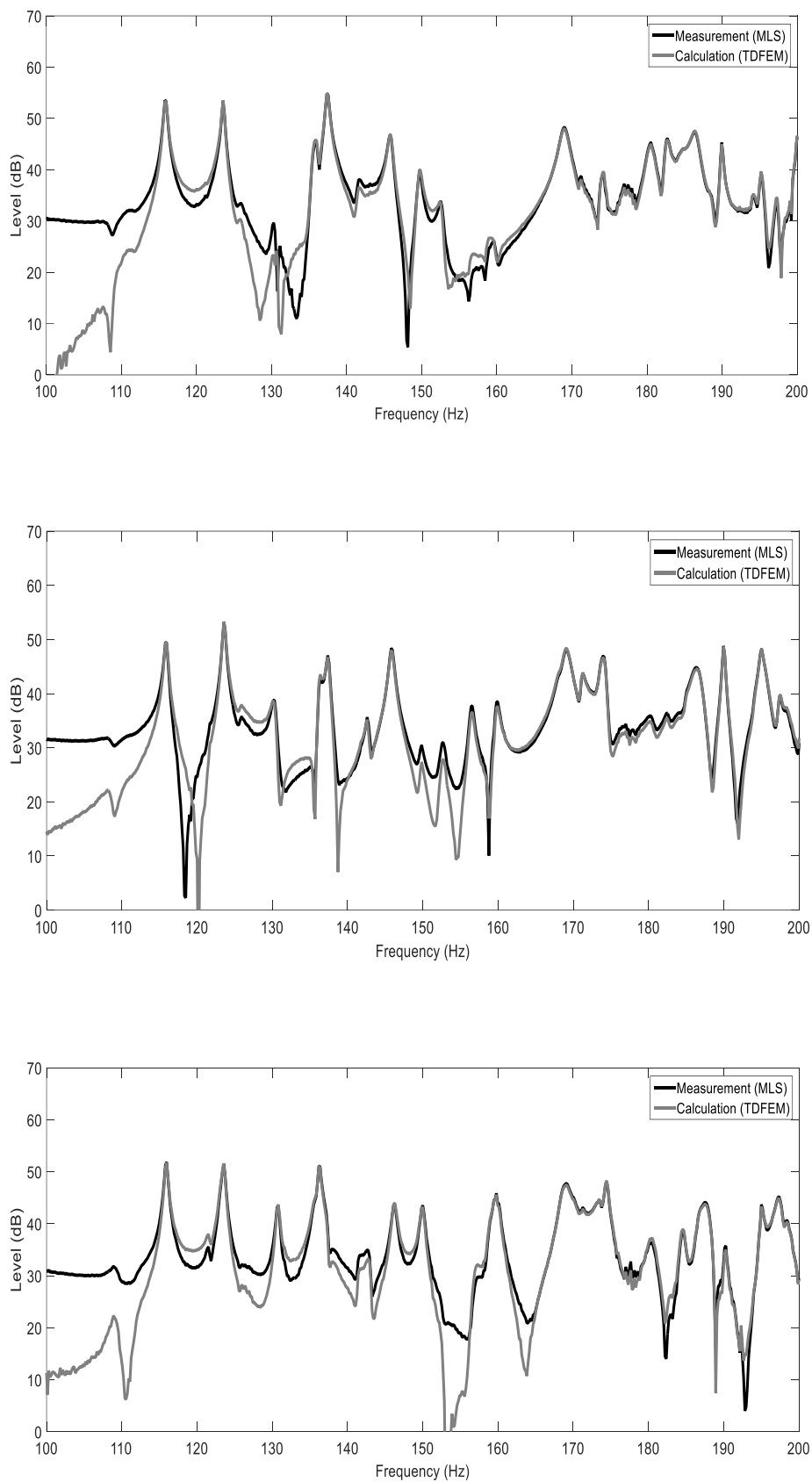


Figure 6-3 Measured and Computed Frequency Responses for three points in the reverberant room

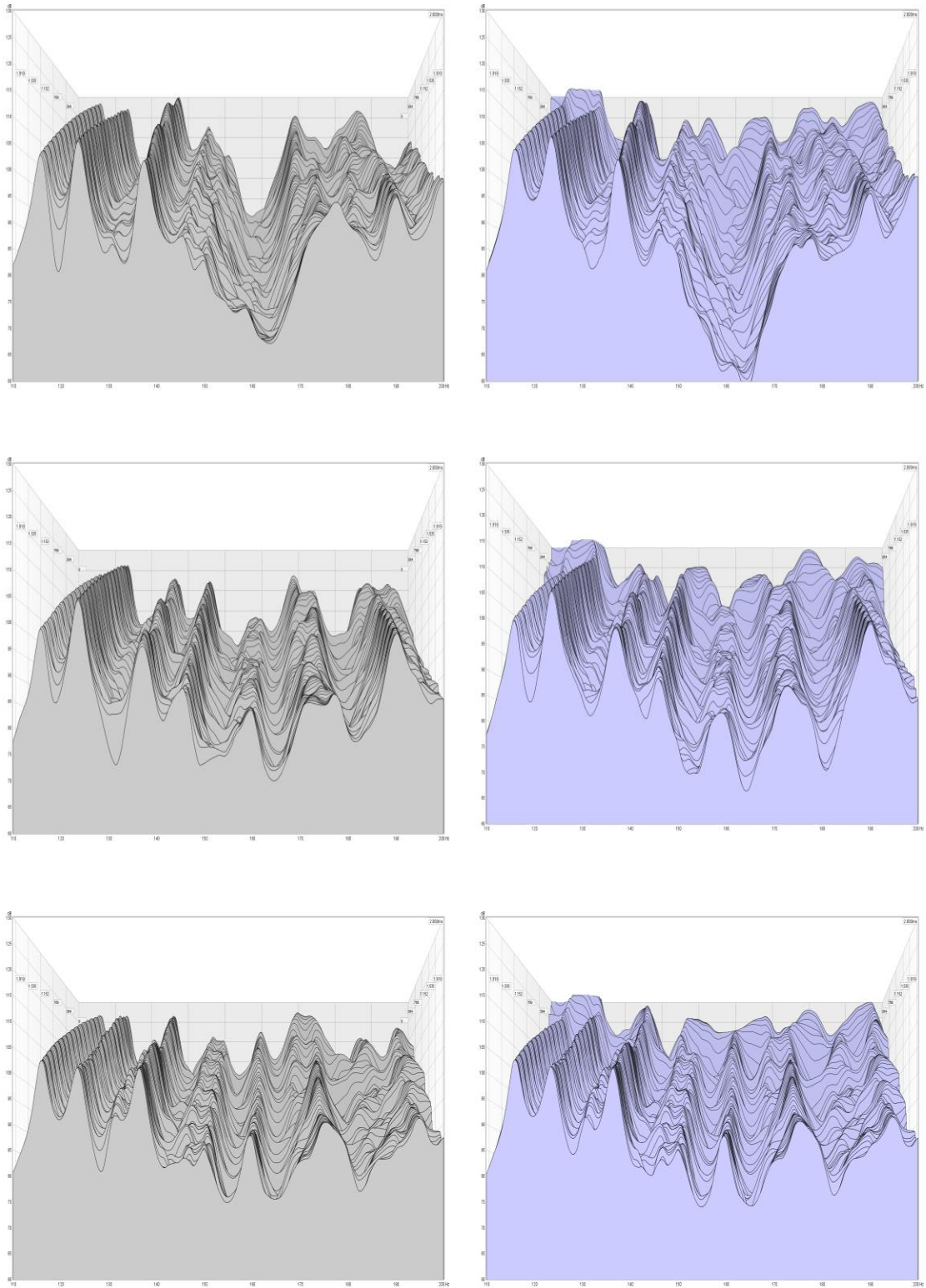


Figure 6-4 Measured (gray) and Computed (light blue) Cumulative Spectral Decays for three points in the reverberant room

there is a difference that is probably due to background noise that existed in the room. In general there are small variations due to differences observed in impulse responses measurements and calculations as previously stated. We note that the method has managed to predict the decay rate of the main resonant frequencies.

6.1.3 Acoustic parameters

Acoustic parameters of the reverberant space were derived from the measured and calculated impulse responses. The reverberation time, early decay time, clarity (C_{80}) and definition (D_{50}) were chosen to be presented in this thesis as some of the most important parameters for room analysis. These parameters are adequate for a satisfying representation of the room characteristics.

The results are presented in the following tables both for the TDFEM and MLS measurement and for octave bands with center frequencies of 125, 250 and 500 Hz. The results are presented in the tables for six arbitrary points in the reverberant room.

RT (sec)	125 (Hz)		250 (Hz)		500 (Hz)	
	MLS	TDFEM	MLS	TDFEM	MLS	TDFEM
1	5.01	5.00	3.10	2.75	2.61	2.45
2	5.34	5.11	3.30	3.43	2.46	2.62
3	5.96	5.04	2.88	3.29	2.84	2.57
4	5.07	4.99	2.59	3.00	2.94	2.54
5	5.49	5.12	3.15	2.89	2.55	2.70
6	5.55	4.96	3.08	2.93	2.54	2.49

Table 6-1 Measured and calculated Reverberation Time of the reverberant space

EDT (sec)	125 (Hz)		250 (Hz)		500 (Hz)	
	MLS	TDFEM	MLS	TDFEM	MLS	TDFEM
1	4.63	4.96	3.03	2.80	3.01	2.88
2	5.44	4.97	2.92	3.24	3.03	2.72
3	5.52	4.89	2.89	3.41	2.94	2.94
4	5.10	4.86	1.96	3.10	2.49	2.87
5	5.06	5.02	3.09	3.16	2.64	3.03
6	5.20	4.84	2.26	3.02	2.36	2.96

Table 6-2 Measured and calculated Early Decay Time of the reverberant space

C ₈₀ (dB)	125 (Hz)		250 (Hz)		500 (Hz)	
	MLS	TDFEM	MLS	TDFEM	MLS	TDFEM
1	-4.65	-4.13	-5.82	-5.07	-5.32	-0.21
2	-8.17	-5.80	-1.54	-3.56	-2.87	-0.44
3	-8.22	-6.62	-2.66	-5.96	-0.54	-2.11
4	-3.15	-3.26	-2.92	-7.52	-0.71	-1.40
5	-6.85	-3.96	-0.92	-1.71	-1.20	-0.96
6	-3.65	-3.10	-4.43	-5.72	-4.08	-1.95

Table 6-3 Measured and calculated Clarity of the reverberant space

D ₅₀ (%)	125 (Hz)		250 (Hz)		500 (Hz)	
	MLS	TDFEM	MLS	TDFEM	MLS	TDFEM
1	9.9	11.6	11.4	17.8	8.8	29.3
2	10.9	17.0	31.4	18.0	22.6	29.9
3	10.7	11.3	20.8	17.2	35.3	44.1
4	22.7	16.7	20.1	8.2	27.4	35.1
5	8.5	19.7	35.3	22.6	27.3	47.6
6	21.0	16.9	20.8	8.6	16.8	31.8

Table 6-4 Measured and calculated Definition of the reverberant space

To evaluate the similarity between the measured and computed acoustic parameters the averages are presented in table 6-5.

Average	125 (Hz)		250 (Hz)		500 (Hz)	
	MLS	TDFEM	MLS	TDFEM	MLS	TDFEM
RT(sec)	5.42	5.05	3.02	3.05	2.66	2.56
EDT(sec)	5.16	4.92	2.69	3.12	2.75	2.88
C ₈₀ (dB)	-5.78	-4.47	-3.05	-4.92	-2.45	-1.18
D ₅₀ (%)	13.9	15.5	23.3	15.4	23.0	36.3

Table 6-5 Averages of measured and calculated acoustic parameters

The results for the measured averages correspond closely to the calculated ones. The calculated averages succeeded to predict the decrease in the reverberation time and early decay time for higher frequencies. Reverberation time is the most important acoustic parameter. The differences between the calculated and the measured values are small which allows practical use of results in acoustic studies of rooms. Also differences in specific measurement points are small. Combining results with results of geometric acoustics allows for a complete study in the whole frequency spectrum. Similar results are also observed for the values of early decay time. We can see that the results for reverberation time are not the same as the early decay time which shows that the space is not

completely diffused. Nevertheless the combination of results both for RT and EDT will allow acoustic treatment for a specific point in an acoustic space. With respect to clarity and definition, we see that we have good results but with a slight bigger variation from the measured values. This is may be due to the fact that the values arise from the comparison of the first section of the impulse response with the rest of the impulse response. More research on real rooms about the accuracy of measurements for room results is necessary.

6.1.4 Application of the TDFEM in real life rooms

The results for the reverberant room show that the method can provide good results for the impulse responses, frequency responses, cumulative spectral decays and the acoustic parameters. An important question that rises, is if the method is applicable in real life rooms. Two seem to be the most important issues.

The first one is the computational cost which currently prohibits the method from widespread use. The use of the method over the entire frequency range (up to 20 kHz) at present time is prohibitive. However, there is the possibility of applying the time domain finite element method up to the Schroeder frequency for real life rooms. The method can then be combined with geometrical acoustics for higher frequencies. Hence a hybrid method would be a possible practical option.

The second issue seems to be the application of boundaries. For this thesis the boundaries are locally reacting. In reality, there are many kinds of boundary conditions which correspond to different acoustic materials such as porous absorbers, combination of porous absorbers, panel absorbers, Helmholtz resonators etc. There would be a problem in precisely defining the boundary conditions for all the absorbent surfaces that may exist in a space. For example, the modeling of a common object that may exist in a space e.g. a chair would require different finite element modeling for different parts. A probable solution would be to apply locally reacting boundary conditions for every absorptive

material in a room, similar with the approach in geometrical acoustics (absorption coefficient). The results of this approach in real life rooms will be examined in a future study.

6.2 ABSORPTION COEFFICIENT OF ACOUSTIC MATERIAL

In the second part of this thesis the ability of calculating impulse responses with the use of the finite element method in the time domain was utilized for the computation of the absorption coefficient of an acoustic panel. For that purpose at first the acoustic coefficient of an acoustic panel was measured in the reverberant space according to the ISO 354. The ISO requests the procedure to be performed in a reverberant space. The same process was performed virtually with the use of the TDFEM. The results are compared in the following section.

6.2.1 Absorption Coefficient

The sound absorption coefficients for third octave bands were calculated from the mean reverberation times for the empty room and the room with the sample installed after. The reverberation times were extracted from the impulse responses both for the measured and calculated ones [6]. The specimen is treated as a planar sample as suggested by the ISO 354. In Figure 6-6 the absolute error and the percent error for the measured and calculated absorption coefficient are presented. The mean absolute error is 0.04 sec. These results indicate that the absorption coefficient can be calculated using the method with acceptable accuracy. Consequently, the method may be considered to have sufficient reliability for calculating absorption characteristics of porous materials and acoustic panels with variant shapes.

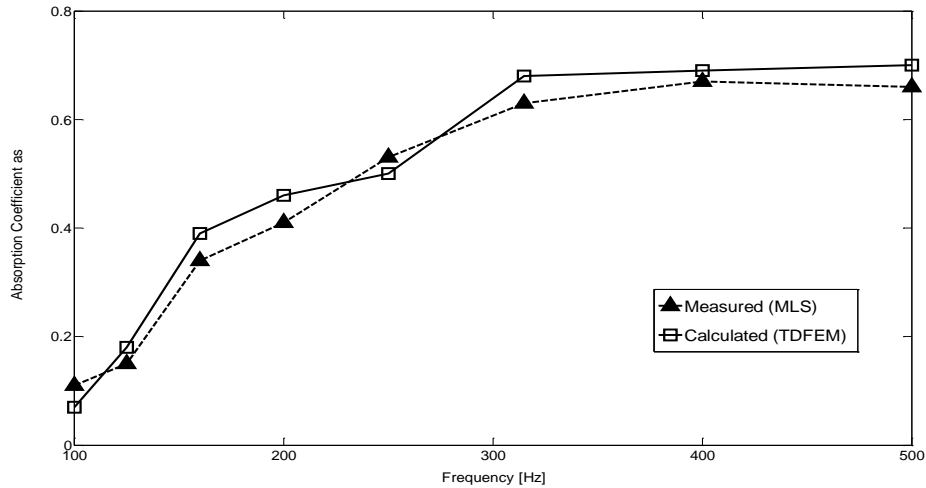


Figure 6-5 Measured and calculated absorption coefficient of an acoustic panel

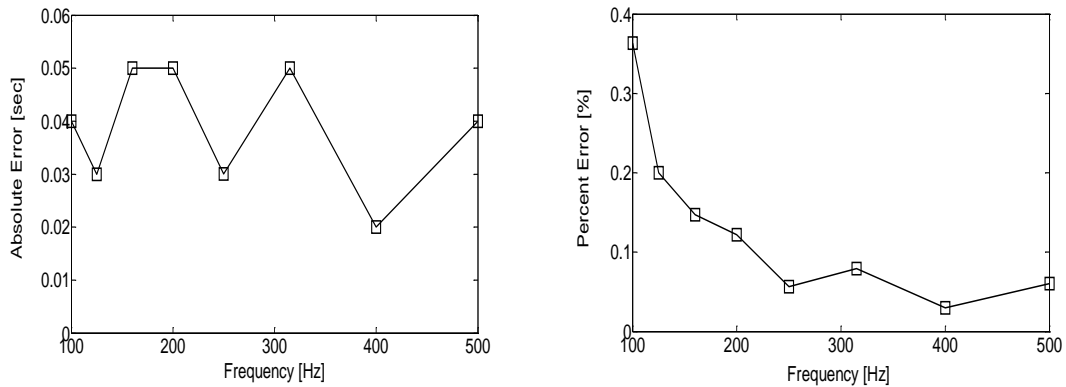


Figure 6-6 Absolute error and percent error for measured and calculated absorption coefficient of an acoustic panel

6.2.2 Applications for a 'virtual' reverberation chamber

The main goal of this part of the thesis was the utilization of the finite element method in the time domain in order to calculate the absorption coefficient of an acoustic panel. The results support this goal and show that the method can be useful in practical real world applications. The method is yet to be applied in reverberation chambers which are in full agreement with the specification of the ISO 354 in order the applicability of the method to be checked and the results to be refined.

A possible application of the method is that it can be applied for the development of acoustic panels. Acoustic panels are created in various shapes for which it is difficult to ascertain their absorption coefficient before they are built. This process can play a major role in the manufacturing process. It could also be combined with an optimization process in order to achieve the best results. In this way, novel shapes of absorption panels could be tested and validated in a virtual environment with minimum cost.

Another possible application of this approach is that other acoustic characteristics of materials can be tested in a virtual environment. An obvious possibility is the random incidence scattering coefficient which also requires a reverberation chamber for its accurate measurement [208, 209].

6.3 EIGENFREQUENCIES-EIGENMODES

In the previous sections by using the finite element method in the time domain, we were able to measure a room's impulse response, the acoustic parameters that characterize it as well as the frequency responses and cumulative spectral decay. From the frequency responses we can observe the eigenfrequencies of the room that exist at the points of measurement. The eigenfrequencies can also be found using the finite element method in the frequency domain (Helmholtz equation). Also with the use of equation 2-28 we can calculate eigenfrequencies of the acoustic space. The purpose of this chapter is to compare the eigenfrequencies for these three cases.

Figure 6-7 presents the eigenfrequencies and the eigenmodes for four frequencies in the reverberant room. In figure 6-7 those frequencies can be identified as resonant from the frequency response obtained from the time domain finite element method in three different points in the acoustic space. Table 6-6 presents the comparison of the eigenfrequencies along with the solution for the eigenfrequencies from equation 2-28. The results obtained from the TDEFEM, the FEM element (Helmholtz) and the analytical solution have very close values.

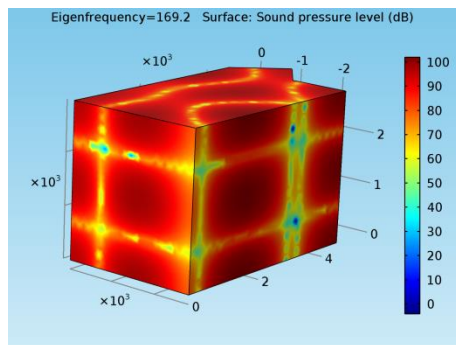
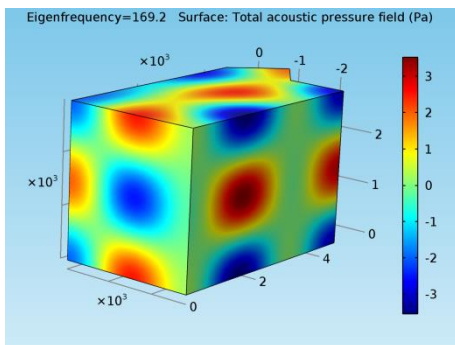
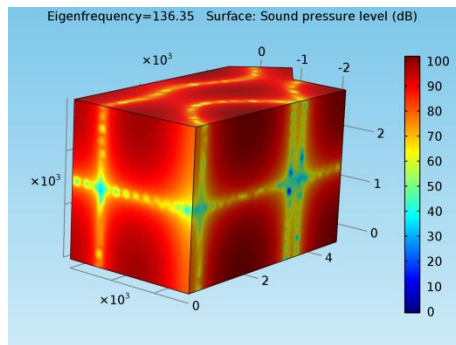
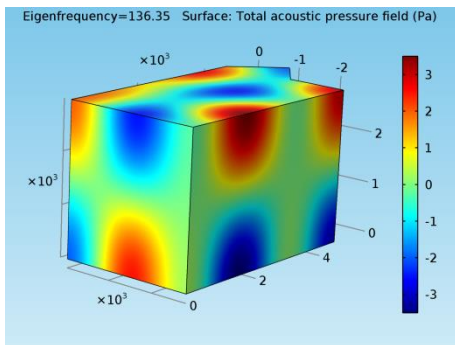
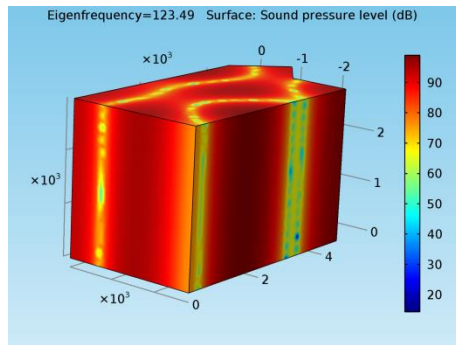
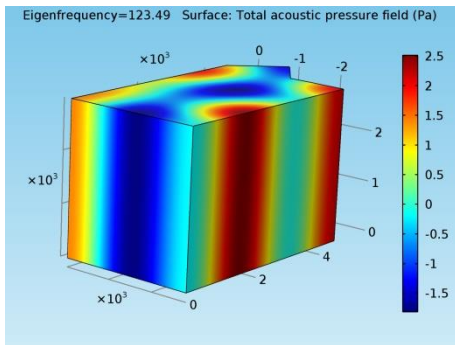
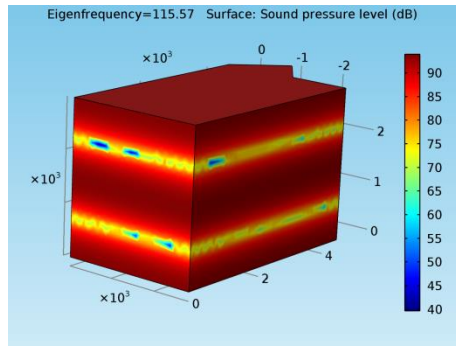
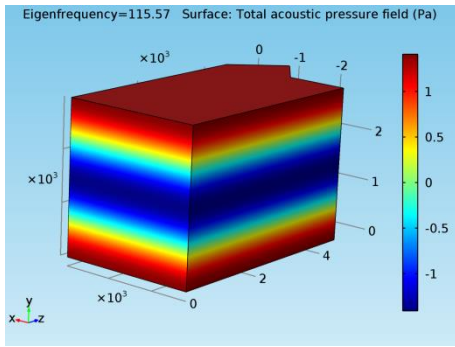


Figure 6-7 Eigen frequencies, Eigen modes and Sound Pressure Levels in the Reverberant Room

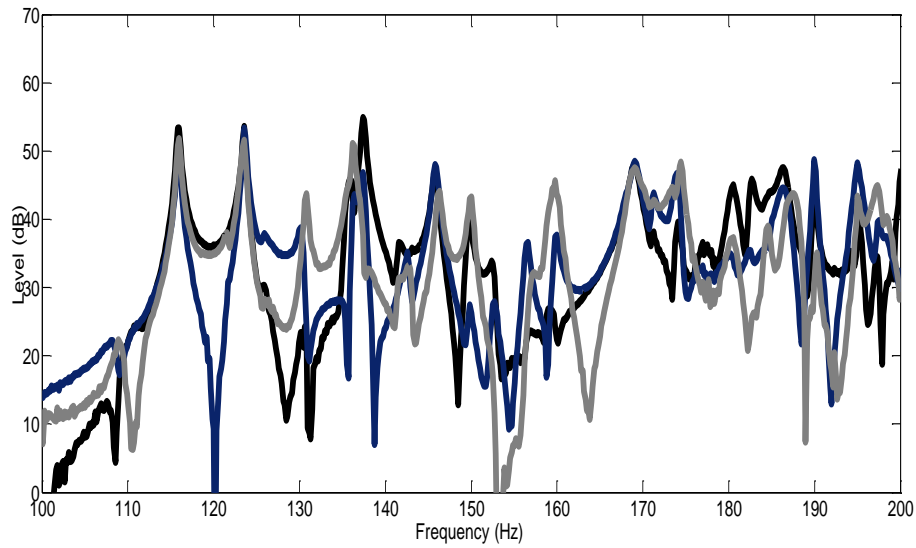


Figure 6-8 Calculated frequency responses for three measurement points in the reverberant room

Analytical	FEM (Helmholtz)	TDFEM
115.49	115.57	115.98
123.38	123.49	123.32
136.23	136.35	136.03
169	169.2	168.92

Table 6-6 Analytical, FEM (Helmholtz) and TDFEM Eigen frequencies for the reverberant room

This latter section, in addition to showing that TDFEM, FEM (Helmholtz) and the analytical solution can provide very close results, has another significant meaning. In practical, real life acoustic studies of rooms the knowledge of the impulse response along with the eigenfrequencies and eigenmodes is very important. In room acoustics it is desirable that the frequency spectrum of a room is as flat as possible in the desired listening position. It is also desirable that the cumulative spectral decay does not reveal significant resonances with a great duration in the time domain.

For this reason, the eigenmodes can be utilized in order the appropriate acoustic interventions to be applied. The eigenmodes provide vital information on which positions the absorbent elements must be placed in order to achieve maximum absorptivity of the acoustic energy. The maximum absorption capacity is achieved where the particle velocity has a maximum, i.e. at a distance from the hard surfaces equal to $\lambda / 4$ [210].

A representation of the eigenmodes with the use of isosurfaces is very helpful for that cause. Some charecteristic isosurfaces for eigenmodes are presented in the following figures. The problematic frequencies can be identified with measurements or with the use of the time domain finite element method. The effect of placing absorbing material in position with maximum absorptivity for the problematic frequency in a room can be predicted with the use of the time domain finite element method.

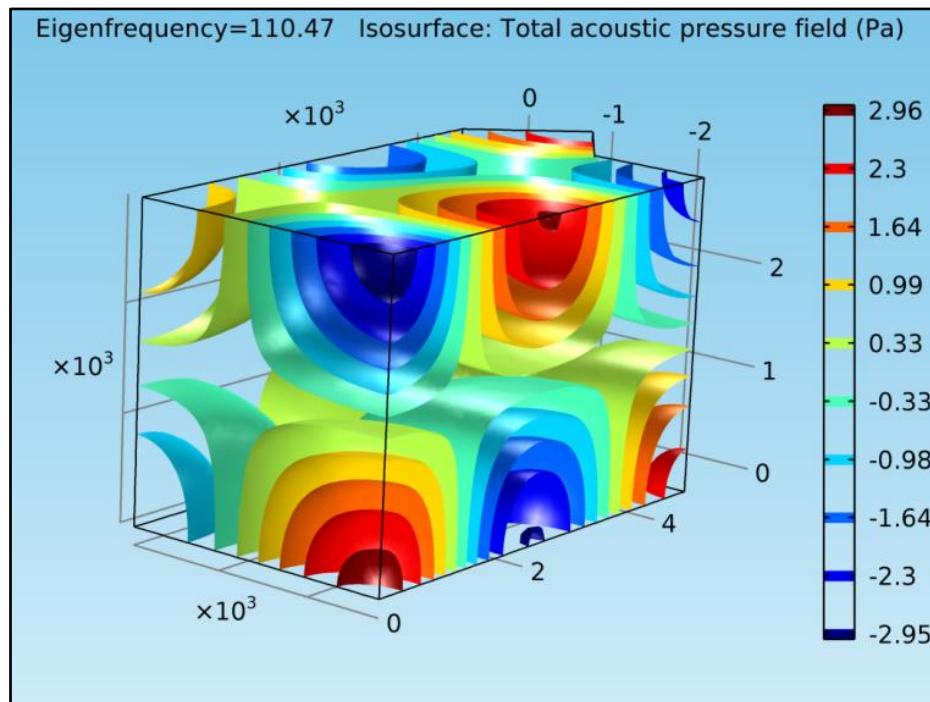


Figure 6-9 Isosurface for Eigenfrequency 110.47 Hz

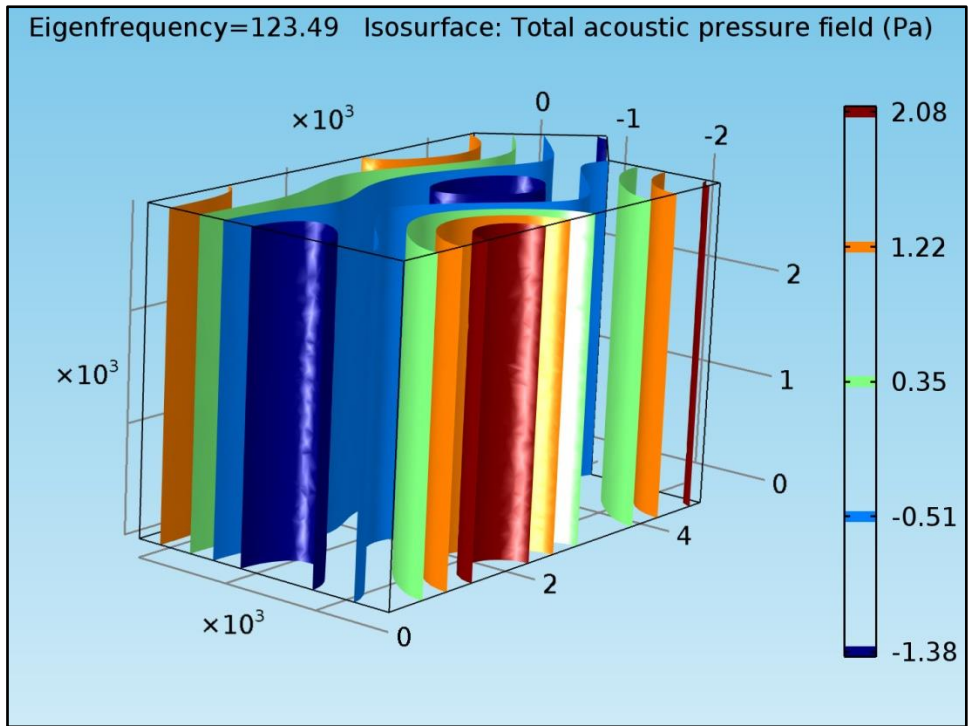


Figure 6-10 Isosurface for Eigenfrequency 123.49 Hz

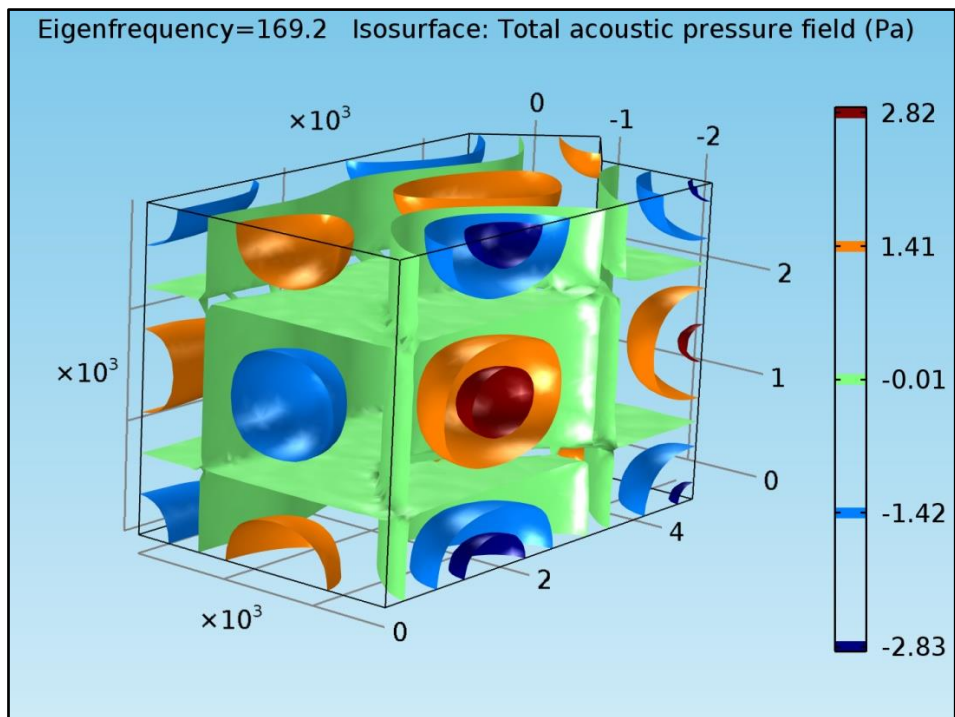


Figure 6-11 Isosurfaces for Eigenfrequency 169.2 Hz

Chapter 7

7. CONCLUSION AND FUTURE RESEARCH



Conclusions and future work for this thesis are presented in this chapter. The most salient points are discussed, along with major strengths and limitations of this thesis. Finally some avenues for future work which are already underway are conferred.

7.1 CONCLUSIONS

This thesis has attempted to propose, validate and utilize a time domain finite element method for modeling the sound field of an acoustic space. A methodology developed for resolving the most crucial problems involving the calculation of the impulse response of a reverberant shape. The steps in the research methods that were taken into account for the development of an accurate method were the source selection, correct modeling of walls, time step-time scales, finite element meshes, modeling of acoustic material and the time stepping method.

The results after the impulse responses and the acoustic parameters of a reverberant space were computed and then compared with the measured ones showed that the time domain finite element method is an applicable method that provides good results for the calculation of the impulse response and acoustic parameters in a reverberant room. The high computational cost along with lack of research in real life rooms currently prohibits the method from widespread use.

The results of this thesis show that the modeling of walls by substituting the normalized acoustic impedance from in situ measurements of the absorption coefficient is satisfactory in the case of a reverberant room. The results for calculated acoustic parameters are very close to the measured ones, which allows for the method to be used in practical application. In reality, this is not the ideal modeling for every kind of absorbing surface. There exist absorbent surfaces and materials that cannot be treated as locally reacting. However, the practicality of this approach if it leads to acceptable results in real life rooms is very promising. The acoustic impedance of materials can be immediately calculated and used in the finite element method in the time domain for measuring acoustic parameters in real rooms. The impedances of a large number of acoustic materials can be extracted from the absorption coefficients of acoustic materials since the majority of the absorption coefficient is already measured with the use of a reverberation chamber.

It therefore stands to reason that this thesis approach for calculating the impulse response could prove to be of considerable commercial interest. This development would presumably lend itself to such applications such software that can predict the sound field of rooms, halls prior to the manufacturing and address the problems that are not possible to solve with current methods such as geometric or statistical acoustics. From the standpoint of low frequency calculation of impulse responses the time domain finite element method can provide better results than the current methods. Combining the method with a geometrical acoustics approach above the Schroeder frequency (hybrid method) could be the best practical solution. Future improvements in computer processing power are likely to make the method more accessible. The above implementation in real life rooms is an obvious avenue of future work.

For this thesis the number of nodes per wavelength that was used for mesh construction was adequate. However it was observed that the correlation coefficient of the impulse responses was reduced overtime. Accuracy, however, was still satisfactory, which also is evident in the results for the acoustic parameters. There were also indications that for shorter impulse responses and smaller rooms with higher absorption this necessity reduces. Hence acceptable results for impulse response can be obtained with fewer nodes per wavelength. This observation may be particularly useful for the appropriate setting of number of nodes per wavelength depending on the room size and absorption.

The second aim of this study was to investigate the usability of the method for predicting the absorption coefficient of a material. The time domain finite element method was utilized in the form of a virtual reverberation chamber for the measurement of the absorption coefficient of an acoustic panel. The results showed that the method can be used for the prediction of the absorption characteristics of acoustic panels. The method can be used for a virtual replication of a reverberation chamber that is commonly used for the measurement of the absorption coefficient of materials. This is an indication that the method can be applied for calculating the absorption coefficient of materials with various shapes prior to their manufacturing.

The findings of this thesis also showed that there is compatibility of the results with the frequency domain finite element method by solving the Helmholtz equation. The combination of methods is very useful for acoustic field studies at low frequencies and proper treatment of a room.

With regard to the research methods, some limitations need to be acknowledged. The method was only applied in a reverberant room. This limitation means that study findings need to be interpreted cautiously. The generalizability of these results needs to be tested in real life rooms, halls and open spaces. Only further study will resolve whether the method can be applicable in real life rooms.

Strength of this thesis is that it can serve as a basis for modeling acoustic phenomena in the time domain. This thesis has provided a deeper insight into the application of time domain finite element method in the field of room acoustics. Many applications exist for an efficient time domain finite element method. Also the accurate prediction of the sound field of any enclosed space is of great interest in many scientific fields and has many useful and interesting applications. The importance of the time domain finite element method is going to be enhanced on the near future because of the emergence of low-cost, high-speed computers. More development and advancement is to be expected for the method in further studies.

7.2 FUTURE WORK

As it was stated earlier a natural progression of this work is the application of the method in real life rooms with different symmetries, larger volumes and with different absorbing materials. The method can also be combined with geometrical acoustics above the Schroeder frequency for a full spectrum hybrid approach of room acoustics problems in the time domain.

Another area of application is the utilization of the virtual reverberation chamber for measuring the absorption coefficient of acoustic panels with

different shapes. Optimization methods can also be used for the proposal of shapes of acoustic panels with better acoustic characteristics.

Accordingly to the method used to measure the absorption coefficient, a similar method can be used to measure the diffusion coefficient of materials. A virtual method for measuring the diffusion of acoustic panels will be of great use and could lead to new shapes and configurations.

The finite element method in the time domain can also be considered for modeling other wave phenomena. Diffraction may be an applicable candidate. The time domain finite element method can be utilized for the development and optimization of sound barriers. The effects of diffraction can be examined and evaluated both in the frequency and the time domain. The open pressure acoustics domain can be modeled with the use of a perfectly matched layer.

The use of the method may be also important in the field of loudspeaker design where the response of the speaker cabinet in the time domain is crucial. Resonances in the time domain can be extracted from the cumulative spectral decay and treated accordingly.

8. APPENDIX

8.1 DERIVATION OF THE FEM FORMULATION VIA THE PRINCIPLE OF MINIMUM POTENTIAL ENERGY

An alternative derivation of the FEM formulation based on the principle of minimum potential energy is presented in this section [211]. In a three-dimensional sound field Ω with sound pressure distribution $p(x, y, z)$, kinetic energy T and potential energy U of sound at an angular frequency ω are in the forms of:

$$T = \frac{1}{2} \frac{1}{\rho \omega^2} \int_{\Omega} (\nabla p \cdot \nabla p) dV \quad (8-1)$$

$$U = \frac{1}{2} \frac{1}{\rho c^2} \int_{\Omega} p^2 dV \quad (8-2)$$

As previously stated, ρ and c , respectively, denote air density and speed of sound. Furthermore, the work W done by an external force at a surface area Γ is obtained by

$$W = \int_{\Gamma} u_n p ds \quad (8-3)$$

where u_n denotes normal displacement at Γ .

Then, total energy Π in the system becomes

$$\Pi = U - T - W \quad (8-4)$$

and, based on the principle of minimum potential energy, i.e. $\delta\Pi = 0$, one can derive the sound field. The same result can be derived as a weak form solution by applying Galerkin's method onto the wave equation as previously stated.

At this point, let us discretize the system by FEM: following the standard FEM procedure, Ω is divided into a number of elements and sound pressure $p(x, y, z)$ at an arbitrary point $Q(x, y, z)$ in an element e can be approximated as

$$p(x, y, z) = N(x, y, z)^T p_e \quad (8-5)$$

Here, p_e and $N(x, y, z)$ are element nodal sound pressure vector and interpolation (shape) function vector, respectively. Hence we can rewrite:

$$T = \sum_e \left(\frac{1}{2} \frac{1}{\rho \omega^2} \int_e \left\{ \left(\frac{\partial N^T p_e}{\partial x} \right)^2 + \left(\frac{\partial N^T p_e}{\partial y} \right)^2 + \left(\frac{\partial N^T p_e}{\partial z} \right)^2 \right\} dV \right) \quad (8-6)$$

$$= \sum_e \left(p_e^T \frac{1}{2} \frac{1}{\rho \omega^2} \int_e \left\{ \frac{\partial N}{\partial x} \frac{\partial N^T}{\partial x} + \frac{\partial N}{\partial y} \frac{\partial N^T}{\partial y} + \frac{\partial N}{\partial z} \frac{\partial N^T}{\partial z} \right\} dV p_e \right)$$

$$U = \sum_e \left(p_e^T \frac{1}{2} \frac{1}{\rho c^2} \int_e [NN^T] dV p_e \right) \quad (8-7)$$

$$W = \sum_e \left(p_e^T u_n \int_{\Gamma_e} N dS \right) \quad (8-8)$$

Then, the following discretized equation can be derived for each element e ,

$$\Pi_e = \frac{1}{2} \frac{1}{\rho \omega^2} p_e^T K_e p_e - \frac{1}{2\rho} p_e^T M_e p_e - p_e^T u_n W_e \quad (8-9)$$

Herein, element matrices, K_e, M_e and W_e , are respectively defined by

$$K_e = \int_e \left\{ \frac{\partial N}{\partial x} \frac{\partial N^T}{\partial x} + \frac{\partial N}{\partial y} \frac{\partial N^T}{\partial y} + \frac{\partial N}{\partial z} \frac{\partial N^T}{\partial z} \right\} dV \quad (8-10)$$

$$M_e = \frac{1}{c^2} \int_e [N N^T] dV \quad (8-11)$$

$$W_e = \int_{\Gamma_e} N dS \quad (8-12)$$

The total energy Π in Ω equals the summation of energies in all the elements.

Therefore, by performing $\delta\Pi = 0$, one can obtain the discretized equation of motion with global matrices K, M and W as

$$(K + j\omega C - \omega^2 M)p = \rho \omega^2 u_n W \quad (8-13)$$

Here, C denotes global dissipation matrix which is constructed using all the element dissipation matrices C_e in Ω .

BIBLIOGRAPHY

1. Papadakis, N. and G.E. Stavroulakis, *Validation of Time Domain Finite Element method via calculations of acoustic parameters in a reverberant space*, in *10th HSTAM International Congress on Mechanics*. 2013: Chania, Crete, Greece.
2. Papadakis, N. and G.E. Stavroulakis. *Time domain finite element method for the calculation of impulse response of enclosed spaces. Room acoustics application*. in *MECHANICS OF HEARING: PROTEIN TO PERCEPTION: Proceedings of the 12th International Workshop on the Mechanics of Hearing*. 2015. AIP Publishing.
3. Papadakis, N.M. and G.E. Stavroulakis, *Estimation Of Insertion Loss of Sound Barriers via Finite Element Method*, in *9th GRACM International Congress on Computational Mechanics*. 2018: Chania, Crete, Greece.
4. Antoniadou, S., N.M. Papadakis, and G.E. Stavroulakis, *Measuring Acoustic Parameters with ESS and MLS: Effect of Artificially Varying Background Noises*, in *Euronoise 2018*. 2018: Heraclion, Crete, Greece.
5. Papadakis, N.M., A. Serras, and G.E. Stavroulakis, *Mimicking the Sound Field of a Dodecahedral Loudspeaker by a Common Directional Loudspeaker for Reverberation Time Measurements*, in *Euronoise 2018* 2018: Heraclion, Crete, Greece.
6. Papadakis, N. and G.E. Stavroulakis, *Virtual Reverberation Chamber Method with the use of Time Domain Finite Element Method* (Submitted to) *Building Acoustics*, 2017.
7. Papadakis, N.M. and G.E. Stavroulakis, *Effect of Mesh Size for Modeling Impulse Responses of Acoustic Spaces via Finite Element Method in the Time Domain*, in *Euronoise 2018* 2018: Heraclion, Crete, Greece.
8. Okuzono, T., et al., *Fundamental accuracy of time domain finite element method for sound-field analysis of rooms*. *Applied Acoustics*, 2010. **71**(10): p. 940-946.

9. Okuzono, T., T. Otsuru, and K. Sakagami, *Applicability of an explicit time-domain finite-element method on room acoustics simulation*. *Acoustical Science and Technology*, 2015. **36**(4): p. 377-380.
10. Kinsler, L.E., et al., *Fundamentals of acoustics*. 1999, Wiley. p. 1.
11. Fahy, F.J., *Foundations of engineering acoustics*. 2000, Academic press. p. 7.
12. Kleiner, M. and J. Tichy, *Acoustics of small rooms*. 2014, CRC Press. p. 1.
13. Beranek, L.L. and T.J. Mellow, *Acoustics: sound fields and transducers*. 2012, Academic Press. p. 5.
14. Beranek, L.L. and T.J. Mellow, *Acoustics: sound fields and transducers*. 2012, Academic Press. p. 13.
15. ISO, B., *9613-1:93*, in *Acoustics-Attenuation of sound during propagation outdoors (part 1)*. 1993.
16. ISO, B., *80000-8:2007*, in *Quantities and units -- Part 8: Acoustics*. 2007.
17. Kleiner, M., *Acoustics and audio technology*. 2011, J. Ross Publishing. p. 2.
18. Kleiner, M. and J. Tichy, *Acoustics of small rooms*. 2014, CRC Press. p. 3.
19. Kleiner, M. and J. Tichy, *Acoustics of small rooms*. 2014, CRC Press. p. 4.
20. Pierce, A.D., *Acoustics: an introduction to its physical principles and applications*. 1981, McGraw-Hill New York. p. 11.
21. Crocker, M.J., *Handbook of noise and vibration control*. 2007, John Wiley & Sons. p. 44.
22. Campos, L., *On 24 forms of the acoustic wave equation in vortical flows and dissipative media*. *Applied Mechanics Reviews*, 2007. **60**(6): p. 291-315.

23. Campos, L., *On 36 forms of the acoustic wave equation in potential flows and inhomogeneous media*. Applied Mechanics Reviews, 2007. **60**(4): p. 149-171.
24. Fahy, F.J., *Foundations of engineering acoustics*. 2000, Academic press. p. 103.
25. Kleiner, M. and J. Tichy, *Acoustics of small rooms*. 2014, CRC Press. p. 7.
26. Lamb Jr, G., *Introductory Applications of Partial Differential Equations: With Emphasis on Wave Propagation and Diffusion*. 2011, John Wiley & Sons. p. 46.
27. APDL, A.M., *Mechanical applications Theory reference*, in *ANSYS Release*. 2013. p. 254.
28. Atalla, N. and F. Sgard, *Finite Element and Boundary Methods in Structural acoustics and vibration*. 2015, CRC Press. p. 10.
29. Kuttruff, H., *Room acoustics*. 2016, Crc Press. p. 68.
30. Crocker, M.J., *Handbook of noise and vibration control*. 2007, John Wiley & Sons. p. 39.
31. Crocker, M.J., *Handbook of noise and vibration control*. 2007, John Wiley & Sons. p. 52.
32. Kleiner, M., *Acoustics and audio technology*. 2011, J. Ross Publishing. p. 101.
33. Crocker, M.J., *Handbook of noise and vibration control*. 2007, John Wiley & Sons. p. 53.
34. Krokstad, A., S. Strom, and S. Sørstal, *Calculating the acoustical room response by the use of a ray tracing technique*. Journal of Sound and Vibration, 1968. **8**(1): p. 118-125.
35. Kulowski, A., *Algorithmic representation of the ray tracing technique*. Applied Acoustics, 1985. **18**(6): p. 449-469.
36. Allen, J.B. and D.A. Berkley, *Image method for efficiently simulating small-room acoustics*. The Journal of the Acoustical Society of America, 1979. **65**(4): p. 943-950.

37. Kirszenstein, J., *An image source computer model for room acoustics analysis and electroacoustic simulation*. Applied Acoustics, 1984. **17**(4): p. 275-290.
38. Schröder, D. and A. Pohl. *Real-time hybrid simulation method including edge diffraction*. in *EAA auralization symposium*. 2009.
39. Antani, L., et al., *Fast geometric sound propagation with finite edge diffraction*. Technical Report TR10-011, University of North Carolina at Chapel Hill, 2010.
40. Sabine, W.C., *Collected papers on acoustics*. 1922: Harvard university press.
41. Mechel, F.P. and P.J. Morris, *Formulas of acoustics*. 2004, Springer. p. 879.
42. Crocker, M.J., *Handbook of noise and vibration control*. 2007, John Wiley & Sons. p. 10.
43. Fahy, F.J., *Foundations of engineering acoustics*. 2000, Academic press. p. 258.
44. Long, M., *Architectural acoustics*. 2005, Elsevier. p. 298.
45. Fahy, F.J., *Foundations of engineering acoustics*. 2000, Academic press.
46. Schroeder, M., *Die statistischen Parameter der Frequenzkurven von großen Räumen*. Acta Acustica united with Acustica, 1954. **4**(5): p. 594-600.
47. Schroeder, M.R., *The "Schroeder frequency" revisited*. The Journal of the Acoustical Society of America, 1996. **99**(5): p. 3240-3241.
48. Kleiner, M. and J. Tichy, *Acoustics of small rooms*. 2014, CRC Press. p. 100.
49. Gunel, B. *Room shape and size estimation using directional impulse response measurements*. in *Proc. Forum Acusticum Sevilla*. 2002.

50. Kuo, S.M., B.H. Lee, and W. Tian, *Real-time digital signal processing: fundamentals, implementations and applications*. 2013, John Wiley & Sons. p. 126.
51. Havelock, D., S. Kuwano, and M. Vorländer, *Handbook of signal processing in acoustics*. 2008, Springer Science & Business Media. p. 12.
52. Ballou, G., *Handbook for sound engineers*. 2013, Taylor & Francis. p. 1613.
53. Havelock, D., S. Kuwano, and M. Vorländer, *Handbook of signal processing in acoustics*. 2008, Springer Science & Business Media. p. 35.
54. Crocker, M.J., *Handbook of noise and vibration control*. 2007, John Wiley & Sons. p. 479.
55. Bunton, J.D. and R.H. Small, *Cumulative spectra, tone bursts, and apodization*. *Journal of the Audio Engineering Society*, 1982. **30**(6): p. 386-395.
56. Kleiner, M., B.-I. Dalenbäck, and P. Svensson, *Auralization-an overview*. *Journal of the Audio Engineering Society*, 1993. **41**(11): p. 861-875.
57. Vorländer, M., et al., *Virtual reality for architectural acoustics*. *Journal of Building Performance Simulation*, 2015. **8**(1): p. 15-25.
58. Standard, I., *3382. Acoustics–Measurement of the reverberation time of rooms with reference to other acoustical parameters*. International Standards Organization, 1997.
59. Mateljan, I., *ARTA Program for Impulse Rresponse Measurement and Real Time Analysis of Spectrum and Frequency Response User Manual*, in *Electroacoustics Laboratory, Faculty of electrical engineering, R. Boskovic bb*. 2011.
60. Schroeder, M., *New method of measuring reverberation time*. *J. Acoust. Soc. Am.*, 1965. **37**: p. 409-412.

61. Schroeder, M.R., *Integrated impulse method measuring sound decay without using impulses*. The Journal of the Acoustical Society of America, 1979. **66**(2): p. 497-500.
62. Jordan, V.L., *Acoustical criteria for auditoriums and their relation to model techniques*. The Journal of the Acoustical Society of America, 1970. **47**(2A): p. 408-412.
63. Rossing, T.D., *Springer Handbook of Acoustics*. 2007, Springer. p. 323.
64. Reichardt, W., O.A. Alim, and W. Schmidt, *Abhängigkeit der grenzen zwischen brauchbarer und unbrauchbarer durchsichtigkeit von der art des musikmotives, der nachhallzeit und der nachhalleinsatzzeit*. Applied Acoustics, 1974. **7**(4): p. 243-264.
65. Thiele, R., *Richtungsverteilung und zeitfolge der schallrückwürfe in räumen*. Acta Acustica United with Acustica, 1953. **3**(4): p. 291-302.
66. Kuttruff, H., *Room acoustics*. 2016, Crc Press. p. 225.
67. Kuttruff, H., *Room acoustics*. 2016, Crc Press. p. 238.
68. Long, M., *Architectural acoustics*. 2005, Elsevier. p. 249.
69. Kinsler, L.E., et al., *Fundamentals of acoustics*, in *Fundamentals of Acoustics, 4th Edition* 1999, Wiley. p. 341.
70. Segerlind, L.J. and H. Saunders, *Applied finite element analysis*. 1987, American Society of Mechanical Engineers. p. 3.
71. Gladwell, G. *A finite element method for acoustics*. in *Proceedings of the Fifth International Congress of Acoustics, Liege L*. 1965.
72. Craggs, A., *The use of simple three-dimensional acoustic finite elements for determining the natural modes and frequencies of complex shaped enclosures*. Journal of Sound and Vibration, 1972. **23**(3): p. 331-339.
73. Shuku, T. and K. Ishihara, *The analysis of the acoustic field in irregularly shaped rooms by the finite element method*. Journal of Sound and Vibration, 1973. **29**(1): p. 67IN1-76.

74. Milner, J.R. and R.J. Bernhard, *An investigation of the modal characteristics of nonrectangular reverberation rooms*. The Journal of the Acoustical Society of America, 1989. **85**(2): p. 772-779.
75. Craggs, A., *The transient response of a coupled plate-acoustic system using plate and acoustic finite elements*. Journal of Sound and Vibration, 1971. **15**(4): p. 509-528.
76. Craggs, A., *A finite element model for rigid porous absorbing materials*. Journal of Sound and Vibration, 1978. **61**(1): p. 101-111.
77. Craggs, A., *Coupling of finite element acoustic absorption models*. Journal of sound and vibration, 1979. **66**(4): p. 605-613.
78. Richards, T. and S. Jha, *A simplified finite element method for studying acoustic characteristics inside a car cavity*. Journal of Sound and Vibration, 1979. **63**(1): p. 61-72.
79. Nefske, D., J. Wolf, and L. Howell, *Structural-acoustic finite element analysis of the automobile passenger compartment: a review of current practice*. Journal of sound and vibration, 1982. **80**(2): p. 247-266.
80. Craggs, A., *A finite element method for the free vibration of air in ducts and rooms with absorbing walls*. Journal of sound and vibration, 1994. **173**(4): p. 568-576.
81. Wright, J.R., *An exact model of acoustic radiation in enclosed spaces*. Journal of the Audio Engineering Society, 1995. **43**(10): p. 813-820.
82. Pietrzyk, A. *Computer modeling of the sound field in small rooms*. in *Audio Engineering Society Conference: 15th International Conference: Audio, Acoustics & Small Spaces*. 1998. Audio Engineering Society.
83. Okamoto, N., et al., *Numerical analysis of large-scale sound fields using iterative methods part II: application of Krylov subspace methods to finite element analysis*. Journal of Computational Acoustics, 2007. **15**(04): p. 473-493.

84. Okuzono, T., et al., *An explicit time-domain finite element method for room acoustics simulations: Comparison of the performance with implicit methods*. Applied Acoustics, 2016. **104**: p. 76-84.
85. Ayr, U., F. Martellotta, and G. Rospi, *A method for the low frequency qualification of reverberation test rooms using a validated finite element model*. Applied Acoustics, 2017. **116**: p. 33-42.
86. Noh, G. and K.-J. Bathe, *An explicit time integration scheme for the analysis of wave propagations*. Computers & structures, 2013. **129**: p. 178-193.
87. Lam, Y.W., *Issues for computer modelling of room acoustics in non-concert hall settings*. Acoustical science and technology, 2005. **26**(2): p. 145-155.
88. Sakuma, T., S. Sakamoto, and T. Otsuru, *Computational simulation in architectural and environmental acoustics*. 2014, Springer. p. 117.
89. Ballou, G., *Handbook for sound engineers*. 2013, Taylor & Francis. p. 228.
90. Botteldooren, D., *Finite-difference time-domain simulation of low-frequency room acoustic problems*. The Journal of the Acoustical Society of America, 1995. **98**(6): p. 3302-3308.
91. Sakamoto, S., et al., *Calculation of impulse responses and acoustic parameters in a hall by the finite-difference time-domain method*. Acoustical science and technology, 2008. **29**(4): p. 256-265.
92. Sakuma, T., S. Sakamoto, and T. Otsuru, *Computational simulation in architectural and environmental acoustics*. 2014, Springer.
93. Kowalczyk, K. and M. Van Walstijn, *Room acoustics simulation using 3-D compact explicit FDTD schemes*. IEEE Transactions on Audio, Speech, and Language Processing, 2011. **19**(1): p. 34-46.
94. Kanarachos, A. and C. Provatidis, *Potential and wave propagation problems using the boundary element method and*

- BEM-subregions*. Engineering analysis with boundary elements, 1992. **9**(2): p. 117-124.
95. Kleiner, M. and J. Tichy, *Acoustics of small rooms*. 2014, CRC Press. p. 395.
 96. Crocker, M.J., *Handbook of noise and vibration control*. 2007, John Wiley & Sons. p. 101.
 97. Harari, I. and T.J. Hughes, *A cost comparison of boundary element and finite element methods for problems of time-harmonic acoustics*. Computer Methods in Applied Mechanics and Engineering, 1992. **97**(1): p. 77-102.
 98. Davies, A.J., *The finite element method: An Introduction with Partial Differential Equations*. 2011, Oxford University Press. p. 274.
 99. Chapra, S.C. and R.P. Canale, *Numerical methods for engineers*. McGraw-Hill New York. p. 890.
 100. Atalla, N. and F. Sgard, *Finite Element and Boundary Methods in Structural acoustics and vibration*. 2015, CRC Press. p. 63.
 101. Segerlind, L.J. and H. Saunders, *Applied finite element analysis*. 1987, American Society of Mechanical Engineers. p. 4.
 102. Lo, D.S., *Finite element mesh generation*. 2014, CRC Press. p. 2.
 103. Atalla, N. and F. Sgard, *Finite Element and Boundary Methods in Structural acoustics and vibration*. 2015, CRC Press. p. 170.
 104. Chapra, S. and R. Canale, *Numerical Methods for Engineers in McGraw-Hill*. 2015. p. 278.
 105. Ihlenburg, F., *Finite element analysis of acoustic scattering*. 2006, Springer Science & Business Media. p. 102.
 106. Crocker, M.J., *Handbook of noise and vibration control*. 2007, John Wiley & Sons. p. 107.
 107. Ihlenburg, F., *Finite element analysis of acoustic scattering*. 2006, Springer Science & Business Media. p. 154.

108. Stanescu, D., et al., *Computation of engine noise propagation and scattering off an aircraft*. International Journal of Aeroacoustics, 2002. **1**(4): p. 403-420.
109. Gockenbach, M.S., *Partial differential equations: analytical and numerical methods*. 2005, Siam. p. 305.
110. APDL, A.M., *Mechanical applications Theory reference*, in *ANSYS Release*. 2013. p. 289.
111. COMSOL, *COMSOL Multiphysics Reference Guide, Version 4.2*. 2011. p. 486.
112. Yue, B. and M.N. Guddati, *Dispersion-reducing finite elements for transient acoustics*. The Journal of the Acoustical Society of America, 2005. **118**(4): p. 2132-2141.
113. Hargreaves, J. and Y. Lam, *Time domain modelling of room acoustics*. Proceedings of the Institute of Acoustics, 2012.
114. Jeong, H. and Y.W. Lam, *Source implementation to eliminate low-frequency artifacts in finite difference time domain room acoustic simulation*. The Journal of the Acoustical Society of America, 2012. **131**(1): p. 258-268.
115. Murphy, D.T., A. Southern, and L. Savioja, *Source excitation strategies for obtaining impulse responses in finite difference time domain room acoustics simulation*. Applied Acoustics, 2014. **82**: p. 6-14.
116. Multiphysics, C., *Acoustic Module–User’s Guide*. 2013, Version. p. 105.
117. Ziolkowski, R.W., *Exact solutions of the wave equation with complex source locations*. Journal of Mathematical Physics, 1985. **26**(4): p. 861-863.
118. Asghar, S., et al., *Scattering of a spherical Gaussian pulse near an absorbing half plane*. Applied Acoustics, 1998. **54**(4): p. 323-338.
119. Long, M., *Architectural acoustics*. 2005, Elsevier. p. 251.

120. Möser, M., *Engineering acoustics: an introduction to noise control*. 2009, Springer Science & Business Media. p. 184.
121. Kuttruff, H., *Room acoustics*. 2016, Crc Press. p. 38.
122. Mommertz, E., *Angle-dependent in-situ measurements of reflection coefficients using a subtraction technique*. *Applied Acoustics*, 1995. **46**(3): p. 251-263.
123. Kimura, K. and K. Yamamoto, *A method for measuring oblique incidence absorption coefficient of absorptive panels by stretched pulse technique*. *Applied Acoustics*, 2001. **62**(6): p. 617-632.
124. Robinson, P. and N. Xiang, *On the subtraction method for in-situ reflection and diffusion coefficient measurements*. *The Journal of the Acoustical Society of America*, 2010. **127**(3): p. EL99-EL104.
125. Benedetto, G. and R. Spagnolo, *Reverberation time in enclosures: The surface reflection law and the dependence of the absorption coefficient on the angle of incidence*. *The Journal of the Acoustical Society of America*, 1985. **77**(4): p. 1447-1451.
126. Kuttruff, H., *Room acoustics*. 2016, Crc Press. p. 43.
127. Kuttruff, H., *Room acoustics*. 2016, Crc Press. p. 45.
128. Bermúdez, A., et al., *Perfectly matched layers, in Computational acoustics of noise propagation in fluids-finite and boundary element methods*. 2008, Springer. p. 167-196.
129. Gao, H. and J. Zhang, *Implementation of perfectly matched layers in an arbitrary geometrical boundary for elastic wave modelling*. *Geophysical Journal International*, 2008. **174**(3): p. 1029-1036.
130. ISO, B., *354: 2003 Acoustics–Measurement of sound absorption in a reverberation room*. British Standards Institution, 2003.
131. Vercammen, M. *Improving the accuracy of sound absorption measurement according to ISO 354*. in *Proceedings of the International Symposium on Room Acoustics, Melbourne, Australia*. 2010.

132. ISO, I.S., *10534-1. Acoustics—determination of sound absorption coefficient and impedance in impedance tubes—Part 1: method using standing wave ratio*. International Standard, 1996.
133. ISO, E., *10534-2 2001 Acoustics—determination of sound absorption coefficient and impedance in impedance tube: Part 2. Method use standing wave ratio*.
134. Courant, R., K. Friedrichs, and H. Lewy, *Über die partiellen Differenzgleichungen der mathematischen Physik*. *Mathematische annalen*, 1928. **100**(1): p. 32-74.
135. Courant, R., K. Friedrichs, and H. Lewy, *On the partial difference equations of mathematical physics*. 1959, CALIFORNIA UNIV LOS ANGELES.
136. Trefethen, L.N., *Finite difference and spectral methods for ordinary and partial differential equations*. 1996. p. 162.
137. *CFD Online*. [cited 2017 5/5/2017]; Available from: https://www.cfd-online.com/Wiki/Courant%E2%80%93Friedrichs%E2%80%93Lewy_condition.
138. Zölzer, U., *Digital audio signal processing*. 2008, John Wiley & Sons. p. 241.
139. Kleiner, M. and J. Tichy, *Acoustics of small rooms*. 2014, CRC Press. p. 400.
140. Łodygowski, T. and W. Sumelka, *Limitations in application of finite element method in acoustic numerical simulation*. *Journal of theoretical and applied mechanics*, 2006. **44**: p. 849-865.
141. Schmiechen, P., *Travelling Wave Speed Coincidence (Ph. D. thesis)*. Imperial College of London, 1997.
142. Wojcik, G.L., et al. *Laser alignment modeling using rigorous numerical simulations*. in *Proc. SPIE*. 1991.
143. Marburg, S. and B. Nolte, *Computational acoustics of noise propagation in fluids: finite and boundary element methods*. Springer. p. 47.

144. Thompson, L.L. and P.M. Pinsky, *Complex wavenumber Fourier analysis of the p-version finite element method*. Computational Mechanics, 1994. **13**(4): p. 255-275.
145. O.C. Zienkiewicz and R.L. Taylor, *The finite element method: fluid dynamics, Fifth Edition*. 2000, Butterworth-Heinemann. p. 244.
146. Marburg, S., *Six boundary elements per wavelength: Is that enough?* Journal of Computational Acoustics, 2002. **10**(01): p. 25-51.
147. Ihlenburg, F., *Finite element analysis of acoustic scattering*. Vol. 132. 2006: Springer Science & Business Media.
148. Otsuru, T. and R. Tomiku, *Basic characteristics and accuracy of acoustic element using spline function in finite element sound field analysis*. Acoustical Science and Technology, 2001. **21**(2): p. 87-95.
149. George, P.L., *Improvements on Delaunay-based three-dimensional automatic mesh generator*. Finite Elements in Analysis and Design, 1997. **25**(3-4): p. 297-317.
150. Johnson, A.A. and T.E. Tezduyar, *Parallel computation of incompressible flows with complex geometries*. International Journal for Numerical Methods in Fluids, 1997. **24**(12): p. 1321-1340.
151. Delaunay, B., *Sur la sphere vide*. Izv. Akad. Nauk SSSR, Otdelenie Matematicheskii i Estestvennyka Nauk, 1934. **7**(793-800): p. 1-2.
152. Lo, S., *Volume discretization into tetrahedra—I. Verification and orientation of boundary surfaces*. Computers & Structures, 1991. **39**(5): p. 493-500.
153. Löhner, R., *Progress in grid generation via the advancing front technique*. Engineering with computers, 1996. **12**(3): p. 186-210.
154. Rassineux, A., *3D mesh adaptation. Optimization of tetrahedral meshes by advancing front technique*. Computer Methods in

- Applied Mechanics and Engineering, 1997. **141**(3-4): p. 335-354.
155. Lo, D.S., *Finite element mesh generation*. 2014, CRC Press. p. 239.
 156. Cheng, S.-W., T.K. Dey, and J. Shewchuk, *Delaunay mesh generation*. 2012, CRC Press. p. 8.
 157. Long, M., *Architectural acoustics*. 2005, Elsevier. p. 261.
 158. Delany, M. and E. Bazley, *Acoustical properties of fibrous absorbent materials*. Applied acoustics, 1970. **3**(2): p. 105-116.
 159. Wang, C.-N. and J.-H. Torng, *Experimental study of the absorption characteristics of some porous fibrous materials*. Applied Acoustics, 2001. **62**(4): p. 447-459.
 160. Hulbert, G., *A Time Integration Algorithm for Structural Dynamics With Improved Numerical Dissipation: The Generalized- α Method*. Ann Arbor, 1993. **1050**: p. 48109-2125.
 161. Jansen, K.E., C.H. Whiting, and G.M. Hulbert, *A generalized- α method for integrating the filtered Navier–Stokes equations with a stabilized finite element method*. Computer Methods in Applied Mechanics and Engineering, 2000. **190**(3): p. 305-319.
 162. Newmark, N.M., *A method of computation for structural dynamics*. Journal of the engineering mechanics division, 1959. **85**(3): p. 67-94.
 163. Sakuma, T., S. Sakamoto, and T. Otsuru, *Computational simulation in architectural and environmental acoustics*. 2014, Springer. p. 56.
 164. Dettmer, W. and D. Perić, *An analysis of the time integration algorithms for the finite element solutions of incompressible Navier–Stokes equations based on a stabilised formulation*. Computer Methods in Applied Mechanics and Engineering, 2003. **192**(9): p. 1177-1226.

165. *MUltifrontal Massively Parallel sparse direct Solver (MUMPS)* 2017 [cited 2017 27/7/2017]; Available from: <http://mumps.enseeiht.fr/index.php?page=home>.
166. Amestoy, P.R., I.S. Duff, and J.-Y. L'Excellent, *Multifrontal parallel distributed symmetric and unsymmetric solvers*. Computer methods in applied mechanics and engineering, 2000. **184**(2): p. 501-520.
167. *PARAllel Sparse DIrect SOLver (PARDISO)*. [cited 2017 8/6/2017]; Available from: <http://www.pardiso-project.org/>.
168. Greenbaum, A., *Iterative methods for solving linear systems*. 1997: SIAM.
169. Saad, Y., *A flexible inner-outer preconditioned GMRES algorithm*. SIAM Journal on Scientific Computing, 1993. **14**(2): p. 461-469.
170. Van der Vorst, H.A., *Bi-CGSTAB: A fast and smoothly converging variant of Bi-CG for the solution of nonsymmetric linear systems*. SIAM Journal on scientific and Statistical Computing, 1992. **13**(2): p. 631-644.
171. Sakuma, T., S. Sakamoto, and T. Otsuru, *Computational simulation in architectural and environmental acoustics*. 2014, Springer. p. 62.
172. Atalla, N. and F. Sgard, *Finite Element and Boundary Methods in Structural acoustics and vibration*. 2015, CRC Press. p. 105.
173. Fahy, F. and J. Walker, *Advanced applications in acoustics, noise and vibration*. 2004, CRC Press. p. 53.
174. Crocker, M.J., *Handbook of noise and vibration control*. 2007, John Wiley & Sons. p. 104.
175. Ballou, G., *Handbook for sound engineers*. 2013, Taylor & Francis. p. 1620.
176. Ream, N. *Nonlinear identification using inverse-repeatm sequences*. in *Proceedings of the Institution of Electrical Engineers*. 1970. IET.

177. Farcas, A.C. and M.D. Topa, *On The Choice Of The Method For Obtaining The Room Impulse Response*. Acta Technica Napocensis, 2013. **54**(1): p. 34.
178. Aoshima, N., *Computer-generated pulse signal applied for sound measurement*. The Journal of the Acoustical Society of America, 1981. **69**(5): p. 1484-1488.
179. Farina, A. *Simultaneous measurement of impulse response and distortion with a swept-sine technique*. in *Audio Engineering Society Convention 108*. 2000. Audio Engineering Society.
180. Farina, A. and E. Ugolotti. *Subjective comparison between Stereo Dipole and 3D Ambisonic surround systems for automotive applications*. in *Audio Engineering Society Conference: 16th International Conference: Spatial Sound Reproduction*. 1999. Audio Engineering Society.
181. Müller, S. and P. Massarani, *Transfer-function measurement with sweeps*. Journal of the Audio Engineering Society, 2001. **49**(6): p. 443-471.
182. Mateljan, I. and K. Ugrinović. *The comparison of room impulse response measuring systems*. in *Proceedings of the First Congress of Alps Adria Acoustics Association*. 2003.
183. Stan, G.-B., J.-J. Embrechts, and D. Archambeau, *Comparison of different impulse response measurement techniques*. Journal of the Audio Engineering Society, 2002. **50**(4): p. 249-262.
184. Schroeder, M.R., *Integrated-impulse method measuring sound decay without using impulses*. The Journal of the Acoustical Society of America, 1979. **66**(2): p. 497-500.
185. Dunn, C. and M.J. Hawksford, *Distortion immunity of MLS-derived impulse response measurements*. Journal of the Audio Engineering Society, 1993. **41**(5): p. 314-335.
186. Bleakley, C. and R. Scaife, *New formulas for predicting the accuracy of acoustical measurements made in noisy environments using the averaged m-sequence correlation technique*. The Journal of the Acoustical Society of America, 1995. **97**(2): p. 1329-1332.

187. Vorländer, M. and M. Kob, *Practical aspects of MLS measurements in building acoustics*. Applied Acoustics, 1997. **52**(3): p. 239-258.
188. Vanderkooy, J., *Aspects of MLS measuring systems*. Journal of the Audio Engineering Society, 1994. **42**(4): p. 219-231.
189. MacWilliams, F.J. and N.J. Sloane, *Pseudo-random sequences and arrays*. Proceedings of the IEEE, 1976. **64**(12): p. 1715-1729.
190. San Martín, R., et al., *Impulse source versus dodecahedral loudspeaker for measuring parameters derived from the impulse response in room acoustics*. The Journal of the Acoustical Society of America, 2013. **134**(1): p. 275-284.
191. Arana, M., A. Vela, and L. San Martin, *Calculating the impulse response in rooms using pseudo-impulsive acoustic sources*. Acta Acustica United with Acustica, 2003. **89**(2): p. 377-380.
192. Szłapa, P., et al., *A Comparison of Handgun Shots, Balloon Bursts, and a Compressor Nozzle Hiss as Sound Sources for Reverberation Time Assessment*. Archives of Acoustics, 2016. **41**(4): p. 683-690.
193. Vorländer, M. and G. Raabe, *Calibration of reference sound sources*. Acta Acustica united with Acustica, 1995. **81**(3): p. 247-263.
194. Beranek, L.L. and N. Nishihara, *Mean-free-paths in concert and chamber music halls and the correct method for calibrating dodecahedral sound sources*. The Journal of the Acoustical Society of America, 2014. **135**(1): p. 223-230.
195. Christensen, C.L., et al., *Applying in-situ recalibration for sound strength measurements in auditoria*. Proceedings of the Institute of Acoustics, 2015. **37**.
196. Small, R.H., *Simplified loudspeaker measurements at low frequencies*. Journal of the Audio Engineering Society, 1972. **20**(1): p. 28-33.
197. Keele Jr, D., *Low-frequency loudspeaker assessment by nearfield sound-pressure measurement*. Journal of the audio engineering society, 1974. **22**(3): p. 154-162.

198. Havelock, D., S. Kuwano, and M. Vorländer, *Handbook of signal processing in acoustics*. 2008, Springer Science & Business Media. p. 1293.
199. Commission, I.E., *IEC61094-6: Measurement Microphones, Part 6: Electrostatic Actuators for Determination of Frequency Response*.
200. Wong, G.S., T.F. Embleton, and S.L. Ehrlich, *AIP Handbook of Condenser Microphones (Theory, Calibration, and Measurements)*, in *The Journal of the Acoustical Society of America*. 1995. p. 231.
201. San Martín, R. and M. Arana, *Uncertainties caused by source directivity in room-acoustic investigations*. *The Journal of the Acoustical Society of America*, 2008. **123**(6): p. EL133-EL138.
202. Martín, R.S., et al., *Influence of the source orientation on the measurement of acoustic parameters*. *Acta acustica united with acustica*, 2007. **93**(3): p. 387-397.
203. Schneider, J.B., C.L. Wagner, and S.L. Broschat, *Implementation of transparent sources embedded in acoustic finite-difference time-domain grids*. *The Journal of the Acoustical Society of America*, 1998. **103**(1): p. 136-142.
204. Martellotta, F., *Optimizing stepwise rotation of dodecahedron sound source to improve the accuracy of room acoustic measures*. *The Journal of the Acoustical Society of America*, 2013. **134**(3): p. 2037-2048.
205. Kleiner, M., *Acoustics and audio technology*. 2011, J. Ross Publishing. p. 7.
206. Katz, B.F., *International round robin on room acoustical impulse response analysis software 2004*. *Acoustics Research Letters Online*, 2004. **5**(4): p. 158-164.
207. Cabrera, D., J. Xun, and M. Guski, *Calculating reverberation time from impulse responses: a comparison of software implementations*. *Acoustics Australia*, 2016. **44**(2): p. 369-378.

208. ISO, 17497-1: *Acoustics - Measurement of the sound scattering properties of surfaces – Part 1: Measurement of the random-incidence scattering coefficient in a reverberation room*. 2000.
209. Cox, T.J., et al., *A tutorial on scattering and diffusion coefficients for room acoustic surfaces*. *Acta Acustica united with ACUSTICA*, 2006. **92**(1): p. 1-15.
210. Λουτρίδης, Σ., *Ακουστική, Αρχές και Εφαρμογές*. Εκδόσεις Τζιόλα. p. 137.
211. Sakuma, T., S. Sakamoto, and T. Otsuru, *Computational simulation in architectural and environmental acoustics*. 2014, Springer. p. 54.